AN ABSTRACT OF THE DISSERTATION OF

Timothy J. Sheehan for the degree of Doctor of Philosophy in Environmental Sciences, presented on June 3, 2019.

Title: A Climate of Risk: Modeled Vegetation, Carbon, Fire, and Biomass Loss Risk in Western Oregon and Washington under Climate Change

Abstract approved: _____
Dominique Bachelet

Managing wildlands to protect species and ecosystem services in response to climate change is challenging. To develop effective long-term strategies, natural resource managers need to account for the projected effects of climate change as well as the uncertainty inherent in those projections. Vegetation models are one important source of projected climate impacts. Interpreting those model results can be difficult due to both uncertainty in results and model limitations. Factors contributing to uncertainty include embedded assumptions about atmospheric CO_2 levels, uncertain climate projections driving models, and model algorithm selection. Limitations include processes excluded by models, such as mortality from maladaptation and succession, as well as algorithmic simplifications such as assumptions about wildfire ignitions.

To understand the potential impacts of climate change on vegetation and wildfire in 21st century, I used the MC2 dynamic global vegetation model (DGVM) to simulate vegetation for the Northwest conterminous United States using results from 20 different Climate Model Intercomparison Project Phase 5 (CMIP5) models downscaled using the MACA algorithm. Results were generated for representative concentration pathways (RCP) 4.5 and 8.5 under vegetation modeling scenarios with and without fire suppression for a total of 80 model runs for future projections. For analysis, results were aggregated by three subregions: the western Northwest (WNW), from the crest of the Cascade Mountains west; Northwest plains and plateau

(NWPP), the non-mountainous areas east of the Cascade Mountains; and eastern Northwest mountains (ENWM), the mountainous areas east of the Cascade Mountains.

To understand MC2 sensitivity to model assumptions, I further explored results and associated uncertainties from the MC2 Dynamic Global Vegetation Model for the WNW subregion. I compared model results for vegetation cover and carbon dynamics over the period 1895-2100 assuming: 1) unlimited wildfire ignitions versus stochastic ignitions, 2) no fire, and 3) a moderate CO_2 fertilization effect versus no CO_2 fertilization effect.

Finally, I implemented an Environmental Evaluation Modeling System (EEMS) decision support model using MC2 DGVM results to characterize biomass loss risk for the WNW subregion. Risk was based on biomass present, fire occurrence and severity, and mortality of climate-maladapted vegetation as indicated by modeled vegetation type change. I characterized the uncertainty due to RCP, fire suppression, and climate projection choice, and I evaluated whether fire or climate maladaptation mortality was the dominant driver of risk.

In the 21st century, in the WNW, mean fire interval (MFI) averaged over all climate projections decreases by up to 48%. By the end of the 21st century, potential vegetation shifts from conifer to mixed forest under RCP 4.5 and 8.5 with and without fire suppression. In the NWPP, MFI averaged over all climate projections decreases by up to 82% without fire suppression and increases by up to 14% with fire suppression resulting in woodier vegetation cover. In the ENWM, MFI averaged across all climate projections decreases by up to 81%, subalpine communities are lost, but conifer forests continue to dominate the subregion in the future.

In evaluating the effects of ignition and CO_2 fertilization assumptions, the greatest carbon stock loss in the WNW, approximately 23% of historical levels, occurs with unlimited ignitions and no CO_2 fertilization effect. With stochastic ignitions and a CO_2 fertilization effect, carbon stocks are more stable than with unlimited ignitions. For all scenarios, the dominant vegetation type shifts from pure conifer to mixed forest, indicating that vegetation cover change is driven solely by climate and that significant mortality due climate-maladapted vegetation as indicated by modeled vegetation shifts are likely through the 21st century regardless of fire regime changes.

The risk of biomass loss in the WNW generally increases in current high biomass areas within the study region through time. The pattern of increased risk is generally south to north and upslope into the Coast and Cascade mountain ranges and along the coast. Uncertainty from climate future choice is greater than that attributable to RCP or +/- fire suppression. Fire dominates as the driving factor for biomass loss risk in more model runs than mortality due to climate maladaptation. This method of interpreting DGVM results and the associated uncertainty provides managers with data in a form directly applicable to their concerns and could prove helpful in adaptive management planning at regional to local scales.

A Climate of Risk: Modeled Vegetation, Carbon, Fire, and Biomass Loss Risk in Western Oregon and Washington under Climate Change

by
Timothy J. Sheehan

A DISSERTATION

submitted to

Oregon State University

in partial fulfillment of
the requirements for the
degree of

Doctor of Philosophy

Presented June 3, 2019
Commencement June 2019

Doctor of Philosophy dissertation of Timothy J. Sheehan presented on June 3, 2019

APPROVED:

Major Professor, representing Environmental Sciences

Director of the Environmental Sciences Program

Dean of the Graduate School

I understand that my dissertation will become part of the permanent collection of Oregon State University libraries. My signature below authorizes release of my dissertation to any reader upon request.

Timothy J. Sheehan Author

ACKNOWLEDGEMENTS

I thank my major advisor Dr. Dominique Bachelet, for her inspiration, guidance, oversight, patience, advice, insights, encouragement, frankness, and friendship throughout my course of study and production of this dissertation. I thank my committee members, Drs. John Bolte, Troy Hall, Meg Krawchuk, and Alexandra Syphard for their encouragement, guidance, patience, faith, and insight. I thank my Graduate Representative, Dr. Stephen Lancaster for fulfilling that important function and for the additional advice and insights he has offered during my studies.

I thank my friend and coworker, Ken Ferschweiler, for help with modeling and analyses and for words of encouragement. I thank Dr. Barry Baker for both informal input on my studies as well as discussions of the methods and meaning for my work. I acknowledge my coworkers at the Conservation Biology Institute for encouragement, resources, research insights, and flexibility, notably Dr. James Strittholt, Pamela Frost, Jerre Stallcup, Dr. Gladwin Joseph, Nik Molnar, Heather Rustigian-Romsos, Kai Foster, Rebecca Degagne, Lisa Alley, Mike Gough, John Gallo, Gwynne Corrigan, and Robert Lount.

I acknowledge the faculty and staff associated with the Environmental Sciences Program, especially Program Director Dr. Carolyn Fonyo whose work makes this program possible and Renee Freeeman, the program's Administrative Assistant, who has always been willing to help with any question or issue.

Above all, I acknowledge my wife, Dr. Kim Sheehan, who has provided encouragement, support, advice on writing, advice on statistics, guidance, infinite patience, the transfer of tuition remission, and time. Without the sacrifices she has made for me, I would never have been able to pursue this degree.

CONTRIBUTION OF AUTHORS

Dr. Dominique Bachelet contributed to this dissertation through advising, editing, and guiding research. She is credited as a coauthor on Chapters 2-4 for her oversight of the research, her input to research ideas and analytical methods, vetting analytical results, guidance in modifying the MC2 computer code, and manuscript editing. Ken Ferschweiler is credited as a coauthor on Chapters 2-3 for his help with modifications to the MC2 computer code, technical input on data analysis, and input on research ideas and analytical methods.

TABLE OF CONTENTS

Page

TABLE OF CONTENTS (Continued)

Page

TABLE OF CONTENTS (Continued)

Page

TABLE OF CONTENTS (Continued)

Page

LIST OF FIGURES

LIST OF FIGURES (Continued)

Figure Page

LIST OF TABLES (Continued)

Table Page

LIST OF TABLES (Continued)

Table Page

DEDICATION

For Kim Sheehan whose encouragement and support know no bounds.

1 Introduction

1.1 Motivation

Over the course of my academic and working careers, I have concentrated on natural sciences and computer science. The specter of global climate change inspired me to pursue a master's in Computer Science with the goal of supporting climate modeling. I successfully met this goal with an internship at the National Center for Atmospheric Research and in a subsequent software engineering position at Oak Ridge National Laboratories. My primary responsibility in both these positions was porting global climate models (GCMs; e.g. Cramer et al., 2001) onto parallel supercomputers.

Circumstances led me to western Oregon, and necessity led me to work in a corporate environment. My desire to do climate-related modeling did not wane and I went back to school for a master's degree in biology, concentrating on modeling wildfire occurrence and its relationship to climate change. That led to a position at an environmental nonprofit in which my modeling work included both vegetation modeling using a dynamic global vegetation model (DGVM) and decision support modeling.

It is a challenge to provide the best science and characterize its uncertainty in a manner suitable for decision makers. The path from climate modeling to environmental management decisions is long and involves scientists, engineers, managers, and stakeholders from disciplines too numerous to name. The work in my dissertation is an effort to span the part of that path that lies between projected climate futures and considering climate risks to some of the ecosystem services provided by wildlands in the natural resource rich region of the Pacific Northwest (PNW). Within this context my dissertation offers both results and methods that may be useful in supporting current and future environmental decision making.

I continue this introduction with a description of the project that funded my initial research and an overview of the research I completed. After that I present a literature review of topics directly applicable to this dissertation's research and that provide context for that research. Some of what is presented in the literature review is taken from or redundant with material in the research chapters as well as a paper I have published on a decision support modeling framework I created (Sheehan and Gough, 2015).

1.2 Dissertation overview

The Northwest Climate Science Center's *Integrated Scenarios of climate, hydrology and vegetation for the Northwest* project (Integrated Scenarios; https://www.sciencebase.gov/catalog/item/55db7caae4b0518e35470be5) was designed to provide climate science results for managers. Its stated goals include "a series of freely available datasets that can be used to address specific management questions" and supporting "a range of management activities to increase the resilience of Northwest ecosystems, agricultural systems, and built environments." This project had several concrete goals: identifying the "best" CMIP5 GCM and earth system model (ESM; IPCC, 2014) projections for the Northwest; providing downscaled climate projections; modeling future vegetation and potential productivity; and modeling future hydrology. My dissertation starts with research undertaken as part of Integrated Scenarios, and then expands on that work.

Chapter 2 is based directly on vegetation modeling research I did for Integrated Scenarios. This chapter focuses on the entire PNW region (Fig. 1, 2A), from the southeast corner of Idaho north to the Canadian border, and west to the Pacific Coast. Fire and vegetation change were modeled using the MC2 DGVM with varied climate inputs and model assumptions regarding fire suppression. Representative concentration pathways (RCPs; van Vuuren et al., 2011) 4.5 and 8.5 were used for CO_2 concentrations and climate futures driving MC2. Projected climate futures from 20 different GCMs and ESMs were used. Simulations were run with and without fire suppression. In total 80 runs of the model were completed (2 RCPs x 2 fire suppression/no fire suppression x 20 climate futures). In this chapter I answer the question, "What is the range of vegetation and fire response to a large set of the most recent projections of future climate and carbon concentration pathways under different assumptions regarding fire suppression?"

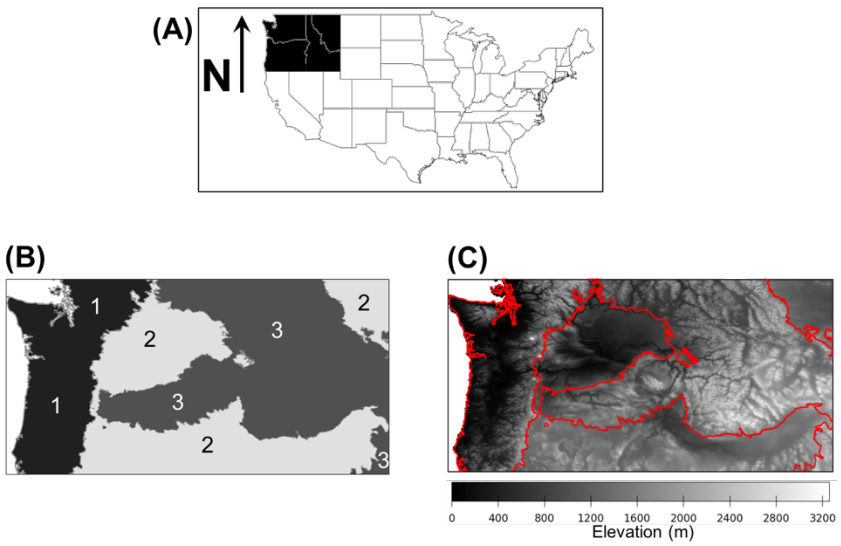

Fig. 1: Study area: (A) Index map of study area within the contiguous United States; (B) subregions defined for this study: 1. western Northwest (WNW); 2. Northwest plains and plateau (NWPP); and 3. eastern Northwest mountains (ENWM); and (C) elevation in meters.

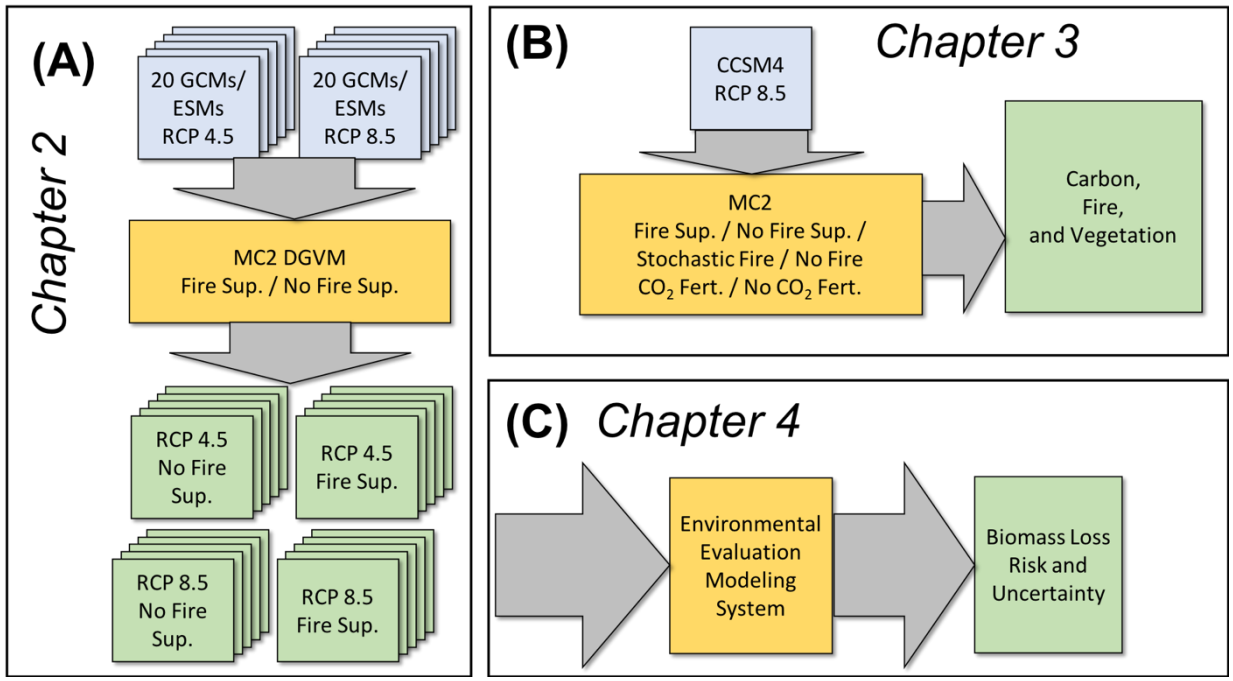

Fig. 2: Schematic of research presented in this dissertation. (A) Climate futures from 20 GCMs/ESMs under RCP 4.5 and 8.5 were used as inputs to MC2, which was run with and without fire suppression for each climate future for Chapter 2. (B) The climate future for CCSM4 was used to analyze the sensitivity of MC2 to assumptions regarding fire occurrence and the effect of CO_2 fertilization. (C) MC2 outputs were in turn used to model biomass loss risk and associated uncertainty using the EEMS modeling framework for chapter 4.

Chapter 3 focuses on the region from the crest of the Cascade mountain range west in Oregon and Washington. In this chapter I answer the question, "How do MC2 assumptions about fire occurrence and the CO_2 fertilization affect fire occurrence, carbon dynamics, and vegetation change?" For a single climate future, it examines uncertainty in model results for fire, carbon dynamics, and vegetation change related to assumptions in MC2's fire modeling algorithm and its application of the CO_2 fertilization effect (Fig. 2B).

Chapter 4 explores how complex model results can be simplified for management decisions. It focuses on biomass loss risk in the region using results from Chapter 2 as inputs to an Environmental Evaluation Modeling System (EEMS; Sheehan and Gough, 2015) decision support model (Fig. 2C). It also quantifies uncertainty in model results, identifies the drivers of uncertainty, and distinguishes whether wildfire or vegetation maladaptation to climate change drives risk.

Each of Chapters 2-4 is presented as an independent research study suitable for publication. In Chapter 5, I present the overall conclusions. The next section begins the literature review and presents a discussion of climate change and its impacts.

1.3 Climate change

Climate change is the major issue driving my research. Anthropogenic emissions have driven atmospheric CO_2 concentrations from approximately 280 parts per million (ppm) in 1850 to over 410 ppm today (https://www.esrl.noaa.gov/gmd/ccgg/trends/). Over two-thirds of this increase has occurred during my lifetime, and this concentration is higher than at any time in the past 800 thousand years (Bereiter et al., 2015; Lüthi et al., 2008). The increase has led to warming of global land and ocean surfaces, reduced snow and ice, rising sea levels, changing patterns of precipitation, and increasing frequency of extreme weather events (IPCC, 2014). Impacts of climate change are observed worldwide, affecting physical (e.g. ice melt, floods, coastal erosion), biological (e.g. ecosystem shifts, wildfires), and human systems (e.g. health, food production; IPCC, 2014). Surface temperatures are projected to continue rising over the 21st century with further, unevenly distributed impacts (IPCC, 2014).

I have focused my work in the Pacific Northwest of the conterminous United States (PNW), where anthropogenic influences are the leading contributor to observed warming (May et al., 2018; Abatzoglou et al., 2014), with impacts including lower winter snowpack and

increased wildfire risk (May et al., 2018). Expected climate change effects on ecosystems include altered fire regimes (e.g. Rogers et al., 2011; Westerling et al., 2006), pest and insect outbreaks (e.g. Kurz et al., 2008), hydrologic changes (e.g. Mote et. al., 2003), altered nutrient cycling (e.g. Fowler et al., 2015), species range shifts (e.g. Chen et al., 2011; Rehfeldt et al., 2009; Rehfeldt et al., 2006), and the emergence of novel species assemblages (e.g. Lurgi et al., 2012; Williams and Jackson, 2007). Vegetation models have been used to simulate such changes and provide resource managers science-based projections to inform their decision process (Littell et al., 2011). Estimating associated uncertainty allows managers to refine their strategies (Littell et al., 2011).

A description of the study area follows next.

1.4 Study area

Chapter 2 focuses on fire and vegetation in the entire PNW region. It defines three subregions based on topographic and climatological characteristics and derived from EPA Level III Ecoregions (Omernik and Griffith, 2014) within the study area (Fig. 1): the Eastern Northwest Mountains (ENWM); the Northwest Plains and Plateau (NWPP); and the Western Northwest (WNW). Chapters 3 and 4 include analyses of carbon and biomass and are geographically limited to the WNW where ecosystem carbon concentrations are among the highest in the world. Here I present a brief introduction of these three regions. More detailed descriptions can be found in Chapters 2-4.

1.4.1 Eastern Northwest Mountains (ENWM)

ENWM covers 41% of the study area and comprises the mountainous regions east of the Cascades. This subregion includes the Wasatch and Uinta Mountains, Wyoming Basin, Blue Mountains, Idaho Batholith, Middle Rockies, Northern Rockies, and Canadian Rockies Level III Ecoregions. It is the coldest of the subregions and has precipitation amounts intermediate to those of the other two. Conifers dominate this subregion with species including Douglas-fir, true firs, cedar, hemlock, lodgepole pine, and ponderosa pine (Kuchler, 1975; Kerns et al., 2018). The fire regime over most of this region is 35-200 years with mixed severity, with some high elevation areas having a 200+ year frequency (Sommers et al., 2011).

There are many climate related risks to forests in this region. For instance, in the Northern Rockies, wildfire, bark beetles, disease, and invasive non-native plants have been identified as climate sensitive disturbances (Loehman et al., 2018), and in the Blue Mountains vegetation range changes and loss of subalpine and alpine vegetation types have been projected (Kerns et al., 2018).

1.4.2 Northwest Plains and Plateau (NWPP)

The Northwest Plains and Plateau (NWPP) subregion comprises 38% of the study area and includes the Eastern Cascades Slopes and Foothills, Northern Basin and Range, Columbia Plateau, Snake River Plain, Northwest Great Plains, and Northwest Glaciated Plains Level III Ecoregions. This subregion is lower in elevation than the Cascades and other Northwest mountain ranges. It is drier than the other two subregions and experiences higher maximum temperatures. Shrubs and grasses dominate the NWPP. The most common potential vegetation type is sagebrush steppe, with grasses in some areas (Kuchler, 1975). While grasslands in the subregion have fire return intervals as short as 5 years (Leenhouts, 1998), FRIs over the majority of the subregion are 35 to 200 years with mixed severity in the northwestern portion of the region and stand replacing severity in the southwestern portion (Sommers et al., 2011).

Native vegetation in this region has been negatively affected by grazing and invasive species (Shinneman and McIlroy, 2016; Loehman et al., 2018; Reeves et al., 2018). Invasive annual grasses, especially cheatgrass, alter fire regimes by providing continuous fuels between native sagebrush or bunch grasses and outcompeting native species for soil and water after fires (Shinneman and McIlroy, 2016; Loehman et al., 2018; Reeves et al., 2018). The effects of climate change on rangelands has not been extensively studied (Shinneman and McIlroy, 2016; Reeves et al., 2018), but sagebrush resilience to disturbance is higher on northern slopes than southern in cold deserts (Reeves et al., 2018), suggesting that climate may play a role in sagebrush resilience.

1.4.3 Western Northwest (WNW)

The Western Northwest (WNW) subregion comprises the area west of the crest of the Cascade Mountains and represents 21% of the study area. It includes the Coast Range, Klamath Mountains/California High North Coast Range, Willamette Valley, Puget Lowlands, Cascades,

and North Cascades Level III Ecoregions. This subregion falls under strong coastal climatological influence with warmer minimum temperatures and much greater precipitation than the other two subregions.

The WNW region includes the Seattle and Portland metropolitan areas, and its total population exceeds six million (www.census.gov), with higher population densities lying along the I-5 corridor. This region includes PNW's moist coniferous forests (detailed description in Franklin et al., 2017). Douglas-fir is dominant over most of this region. Western hemlock, western redcedar, red alder, and big leaf maple are among species also common at lower elevations. Oregon white oak and Pacific madrone are common in drier lowlands. Sitka spruce is common along the Pacific Coast in valleys where marine fog occurs. At mid elevations, noble fir occurs in the Cascade Range, and Pacific silver fir occurs in both the Cascade and the Olympic Range. Douglas-fir does not range into the subalpine regions where true firs, mountain hemlock, and Alaska yellow cedar are common. In the warmer, drier southern portion of the region, mixed conifer hardwood forests are more common, with species including ponderosa pine, tanoak, and live oaks.

Prior to Euro-American settlement, the fire regime in the WNW was predominantly one of large wildfires at 100 to 400-year intervals with more frequent fires in the southern portion of the region (Franklin et al., 2017). Locally, Native Americans had altered the fire regime for hunting and food gathering, for example the oak woodlands and savannahs that dominated the Willamette Valley were maintained through frequent Native American burning prior to Euro-American settlement (Boyd, 1999; Whitlock and Knox, 2002).

Productivity in the WNW is high compared to other boreal and temperate forests (Harmon and Campbell, 2017). Carbon densities in the region are among the highest in the world, with values exceeding 200 MgC/ha over much of the Coast, Cascade, and Olympic mountains (Wilson et al., 2013, in Olsen and Van Horne, 2017). These highly productive forests are valuable for both natural resources and biodiversity. Conflicts between timber production and endangered species – most emblematically the northern spotted owl – are well known in this subregion. The Northwest Forest Plan was created in1994 to balance these conflicting interests. Challenges remain on how to maintain forests in this region sustainably in light of conflicting interests and climate change (Olsen et al., 2017a).

While ecosystem services are not a main focus of this study, they are a driver of land use conflicts in the region, and this dissertation's results have strong implications for them. As background, the next section provides a brief review of ecosystem services.

1.5 Ecosystem services

I examined the ecological impacts of climate change on the landscape. Implicit in those impacts are effects on humans, both within and outside of the study region. The concept of *ecosystem services,* (coined by Ehrlich and Ehrlich, 1981), provides a lens through which impacts on humans can be viewed. Definitions of the ecosystem services, vary. Commonly used definitions include (Fisher et al., 2007): *[T]he conditions and processes through which natural ecosystems, and the species that make them up sustain and fulfill human life* (Daily, 1997); *The benefits human populations derive, directly or indirectly, from ecosystem functions* (Costanza et al., 1997); *The benefits people obtain from ecosystems* (Millennium Ecosystem Assessment, 2005); and *[C]omponents of nature, directly enjoyed, consumed, or used to yield human well-being* (Boyd and Banzhaf, 2006). The value ecosystems provide to humans is central to the concept.

There are various classification schemes for ecosystem services, the most appropriate of which depends on context (Fisher et al., 2007). The Millenium Ecosystem Assessment (2005) uses three broad categories: *Provisioning* which includes the production of consumable goods such as food, fiber, and water; *Regulating* which includes the maintenance of conditions such as air quality, climate, and water quality; and *Cultural* which includes spiritual, aesthetic, and recreational values and activities. De Groot et al. (2002) define four categories based on function: *Regulation,* which includes the capacity of natural systems to maintain ecosystems and their services that benefit humans (e.g. clean air and water); *Habitat,* which includes the provision of natural habitat that conserves biological and genetic diversity; *Production* which includes the production of ecosystem goods for human consumption including food, raw materials, and energy production; and *Information* which includes opportunities for reflection, recreation, and spiritual enrichment. Fisher et al. (2007) outlined a classification scheme based on the relationship of the service to where the benefits are realized: *in situ* where benefits are realized locally; *omni-directional* where the benefits are realized in the surrounding landscape with no directional bias; and *directional* where benefits flow to a specific location.

Valuation of ecosystem services is needed to track and account for them (Costanza et al., 1997; de Groot et al., 2002; Millenium Ecosystem Assessment, 2005; Boyd and Banzhaf, 2006; Fisher et al., 2007; Guerry et al., 2015). Challenges to valuation include the fact that ecosystem services include both market and non-market components (Costanza et al., 1997; Boyd and Banzhaf, 2006; Guerry et al., 2015) and external costs (Millenium Ecosystem Assessment, 2005; Fisher et al., 2007). Costanza et al. (1997) provided a method of valuation and estimated a range of US$16-$54 trillion globally per year, while acknowledging the challenges and uncertainties in doing so. Boyd and Banzhaf (2006) argue for a standardized measure of the value of ecosystem services whose units are clearly defined and consistent both economically and ecologically. Valuation is important for decision support surrounding ecosystem services not only so that beneficiaries can pay providers, but also for evaluating competing stakeholder interests, for instance between carbon sequestration and fuel wood (Fisher et al., 2007). Guerry et al. (2015) examined the adoption of ecosystem services in decision making and found awareness of human well-being/ecosystem interdependence is at an all-time high, for instance with the environment listed as one of the top global risks by the World Economic Forum. However, they found the science of ecosystem services is advancing, but that successful implementation the science in decision making is not yet widespread.

Within the WNW, timber production and salmon are two important provisioning ecosystem services (Deal et al., 2017). Regulating ecosystem services include water quality (Olson et al., 2017b) and carbon sequestration (Harmon and Campbell, 2017). Cultural ecosystem services include recreation and aesthetics (Deal et al., 2017). Within the context of this dissertation (which includes results for carbon dynamics) results are most directly applicable to carbon sequestration. However, results for changes in biomass, changes in vegetation type, and fire occurrence and severity have clear implications for many ecosystem services, which are a logical next step for the decision support modeling method used in Chapter 4.

Having set the context for practical implications of modeling results, I now present descriptions and issues related to this dissertation's methods.

1.6 Vegetation modeling with the MC2 Dynamic Global Vegetation Model

Dynamic Global Vegetation Models (DGVMs) are process-based models that simulate vegetation, carbon, nutrient, and hydrological dynamics. They are driven by historical climate

data or climate projections. I used MC2, the C++ version of the MC1 DGVM (Bachelet et al., 2015), a process-based model with biogeography, biogeochemistry, and fire modules. The model runs on a monthly timestep and is forced by climate inputs (minimum temperature, maximum temperature, precipitation, and either relative humidity or vapor pressure deficit) and by soil characteristics (bulk density, texture, and depth). The model simulates functional types, not species. Woody types (trees and shrubs) are distinguished by leaf phenology (evergreen vs deciduous) and morphology (needleleaf vs broadleaf). Herbaceous vegetation (grasses, forbs, and sedges) are distinguished between C3 and C4. The model always simulates competition for light, water, and nutrients between herbaceous and woody vegetation.

The fire module (Lenihan et al., 1998; Conklin et al., 2015) simulates fire occurrence and fire effects, including area burned, mortality, consumption of aboveground biomass, carbon emission, and nitrogen volatilization. Mortality and consumption of overstory biomass are simulated as a function of fire behavior and the canopy vertical structure. Fire occurrence is simulated as a discrete event. The module runs on a daily time step using a randomly distributed set of daily precipitation values derived from monthly precipitation values. Estimates for fine fuel moisture code (FFMC, Van Wagner, 1987), buildup index (BUI, Canadian Forestry Service, 1984), and energy release component (ERC, Cohen and Deeming, 1985) are calculated daily. An ignition source is always assumed and a fire is simulated the first time FFMC and BUI values exceed their thresholds for current vegetation type and when the fuel load is sufficiently dense to carry a fire. The fire suppression algorithm suppresses fires by limiting fraction of a cell burned to 0.06% if fuel loads fall below a vegetation specific ERC threshold. The assumption is that low severity fires can be extinguished. To reflect a realistic geographic extent of a fire under assumed ignitions, the fire module limits the area burned with an algorithm based on a vegetation type-specific fire return interval (FRI; Leenhouts, 1998) and the number of years since last fire. In the fire module each vegetation type is assigned both a maximum and minimum FRI. A more detailed description of MC2 is presented in Chapter 2, and a more detailed description of its fire module is presented in Chapter 3.

There are several limitations with MC2. It does not account for herbivory, pests, disease, windthrow, or invasive species. Furthermore, reliable soils data are key to projecting accurate

soil water availability and drought stress (Peterman et al., 2014) but are typically not available. More accurate and detailed soils data would likely improve results.

MC2 simulates potential vegetation most adapted to the climate drivers so that when climate (a 15-year average is used in the model) changes the model will simulate an instantaneous change without mortality of legacy maladapted vegetation or succession. In reality vegetation is long lived and endures under suboptimal conditions, preventing better-suited vegetation from rapidly gaining a foothold in the absence of disturbance.

The effects of CO_2 concentration on water use efficiency and plant productivity are still not completely understood because data only exist for a few species mostly from temperate latitudes and may depend on factors such as ontogeny and site conditions, especially soil nutrient content (Camarero et al., 2015; Fernandez-Martinez et al., 2017). MC2 assumes a moderate CO_2 fertilization effect that enhances production and fuel accumulation. CO_2 effects on plant productivity are discussed below, and research results for MC2's sensitivity to CO_2 concentrations are discussed in Chapter 3.

MC2's assumed fire ignitions, built-in thresholds for fire occurrence, and FRI limited fire extent can lead to simulated fire regimes that are more or less frequent, and more uniform than in reality, where ignition sources and ignition propagation vary. The simulated resulting vegetation may be more uniform than in reality. A more detailed description of MC2's fire algorithm is presented in Chapter 3, as are research results for MC2 sensitivity to assumptions surrounding ignition sources and fire occurrence.

A complete understanding of modeling results includes understanding the uncertainties in those results. The next section provides background on sources of uncertainty.

1.7 Uncertainty in DGVM modeling

Sources of uncertainty in DGVM projections come from both external data used to force DGVM simulations, such as climate and soil characteristics, and internal characteristics such as model structure, empirical parameter values, built-in thresholds, and inherent assumptions and simplifications. In this dissertation, I have addressed several aspects of uncertainty: assumptions about future atmospheric concentrations, variations in climate projections, assumptions about the effect of atmospheric CO_2 concentration on water use efficiency and production, and assumptions about wildfire ignitions.

1.7.1 Climate-related uncertainty

Uncertainties in the climate projections used to force this dissertation's MC2 simulations come from two main sources. First is the uncertainty in future levels of atmospheric CO_2, which force GCMs and ESMs. Climate models respond differently to differences in CO_2 concentrations (e.g. Knutti and Sedlácek, 2012; Sillman et al., 2013). To deal with uncertainties in future levels of atmospheric CO_2, suites of projected future concentrations are used. For example, the Coupled Model Intercomparison Project Phase 5 (CMIP5; https://cmip.llnl.gov/cmip5/) used four representative concentration pathways (RCPs; Van Vuuren et al., 2011) based on differing socioeconomic assumptions.

A second source of climate forcing uncertainty is that, when driven by identical CO_2 concentrations, different climate models produce different results. Projects such as CMIP5 seek to discover the reasons for differing model responses (Taylor et al., 2012).

Approaches to characterize and possibly reduce uncertainty introduced by variations in climatic drivers include taking the ensemble average of climate projections from multiple models (Littell et al., 2011), using a range of projections covering the range of future conditions (Littell et al., 2011), using only the ensemble of those results which best match historical conditions (Littell et al., 2011, e.g. Rupp et al., 2013), and selecting the most extreme climate projections (e.g. warmest, coolest, wettest, driest) in order to provide brackets for results (Littell et al., 2011). An issue with ensemble averaging is that it likely modulates intra- and interannual climate variability which affects the response of the vegetation model. Bracketing extreme inputs runs the risk of missing variations at a fine temporal scale that may affect vegetation model behavior. Exposing the true uncertainty due to variations in climate projections, results must be generated for all candidate models or the relationship between climate inputs and model results must be understood in great detail. The latter possibility is unlikely or impossible due to nonlinear responses inherent in process-based vegetation models.

1.7.2 Atmospheric-CO_2 related uncertainty

The CO_2 fertilization effect (Amthor, 1995) is the assumed positive effect on plant growth due to increased water use efficiency under higher concentrations of atmospheric CO_2. MC2 normally models a moderate CO_2 fertilization effect on vegetation (detailed in Chapter 3)

in which production increases and evapotranspiration decreases with increasing atmospheric CO_2 concentrations. However, the effects of CO_2 on water use efficiency and growth are not completely understood, resulting in another source of uncertainty in results. Simulations with and without the CO_2 fertilization are analyzed in Chapter 3 to explore this assumption's effects on model results. This section details research findings regarding the CO_2 fertilization effect.

It is well known that the closure of stomatal guard cells in response to elevated CO_2 increases water use efficiency (Cowan and Farquhar, 1977). For CO_2 concentrations above current ambient levels, this response is strong in angiosperms but much less so in conifers or ferns (Broddribb et al., 2009). At the leaf level, elevated CO_2 has been found to cause reduced stomatal density, reduced stomatal conductance and thus transpiration. However, other climatic factors, such as drought and elevated temperature, may cause reverse responses (see Xu et al., 2016 for summary). Elevated CO_2 may also enhance photosynthesis for a short time but not over periods of weeks to years (Way et al., 2015). In trees, general increases in productivity have been attributed to increases in CO_2, but confidence in tree responses is lower at larger spatial and longer temporal scales as well as in combination with warming (Way et al., 2015). In grasses, both C3 and C4 grasses show similar reductions in stomatal conductance under elevated CO_2, with C3 grasses showing a 68% increase in leaf level WUE and C4 grasses showing none (Ainsworth and Long, 2005).

Free-air CO_2 enrichment experiments (FACE, Hendrey et al., 1999) have been used to explore the effects of elevated CO_2 on vegetation. In a review of FACE experiments on forests, Norby and Zak (2011) found that elevated CO_2 can cause an increase in leaf area index (LAI) in closed stands with relatively low LAI but not produce a substantial increase over larger areas. It can increase net primary production (NPP) per unit LAI, but other factors, such as nitrogen availability and fine root turnover, may constrain that response over time, and increased NPP does not necessarily increase ecosystem carbon.

1.7.3 Uncertainty related to fire modeling

The relationship between fire and vegetation is complex and takes place over a range of spatial and temporal scales (Harris et al., 2016). Shifts in fire regime cause vegetation-altering feedbacks (e.g. Batllori et al., 2015; Kitzberger et al., 2016). The type and level of complexity of

fire models adequate for management-relevant vegetation modeling remains unclear (Hantson et al., 2016). Models generally are one of three types: physical and quasi-physical, based on the physics and chemistry of combustion and fire spread; empirical and quasi-empirical, based on statistical relationships between wind speed and fuel condition and the rate of spread; and mathematical and analog model, based on a non-physical relationship of fire spread (Sullivan, 2009a-c).

Disturbance modeling at the landscape scale has been described (Keane et al., 2015), and fire model limitations and uncertainties in global vegetation models discussed extensively (Hantson et al., 2016; Rabin et al., 2017). The Fire Modeling Intercomparison Project (FireMIP; Rabin et al., 2017) project has examined uncertainty due to assumptions about fire by comparing results among DGVMs with different embedded fire models. FireMIP has analyzed the complexity of fire models used within DGVMs. For fire behavior, these generally utilize algorithms for fuel moisture, fuel load, ignition causes (lightning and anthropogenic), fire suppression, rate of spread, and area burned, although many of them lack algorithms for one or more of these aspects (Hantson et al., 2016). For fire impacts, models FireMIP rates the complexity of fire-associated carbon dynamics and vegetation effects (Hantson et al., 2016).

MC2's fire algorithm falls in the middle range for overall complexity and for carbon dynamics and vegetation complexity. Its fire algorithm assumes ignition sources and models a fire whenever fuel is dense enough to carry a fire and fuel conditions exceed a vegetation type's threshold. To explore how modeling ignition sources would affect MC2's behavior, Chapter 3 examines the effects of using stochastic ignition sources and stochastic ignition propagation based on fuel conditions in MC2. This approach is more parsimonious than that used by FireMIP as it eliminates differences in results due to non-fire modeling aspects of different DGVMs.

1.7.4 Uncertainty related to climate future downscaling

Downscaling methods produce different results in the climate data used to force DGVM runs. I did not explore results produced from different downscaling methods in this dissertation, but have included a brief discussion for completeness.

GCMs and ESMs commonly produce output data at a coarser horizontal scale than that required for DGVM simulations. For instance, horizontal resolutions for GCM and ESM outputs

used in this dissertation's modeling ranged from 0.94 to 3.75 degrees, while the MC2 simulations utilized a 0.0417 degree grid. Climate outputs, therefore, must be downscaled for use with finer resolution models.

The two main methods of downscaling are statistical and dynamical. Statistical downscaling involves two steps (Fowler et al., 2007). The first is bias correction, which removes biases in the GCM/ESM results, normally via adjustments made based on differences between model results and observations on a local basis (e.g., Wood et al., 2002; Fowler et al., 2007; Ahmed et al., 2013). The second step is to downscale the resolution of the data to the target resolution using synoptic-scale meteorology and local physiographic features to develop local predictions based on larger scale predictions. Dynamical downscaling (e.g., Abatzoglou and Brown, 2012) nests regional climate processes within global processes (Abatzoglou and Brown, 2012). Statistical downscaling is more computationally efficient than dynamical downscaling while dynamical downscaling can resolve atmospheric processes on a smaller scale (Fowler et al., 2007; Abatzoglou and Brown, 2012).

MC2 simulations in this dissertation used climate futures downscaled using Multivariate Adapted Constructed Analogs (MACA; Abatzoglou and Brown, 2012), a dynamical downscaling method that performs well in capturing fire weather danger indices across the western United States. Use of this dataset was mandated by Integrated Scenarios.

For decision makers to consider the potential impacts of climate change on ecosystem services, they must have data in a usable form and use it appropriately. In the following section I review issues surrounding methods for producing usable data, how model data fit into management planning, and describe the modeling framework I used to reinterpret MC2 result data into a form intended for decision makers.

1.8 Data for decision making

1.8.1 Usability

Challenges to using climate science in environmental decision making include the usability of the science (Dilling and Lemos, 2011; Kirchhoff et al., 2013) and uncertainty in projected climate and impacts (Millar et al., 2007; Littell et al., 2011; Curry and Webster, 2011).

The push for usable climate science in the United States has been strong. For instance, the 1990 law establishing the United States Global Change Research Program calls for

information usable for policy decision making (Dilling and Lemos, 2011). Dilling and Lemos (2011) explored three models for science agenda setting: *Push*, in which scientists set the information agenda; *Pull,* in which potential users of the information set the agenda; and *Co-Production,* in which scientists and users work iteratively to set the agenda. They found that nearly all cases of successful climate knowledge production involved iteration between the producers and users, underscoring the importance of user-scientist collaboration in producing usable results.

Kirchhoff et al. (2013) examined two factors that affect the usability of science for environmental decision making. The first is motivation for research, which ranges from the generation of knowledge to problem solving. The second is user participation in knowledge production, which ranges from low to high. These two factors were used to characterize different modes of research in relation to producing knowledge for environmental decision making. Advocates for knowledge driven research with little or no user input support the separation of science from society to insure credibility and objectivity and to keep science value-free. Advocates for coproduction, at the other end of the spectrum, see collaborations between scientists and nonscientists as valuable.

Coproduction has proven to be a successful means for producing knowledge that is accepted by some decision makers (e.g. Meadow et al., 2015; Reyers et al., 2015). Google Scholar searches for articles containing the word *climate* and either *coproduction* or *co-production* from 2000 through 2019 returned a total of 41,800 results, indicating coproduction's importance in relation to climate science. Chapter 4 presents a methodology that may prove valuable in coproduced projects.

1.8.2 Adaptive management and model data

Adaptive management (Stankey et al., 2005; Williams, 2011) is a method of managing resources in the face of uncertainty regarding environmental variation and the results of natural actions. Central to its implementation is a cycle in which goals are evaluated, decisions are made and implemented, resources are monitored, and results are assessed (Stankey et al., 2005; Williams, 2011). Environmental variability often dominates natural systems and is often the most dominant source of uncertainty (Williams, 2011).

Climate change is expected to lead to novel ecosystems (Littell et al., 2011), and maintaining or restoring to past conditions could lead to forests less fit for current conditions (Millar, 2007). While quantitative models can project trajectories of environmental change, they are not accurate enough to predict future conditions with the certainty managers need and, therefore, are best used to gain an understanding of the range of possible futures (Millar et al., 2007; Littell et al., 2011). Within this context, the range of results presented in this dissertation may prove valuable for practitioners of adaptive management.

1.8.3 Fuzzy logic modeling for decision support

Fuzzy logic (Zadeh, 1973; Giles, 1976) is a method well suited for working in fields where variables are quantified verbally and imprecisely and provides a way to represent vague and subjective knowledge (Kasabov, 1996). Many concepts associated with environmental conditions are expressed vaguely, making fuzzy logic suited for use in various environmental fields (Sheehan and Gough, 2015) including infrastructure placement (e.g. Bojorquez-Tapia et al., 2002; Boclin and de Mello, 2006; Aydi et al., 2013), aquatic ecosystems (e.g. Cheung et al., 2005; Kaplan et al., 2014; Segui et al., 2013), and soils (McBratney and Odeh, 1997; e.g. Rodríguez et al., 2016).

For decision support modeling in this dissertation I used the Environmental Evaluation Modeling System (EEMS; Sheehan and Gough, 2016), a fuzzy logic modeling platform I developed, patterned after the Ecosystem Management Decision Support system (EMDS; Reynolds et al., 2015). Like EMDS, EEMS is designed to inform answers to management questions. I initially implemented EEMS as an alternative to EMDS in the ArcGIS (ESRI, 1999-2019) ModelBuilder environment to obviate EMDS's need for third party software. Since then, I have expanded EEMS to include a scripting interface for use outside of Arc ModelBuilder and that works with a variety of file types.

An EEMS model is structured as a bottom-up logic tree with leaf nodes iteratively combined into a single root node. The bottom-most nodes in the tree represent input data layers. Each input layer is first normalized (0 to 1 for this study) to produce a node representing its level of agreement with a user-defined statement. For example, a fuel load metric might be mapped to the statement *Simulated Live Biomass is High* using user-defined thresholds to characterize *High*.

Normalized values are combined into higher level nodes using fuzzy logic operators that evaluate the relationship between two or more datasets to another statement. For example, data for *Simulated Live Biomass is High* might be combined with data for *Vegetation Stress is High* to create a resulting node for *Mortality Risk is High.* In a complete model, nodes are repeatedly combined to produce a final, top-level node that informs the original management question.

Formally, each node in a fuzzy logic model corresponds to a factual statement, and the values for the node (the normalized values described above) are the values for the statement's *fuzzy truth value*. Fuzzy truth values range from 0 for *fully false* to 1 for *fully true*. Values between 0.0 and 0.5 are considered *partially false*, 0.5 is *neither true nor false*, and values between 0.5 and 1.0 are *partially true*. Informally, values in the nodes are considered as indices for the attribute associated with the factual statement. For example, a fuzzy value for *Vegetation Stress is High* might be referred to simply as a metric expressing *Vegetation Stress* on a scale from low (0) to high (1).

EEMS models allow decision makers to evaluate a landscape using a simple numerical scale. The model structure and data layers associated with model nodes help decision makers understand the drivers of the top-level metric and provide insights into which actions would help meet management goals. In Chapter 4, not only did I use EEMS to model biomass loss risk, but I expanded its functionality in order to express uncertainty in model results. I also used the data in layers below the top-level node to expose the drivers of biomass loss risk.

1.9 Other studies

Previous modeling studies in this region have used a number of approaches. Methods have included statistical methods such as random forests classification (e.g. Rehfeldt et al., 2006, 2012, 2014a), linear mixed effects models (e.g. Rehfeldt et al., 2014b), the relationship between bioclimatic variables and species (e.g. Shafer et al., 2001), process-based dynamic global vegetation models (DGVMs; e.g. Rogers et al., 2011), and hybrid approaches, such as combining process-based model results with statistical classification tree methods (e.g. Coops and Waring, 2011), with state and transition models (STMs; e.g. Creutzburg et al., 2014; Halofsky et al., 2014), and with a land use model (Turner et al., 2015). Overall these models project climate-related vegetation changes, increased fires, carbon losses, and increased beetle attacks (which MC2 does not simulate). Generally, these results are consistent with the findings in my

dissertation, potentially providing additional confidence in trends from a range of models. Differences, on the other hand, contribute to uncertainty that can be accounted for in planning, and that points to the need for model refinement. Detailed comparisons are presented in Chapters 2-4.

The next three chapters present my dissertation research and are followed by overall conclusions from the dissertation.

1.10 References

Abatzoglou, J. T., & Brown, T. J. (2012). A comparison of statistical downscaling methods suited for wildfire applications. *International Journal of Climatology*, 32(5), 772-780.

Abatzoglou, J. T., Rupp, D. E., & Mote, P. W. (2014). Seasonal climate variability and change in the Pacific Northwest of the United States. *Journal of Climate*, 27(5), 2125-2142.

Ahmed, K. F., Wang, G., Silander, J., Wilson, A. M., Allen, J. M., Horton, R., & Anyah, R. (2013). Statistical downscaling and bias correction of climate model outputs for climate change impact assessment in the US northeast. *Global and Planetary Change*, 100, 320-332.

Ainsworth, E. A., & Long, S. P. (2005). What have we learned from 15 years of free-air CO_2 enrichment (FACE)? A meta-analytic review of the responses of photosynthesis, canopy properties and plant production to rising CO2. *New Phytologist*, 165(2), 351-372.

Amthor, J. S. (1995). Terrestrial higher-plant response to increasing atmospheric CO_2 in relation to the global carbon cycle. *Global Change Biology*, 1(4), 243-274.

Aydi, A., Zairi, M., & Dhia, H. B. (2013). Minimization of environmental risk of landfill site using fuzzy logic, analytical hierarchy process, and weighted linear combination methodology in a geographic information system environment. *Environmental Earth Sciences*, 68(5), 1375-1389.

Bachelet, D., Ferschweiler, K., Sheehan, T. J., Sleeter, B. M., & Zhu, Z. (2015). Projected carbon stocks in the conterminous USA with land use and variable fire regimes. *Global Change Biology*, 21(12), 4548-4560.

Batllori, E., Ackerly, D. D., & Moritz, M. A. (2015). A minimal model of fire-vegetation feedbacks and disturbance stochasticity generates alternative stable states in grassland–shrubland–woodland systems. *Environmental Research Letters*, 10(3), 034018.

Bereiter, B., Eggleston, S., Schmitt, J., Nehrbass-Ahles, C., Stocker, T. F., Fischer, H., Kipfstuhl, S., & Chappellaz, J. (2015). Revision of the EPICA Dome C CO_2 record from 800 to 600 kyr before present. *Geophysical Research Letters*, 42(2), 542-549.

Boyd, J., & Banzhaf, S. (2007). What are ecosystem services? The need for standardized environmental accounting units. *Ecological Economics*, 63(2-3), 616-626.

Boyd, R. (1999). Strategies of Indian burning in the Willamette Valley. In Boyd, R. (Ed.), *Indians, Fire and the Land in the Pacific Northwest* (pp. 94-138). Oregon State University Press, Corvallis, OR, USA.

Brodribb, T. J., McAdam, S. A., Jordan, G. J., & Feild, T. S. (2009). Evolution of stomatal responsiveness to CO_2 and optimization of water-use efficiency among land plants. *New Phytologist*, 183(3), 839-847.

Camarero, J. J., Gazol, A., Galván, J. D., Sangüesa-Barreda, G., & Gutiérrez, E. (2015). Disparate effects of global-change drivers on mountain conifer forests: warming-induced growth enhancement in young trees vs. CO_2 fertilization in old trees from wet sites. *Global Change Biology*, 21(2), 738-749.

Canadian Forestry Service (1984). *Tables for the Canadian Forest Fire Weather Index System*. Forestry technical report 25, 4th ed. Environment Canada, Canadian Forest Service, Ottawa, ON, CA.

Chen, I. C., Hill, J. K., Ohlemüller, R., Roy, D. B., & Thomas, C. D. (2011). Rapid range shifts of species associated with high levels of climate warming. *Science*, 333(6045), 1024-1026.

Cheung, W. W., Pitcher, T. J., & Pauly, D. (2005). A fuzzy logic expert system to estimate intrinsic extinction vulnerabilities of marine fishes to fishing. *Biological Conservation*, 124(1), 97-111.

Cohen, J. D., Deeming, J. E. (1985). *The National Fire Danger Rating System: Basic Equations*. General technical report PSW-82. U. S. Department of Agriculture, Forest Service, Pacific Southwest Research Station, Berkeley, CA, USA.

Conklin, D. R., Lenihan, J. M., Bachelet, D., Neilson, R. P., Kim, J. B. (2015). *MCFire Model Technical Description*. Gen. Tech. Rep. PNW-GTR-904. U.S. Department of Agriculture, Forest Service, Pacific Northwest Research Station, Portland, OR, USA.

Coops, N. C., & Waring, R. H. (2011). Estimating the vulnerability of fifteen tree species under changing climate in Northwest North America. *Ecological Modelling*, 222(13), 2119-2129.

Costanza, R., d'Arge, R., de Groot, R., Farber, S., Grasso, M., Hannon, B., Limburg, K., Naeem, S., O'neill, R. V., Paruelo, J., & Raskin, R. G. (1997). The value of the world's ecosystem services and natural capital. *Nature*, 387, 253-260.

Cowan, I. R., & Farquhar, G. D. (1977). Stomatal function in relation to leaf metabolism and environment. *Symposia of the Society for Experimental Biology*, 31, 471-504.

Cramer, W., Bondeau, A., Woodward, F. I., Prentice, I. C., Betts, R. A., Brovkin, V., Cox, P. M., Fisher, V., Foley, J. A., Friend, A. D., & Kucharik, C. (2001). Global response of terrestrial ecosystem structure and function to CO_2 and climate change: results from six dynamic global vegetation models. *Global Change Biology*, 7(4), 357-373.

Creutzburg, M. K., Halofsky, J. E., Halofsky, J. S., & Christopher, T. A. (2014). Climate change and land management in the rangelands of central Oregon. *Environmental Management*, 55(1), 43-55.

Curry, J. A., & Webster, P. J. (2011). Climate science and the uncertainty monster. *Bulletin of the American Meteorological Society*, 92(12), 1667-1682.

Daily, G. C. (1997). *Nature's Services* (Vol. 19971). Island Press, Washington, DC.

de Groot, R. S., Wilson, M. A., & Boumans, R. M. (2002). A typology for the classification, description and valuation of ecosystem functions, goods and services. *Ecological Economics*, 41(3), 393-408.

Deal, R. L., Hennon, P. E., D'Amore, D. V., Davis, R. J., Smith, J. E., & Lowell, E. C. (2017). Ecosystem services with diverse forest landowners. In *People, Forests, and Change: Lessons from the Pacific Northwest* (pp. 191-206). Island Press, Washington, D.C., USA.

Dilling, L., & Lemos, M. C. (2011). Creating usable science: opportunities and constraints for climate knowledge use and their implications for science policy. *Global Environmental Change*, 21(2), 680-689.

Ehrlich, P., & Ehrlich, A. (1981). *Extinction: The Causes and Consequences of the Disappearance of Species*. Random House, New York, New York, USA.

ESRI (1999-2019). ArcMap (Computer Software). ESRI, Inc., Redlands, CA.

Fernández-Martínez, M., Vicca, S., Janssens, I. A., Ciais, P., Obersteiner, M., Bartrons, M., Sardans, J., Verger, A., Canadell, J. G., Chevallier, F. and Wang, X. (2017). Atmospheric deposition, CO_2, and change in the land carbon sink. *Scientific Reports*, 7(1), 9632.

Fisher, B., Turner, R. K., & Morling, P. (2009). Defining and classifying ecosystem services for decision making. *Ecological Economics*, 68(3), 643-653.

Fowler, D., Steadman, C. E., Stevenson, D., Coyle, M., Rees, R. M., Skiba, U. M., Sutton, M. A., Cape, J. N., Dore, A. J., Vieno, M., & Simpson, D. (2015). Effects of global change during the 21st century on the nitrogen cycle. *Atmospheric Chemistry and Physics*, 15(24), 13849-13893.

Fowler, H. J., Blenkinsop, S., & Tebaldi, C. (2007). Linking climate change modelling to impacts studies: recent advances in downscaling techniques for hydrological modelling. *International Journal of Climatology*, 27(12), 1547-1578.

Franklin, J. F., Spies, T. A., & Swanson, F. J. (2017) Setting the stage: vegetation, ecology, and dynamics. In *People, Forests, and Change: Lessons from the Pacific Northwest* (pp. 16-32). Island Press, Washington, D.C., USA.

Giles, R. (1976). Łukasiewicz logic and fuzzy set theory. *International Journal of Man-Machine Studies*, 8(3), 313-327.

Guerry, A. D., Polasky, S., Lubchenco, J., Chaplin-Kramer, R., Daily, G. C., Griffin, R., Ruckelshaus, M., Bateman, I. J., Duraiappah, A., Elmqvist, T., & Feldman, M. W.

(2015). Natural capital and ecosystem services informing decisions: From promise to practice. *Proceedings of the National Academy of Sciences*, 112(24), 7348-7355.

Halofsky, J. S., Halofsky, J. E., Burcsu, T., & Hemstrom, M. A. (2014). Dry forest resilience varies under simulated climate-management scenarios in a central Oregon, USA landscape. *Ecological Applications*, 24(8), 1908-1925.

Hantson, S., Arneth, A., Harrison, S. P., Kelley, D. I., Prentice, I. C., Rabin, S. S., Archibald, S., Mouillot, F., Arnold, S. R., Artaxo, P., & Bachelet, D. (2016). The status and challenge of global fire modelling. *Biogeosciences*, 13(11), 3359-3375.

Harmon, M. E., & Campbell, J. L. (2017). Managing carbon in the forest sector. In *People, Forests, and Change: Lessons from the Pacific Northwest* (pp. 161-173). Island Press, Washington, D.C., USA.

Harris, R., Remenyi, T. A., Williamson, G. J., Bindoff, N. L., & Bowman, D. M. (2016). Climate–vegetation–fire interactions and feedbacks: trivial detail or major barrier to projecting the future of the Earth system? *Wiley Interdisciplinary Reviews: Climate Change*, 7(6), 910-931.

Hendrey, G. R., Ellsworth, D. S., Lewin, K. F., & Nagy, J. (1999). A free-air enrichment system for exposing tall forest vegetation to elevated atmospheric CO_2. *Global Change Biology*, 5(3), 293-309.

IPCC (2014) *Climate Change 2014: Synthesis Report. Contribution of Working Groups I, II and III to the Fifth Assessment Report of the Intergovernmental Panel on Climate Change,* Core Writing Team, R.K. Pachauri and L.A. Meyer (eds.). IPCC, Geneva, Switzerland.

Kaplan, K. A., Montero-Serra, I., Vaca-Pita, E. L., Sullivan, P. J., Suárez, E., & Vinueza, L. (2014). Applying complementary species vulnerability assessments to improve conservation strategies in the Galapagos Marine Reserve. *Biodiversity and Conservation*, 23(6), 1509-1528.

Kasabov, N.K. (1996). *Foundations of Neural Networks, Fuzzy Systems, and Knowledge Engineering*. MIT Press, Cambridge, MA, and London, England.

Keane, R. E., McKenzie, D., Falk, D. A., Smithwick, E. A., Miller, C., & Kellogg, L. K. B. (2015). Representing climate, disturbance, and vegetation interactions in landscape models. *Ecological Modelling*, 309, 33-47.

Kerns, B. K., Powell, D. C., Mellmann-Brown, S., Carnwath, G., & Kim, J. B. (2018). Effects of projected climate change on vegetation in the Blue Mountains ecoregion, USA. *Climate Services*, 10, 33-43.

Kirchhoff, C. J., Lemos, M. C., & Dessai, S. (2013). Actionable knowledge for environmental decision making: broadening the usability of climate science. *Annual Review of Environment and Resources*, 38, 393-414.

Kitzberger, T., Perry, G. L. W., Paritsis, J., Gowda, J. H., Tepley, A. J., Holz, A., & Veblen, T. T. (2016). Fire–vegetation feedbacks and alternative states: common mechanisms of

temperate forest vulnerability to fire in southern South America and New Zealand. *New Zealand Journal of Botany*, 54(2), 247-272.

Knutti, R., & Sedláček, J. (2013). Robustness and uncertainties in the new CMIP5 climate model projections. *Nature Climate Change*, 3(4), 369-373.

Kuchler, A. W. (1975). *Potential Natural Vegetation of the Conterminous United States*, 2nd ed. American Geographical Society, New York, NY.

Kurz, W. A., Dymond, C. C., Stinson, G., Rampley, G. J., Neilson, E. T., Carroll, A. L., Ebata, T., & Safranyik, L. (2008). Mountain pine beetle and forest carbon feedback to climate change. *Nature*, 452(7190), 987-990.

Leenhouts, B. (1998). Assessment of biomass burning in the conterminous United States. *Conservation Ecology,* 2(1), 1-18. Available at: http://www.consecol.org/vol2/iss1/

Lenihan, J. M., Daly, C., Bachelet, D., & Neilson, R. P. (1998). Simulating broad-scale fire severity in a dynamic global vegetation model. *Northwest Science*, 72(4), 91-101.

Littell, J. S., McKenzie, D., Kerns, B. K., Cushman, S., & Shaw, C. G. (2011). Managing uncertainty in climate-driven ecological models to inform adaptation to climate change. *Ecosphere*, 2(9), 1-19.

Loehman, R. A., Bentz, B. J., DeNitto, G. A., Keane, R. E., Manning, M. E., Duncan, J. P., Egan, J. M., Jackson, M. B., Kegley, S., Lockman, I. B., & Pearson, D.E. (2018). Effects of climate change on ecological disturbance in the Northern Rockies. In *Climate Change and Rocky Mountain Ecosystems* (pp. 115-141). Springer, New York, NY, USA.

Lurgi, M., López, B. C., & Montoya, J. M. (2012). Novel communities from climate change. *Philosophical Transactions of the Royal Society of London B: Biological Sciences*, 367(1605), 2913-2922.

Lüthi, D., Le Floch, M., Bereiter, B., Blunier, T., Barnola, J.M., Siegenthaler, U., Raynaud, D., Jouzel, J., Fischer, H., Kawamura, K., & Stocker, T.F. (2008). High-resolution carbon dioxide concentration record 650,000–800,000 years before present. *Nature*, 453(7193), 379-382.

May, C., Luce, C., Casola, J., Chang, M., Cuhaciyan, J., Dalton, M. , Lowe, S., Morishima, G., Mote, P., Petersen, A., Roesch-McNally, G., & York, E. (2018). Northwest. In *Impacts, Risks, and Adaptation in the United States: Fourth National Climate Assessment, Volume II* (pp. 1036-1100). U.S. Global Change Research Program, Washington, DC, USA.

Meadow, A. M., Ferguson, D. B., Guido, Z., Horangic, A., Owen, G., & Wall, T. (2015). Moving toward the deliberate coproduction of climate science knowledge. *Weather, Climate, and Society*, 7(2), 179-191.

Millar, C. I., Stephenson, N. L., & Stephens, S. L. (2007). Climate change and forests of the future: managing in the face of uncertainty. *Ecological Applications*, 17(8), 2145-2151.

Millennium Ecosystem Assessment (2005). *Ecosystems and Human Well-being: Synthesis*. Island Press, Washington, DC, USA.

Mote, P. W., Parson, E. A., Hamlet, A. F., Keeton, W. S., Lettenmaier, D., Mantua, N., Miles, E. L., Peterson, D. W., Peterson, D. L., Slaughter, R., & Snover, A. K. (2003). Preparing for climatic change: the water, salmon, and forests of the Pacific Northwest. *Climatic Change*, 61(1), 45-88.

Norby, R. J., & Zak, D. R. (2011). Ecological lessons from free-air CO_2 enrichment (FACE) experiments. *Annual Review of Ecology, Evolution, and Systematics*, 42, 181-203.

Olson, D. E., Van Horne, B., Bormann, G. T., Anderson, P. D., & Haynes, R. W. (2017a). Introduction: the human-forest ecosystem. In *People, Forests, and Change: Lessons from the Pacific Northwest* (pp. 3-15). Island Press, Washington, D.C., USA.

Olson, D. H., Johnson, S. L., Anderson, P. D., Penaluna, B. E., & Dunham, J. B. (2017). Aquatic-riparian systems. In *People, Forests, and Change: Lessons from the Pacific Northwest* (pp. 191-206). Island Press, Washington, D.C., USA.

Olson, D. H., & van Horne, B., Eds. (2017). *People, Forests, and Change: Lessons from the Pacific Northwest.* Island Press, Washington, D.C., USA.

Omernik, J. M., & Griffith, G. E. (2014). Ecoregions of the conterminous United States: evolution of a hierarchical spatial framework. *Environmental Management*, 54(6), 1249-1266.

Peterman, W., Bachelet, D., Ferschweiler, K., & Sheehan, T. (2014). Soil depth affects simulated carbon and water in the MC2 dynamic global vegetation model. *Ecological Modelling*, 294, 84-93.

Rabin, S. S., Melton, J. R., Lasslop, G., Bachelet, D., Forrest, M., Hantson, S., Li, F., Mangeon, S., Yue, C., Arora, V. K., & Hickler, T. (2017). The Fire Modeling Intercomparison Project (FireMIP), phase 1: experimental and analytical protocols with detailed model descriptions. *Geoscientific Model Development*, 10(3), 1175.

Reeves, M. C., Manning, M. E., DiBenedetto, J. P., Palmquist, K. A., Lauenroth, W. K., Bradford, J. B., & Schlaepfer, D. R. (2018). Effects of climate change on rangeland vegetation in the Northern Rockies. In *Climate Change and Rocky Mountain Ecosystems* (pp. 97-114). Springer, New York, NY, USA,

Rehfeldt, G. E., Crookston, N. L., Sáenz-Romero, C., & Campbell, E. M. (2012). North American vegetation model for land-use planning in a changing climate: a solution to large classification problems. *Ecological Applications*, 22(1), 119-141.

Rehfeldt, G. E., Crookston, N. L., Warwell, M. V., & Evans, J. S. (2006). Empirical analyses of plant-climate relationships for the western United States. *International Journal of Plant Sciences*, 167(6), 1123-1150.

Rehfeldt, G. E., Ferguson, D. E., & Crookston, N. L. (2009). Aspen, climate, and sudden decline in western USA. *Forest Ecology and Management*, 258(11), 2353-2364.

Rehfeldt, G. E., Jaquish, B. C., López-Upton, J., Sáenz-Romero, C., St Clair, J. B., Leites, L. P., & Joyce, D. G. (2014). Comparative genetic responses to climate for the varieties of

Pinus ponderosa and *Pseudotsuga menziesii*: Realized climate niches. *Forest Ecology and Management*, 324, 126-137.

Rehfeldt, G. E., Leites, L. P., St Clair, J. B., Jaquish, B. C., Sáenz-Romero, C., López-Upton, J., & Joyce, D. G. (2014). Comparative genetic responses to climate in the varieties of *Pinus ponderosa* and *Pseudotsuga menziesii*: Clines in growth potential. *Forest Ecology and Management*, 324, 138-146.

Reyers, B., Nel, J. L., O'Farrell, P. J., Sitas, N., & Nel, D. C. (2015). Navigating complexity through knowledge coproduction: Mainstreaming ecosystem services into disaster risk reduction. *Proceedings of the National Academy of Sciences*, 112(24), 7362-7368.

Reynolds, K., Paplanus, S., Miller, B., & Murphy, P. (2014). Design features behind success of the ecosystem management decision support system and future development. *Forests*, 6(1), 27-46.

Rodríguez, E., Peche, R., Garbisu, C., Gorostiza, I., Epelde, L., Artetxe, U., Irizar, A., Soto, M., Becerril, J. M. and Etxebarria, J. (2016). Dynamic quality index for agricultural soils based on fuzzy logic. *Ecological Indicators*, 60, 678-692.

Rogers, B. M., Neilson, R. P., Drapek, R., Lenihan, J. M., Wells, J. R., Bachelet, D., & Law, B. E. (2011). Impacts of climate change on fire regimes and carbon stocks of the US Pacific Northwest. *Journal of Geophysical Research: Biogeosciences*, 116, G03037.

Rupp, D. E., Abatzoglou, J. T., Hegewisch, K. C., & Mote, P. W. (2013). Evaluation of CMIP5 20th century climate simulations for the Pacific Northwest USA. *Journal of Geophysical Research: Atmospheres*, 118(19), 10-884.

Seguí, X., Pujolasus, E., Betrò, S., Àgueda, A., Casal, J., Ocampo-Duque, W., Rudolph, I., Barra, R., Páez, M., Barón, E. and Eljarrat, E. (2013). Fuzzy model for risk assessment of persistent organic pollutants in aquatic ecosystems. *Environmental Pollution*, 178, 23-32.

Shafer, S. L., Bartlein, P. J., & Thompson, R. S. (2001). Potential changes in the distributions of western North America tree and shrub taxa under future climate scenarios. *Ecosystems*, 4(3), 200-215.

Sheehan, T., & Gough, M. (2016). A platform-independent fuzzy logic modeling framework for environmental decision support. *Ecological Informatics*, 34, 92-101.

Shinneman, D. J., & McIlroy, S. K. (2016). Identifying key climate and environmental factors affecting rates of post-fire big sagebrush (Artemisia tridentata) recovery in the northern Columbia Basin, USA. *International Journal of Wildland Fire*, 25(9), 933-945.

Sillmann, J., Kharin, V. V., Zwiers, F. W., Zhang, X., & Bronaugh, D. (2013). Climate extremes indices in the CMIP5 multimodel ensemble: Part 2. Future climate projections. *Journal of Geophysical Research: Atmospheres*, 118(6), 2473-2493.

Sommers, W. T., Coloff, S. G., & Conard, S. G. (2011). *Fire History and Climate Change*. Joint Fire Science Program project report 09-2-01-09.

Sullivan, A. L. (2009a). Wildland surface fire spread modelling, 1990–2007. 1: Physical and quasi-physical models. *International Journal of Wildland Fire*, 18(4), 349-368.

Sullivan, A. L. (2009b). Wildland surface fire spread modelling, 1990–2007. 2: Empirical and quasi-empirical models. *International Journal of Wildland Fire*, 18(4), 369-386.

Sullivan, A. L. (2009c). Wildland surface fire spread modelling, 1990–2007. 3: Simulation and mathematical analogue models. *International Journal of Wildland Fire*, 18(4), 387-403.

Taylor, K. E., Stouffer, R. J., & Meehl, G. A. (2012). An overview of CMIP5 and the experiment design. *Bulletin of the American Meteorological Society*, 93(4), 485-498.

Turner, D. P., Conklin, D. R., & Bolte, J. P. (2015). Projected climate change impacts on forest land cover and land use over the Willamette River Basin, Oregon, USA. *Climatic Change*, 133(2), 335-348.

Van Der Sleen, P., Groenendijk, P., Vlam, M., Anten, N. P., Boom, A., Bongers, F., Pons, T. L., Terburg, G., & Zuidema, P. A. (2015). No growth stimulation of tropical trees by 150 years of CO_2 fertilization but water-use efficiency increased. *Nature Geoscience*, 8(1), 24-28.

Van Vuuren, D. P., Edmonds, J., Kainuma, M., Riahi, K., Thomson, A., Hibbard, K., Hurtt, G. C., Kram, T., Krey, V., Lamarque, J. F., & Masui, T. (2011). The representative concentration pathways: an overview. *Climatic Change*, 109(1-2), 5-31.

Van Wagner, C. E. (1987). *Development and Structure of the Canadian Forest Fire Weather Index System*. Technical report 35. Petawawa National Forestry Institute, Canadian Forest Service, Chalk River, Ontario, CA.

Way, D. A., Oren, R., & Kroner, Y. (2015). The space-time continuum: the effects of elevated CO_2 and temperature on trees and the importance of scaling. *Plant, Cell & Environment*, 38(6), 991-1007.

Westerling, A. L., Hidalgo, H. G., Cayan, D. R., & Swetnam, T. W. (2006). Warming and earlier spring increase western US forest wildfire activity. *Science*, 313(5789), 940-943.

Whitlock, C., & Knox, M. A. (2002). Prehistoric burning in the Pacific Northwest. In *Fire, Native Peoples, and the Natural Landscape* (pp. 195-231). Island Press, Washington, D.C., USA.

Williams, B. K. (2011). Adaptive management of natural resources—framework and issues. *Journal of Environmental Management*, 92(5), 1346-1353.

Williams, J. W., & Jackson, S. T. (2007). Novel climates, no-analog communities, and ecological surprises. *Frontiers in Ecology and the Environment*, 5(9), 475-482.

Wilson, B. T., Woodall, C. W., & Griffith, D. M. (2013). Imputing forest carbon stock estimates from inventory plots to a nationally continuous coverage. *Carbon Balance and Management*, 8(1), 1.

Wood, A. W., Maurer, E. P., Kumar, A., & Lettenmaier, D. P. (2002). Long-range experimental hydrologic forecasting for the eastern United States. *Journal of Geophysical Research: Atmospheres*, 107(D20), ACL-6.

Xu, Z., Jiang, Y., Jia, B., & Zhou, G. (2016). Elevated-CO_2 response of stomata and its dependence on environmental factors. *Frontiers in Plant Science*, 7, 657.

Zadeh, L. A. (1973). Outline of a new approach to the analysis of complex systems and decision processes. *IEEE Transactions on Systems, Man, and Cybernetics*, 1, 28-44.

PROJECTED MAJOR FIRE AND VEGETATION CHANGES IN THE PACIFIC NORTHWEST OF THE CONTERMINOUS UNITED STATES UNDER SELECTED CMIP5 CLIMATE FUTURES

Timothy J. Sheehan, Dominique Bachelet, and Ken Ferschweiler

Ecological Modeling
Elsevier B.V.
Radarweg 29
Amsterdam, 1043 NX
Issue 317 (2015)

2.1 Abstract

Climate change adaptation and mitigation require understanding of vegetation response to climate change. Using the MC2 dynamic global vegetation model (DGVM) we simulate vegetation for the Northwest United States using results from 20 different Climate Model Intercomparison Project Phase 5 (CMIP5) models downscaled using the MACA algorithm. Results were generated for representative concentration pathways (RCP) 4.5 and 8.5 under vegetation modeling scenarios with and without fire suppression for a total of 80 model runs for future projections. For analysis, results were aggregated by three subregions: the western Northwest (WNW), from the crest of the Cascade Mountains west; Northwest plains and plateau (NWPP), the non-mountainous areas east of the Cascade Mountains; and eastern Northwest mountains (ENWM), the mountainous areas east of the Cascade Mountains. In the WNW, mean fire interval (MFI) averaged over all climate projections decreases by up to 48%, and potential vegetation shifts from conifer to mixed forest under RCP 4.5 and 8.5 with and without fire suppression. In the NWPP MFI averaged over all climate projections decreases by up to 82% without fire suppression and increases by up to 14% with fire suppression resulting in woodier vegetation cover. In the ENWM, MFI averaged across all climate projections decreases by up to 81%, subalpine communities are lost, but conifer forests continue to dominate the subregion in the future.

2.2 Introduction

Effects of warming climate have already been observed in the Pacific Northwest (PNW; e.g. Cayan et al. 2001; Mote et al. 2005), and projections indicate further warming throughout the 21st century (e.g. Mote and Salathé 2010). In some areas, impacts of climate change may lead to widespread ecological disruption (Rehfeldt et al. 2006). Regional efforts towards climate change adaptation and mitigation require some understanding of the vegetation response to climate change (Chmura et al. 2011) and must take into account variation in projected future conditions (Millar et al. 2007).

In this context, a variety of regional studies within or including the Pacific Northwest (PNW) have examined potential climate-driven changes in the distribution of vegetation cover types and species (e.g. Rehfeldt et al. 2006; Littell et al. 2010; Rogers et al. 2011; Coops et al.

2011; Creutzburg et al. 2015; Rehfeldt et al. 2014a,b,c). Other studies have focused on the potential effects of PNW regional climate change on fire regime (Whitlock et al. 2003), insect population dynamics (Bentz et al. 2010), and forest productivity (Latta et al. 2009).

Modeling approaches have included process-based dynamic global vegetation models (DGVMs; e.g. Rogers et al. 2011), statistical methods such as random forests classification (e.g. Rehfeldt et al. 2006; Rehfeldt et al. 2012; Rehfeldt et al. 2014a), linear mixed effects models (e.g. Rehfeldt et al. 2014b), the relationship between bioclimatic variables and species (e.g. Shafer et al. 2001), and hybrid approaches, such as combining process-based model results with statistical classification tree methods (e.g. Coops and Waring 2011) or with state and transition models (STMs; e.g. Creutzburg et al. 2014; Halofsky et al. 2014).

The *Integrated Scenarios of Climate, Hydrology and Vegetation* project (http://bit.ly/104rQiB) was a collaboration between the Northwest Climate Science Center, the University of Idaho, Conservation Biology Institute, and the University of Washington. The goal was to model future changes in climate, hydrology, and vegetation over the western United States from the coast to the Great Plains. Results from the Climate Model Intercomparison Project Phase 5 (CMIP5, http://cmip-pcmdi.llnl.gov/cmip5/) were evaluated for their ability to simulate the climate of the Northwest. The most relevant models (Vano et al. 2015) were downscaled to finer grids and used in regional hydrologic and vegetation models.

This paper presents the regional results from the vegetation modeling efforts using the downscaled CMIP5 projections in the Pacific Northwest and provides an example of the insights produced through the use of a process-based vegetation model with a large number of the most recent global climate projections. Our results suggest that fire plays a major role in shaping climate change influence on vegetation.

2.3 Methods

2.3.1 Study area

For this paper we focused on the Pacific Northwest region of the conterminous United States (north of 42 degrees latitude and west of -111 degrees longitude). Based on topographic and climatological characteristics, we defined three subregions (Fig. 2.1, Table 2.1) derived from the full and partial EPA Level III Ecoregions (Omernik and Griffith 2014) within the study area (Table 2.1). The western Northwest (WNW) subregion comprises the area west of the crest of

the Cascade Mountains and represents 21% of the study area. It includes the Coast Range, Klamath Mountains/California High North Coast Range, Willamette Valley, Puget Lowlands, Cascades, and North Cascades Level III Ecoregions. This subregion falls under strong coastal climatological influence with warmer minimum temperatures and much greater precipitation than the other two subregions. The Northwest Plains and Plateau (NWPP) subregion comprises 38% of the area and includes the Eastern Cascades Slopes and Foothills, Northern Basin and Range, Columbia Plateau, Snake River Plain, Northwest Great Plains, and Northwest Glaciated Plains Level III ecoregions. This subregion is lower in elevation than the Cascades and other Northwest mountain ranges. It is drier than the other two subregions and experiences higher maximum temperatures. The remaining 41% of the area is covered by the Eastern Northwest Mountains (ENWM) comprising the mountainous regions east of the Cascades. This subregion includes the Wasatch and Uinta Mountains, Wyoming Basin, Blue Mountains, Idaho Batholith, Middle Rockies, Northern Rockies, and Canadian Rockies Level III Ecoregions. It is the coldest of the subregions and has precipitation amounts intermediate to those of the other two.

Table 2.1: PNW subregion characteristics. Climate variables are derived from PRISM data and averaged over the historical baseline period (1971-2000).

Region	Area (km^2)	Mean min. monthly temp (°C)	Mean max monthly temp (°C)	Annual precip (mm)	Annual summer precip (mm)	Level III ecoregions
Full study area	784,358	0.56	13.26	842	95.76	
Western Northwest (WNW)	162,620	3.66	13.97	1841	139.95	Coast Range, Klamath Mountains/California High North Coast Range, Willamette Valley, Puget Lowlands, Cascades, North Cascades
Northwest Plains and Plateau (NWPP)	300,393	0.95	14.93	382	55.26	Eastern Cascades Slopes and Foothills, Northern Basin and Range, Columbia Plateau, Snake River Plain, Northwest Great Plains, Northwest Glaciated Plains
Eastern Northwest Mountains (ENWM)	321,345	-0.75	12.43	643	109.8	Wasatch and Uinta Mountains, Wyoming Basin, Blue Mountains, Idaho Batholith, Middle Rockies, Northern Rockies, Canadian Rockies

(min: minimum; max: maximum; precip: precipitation)

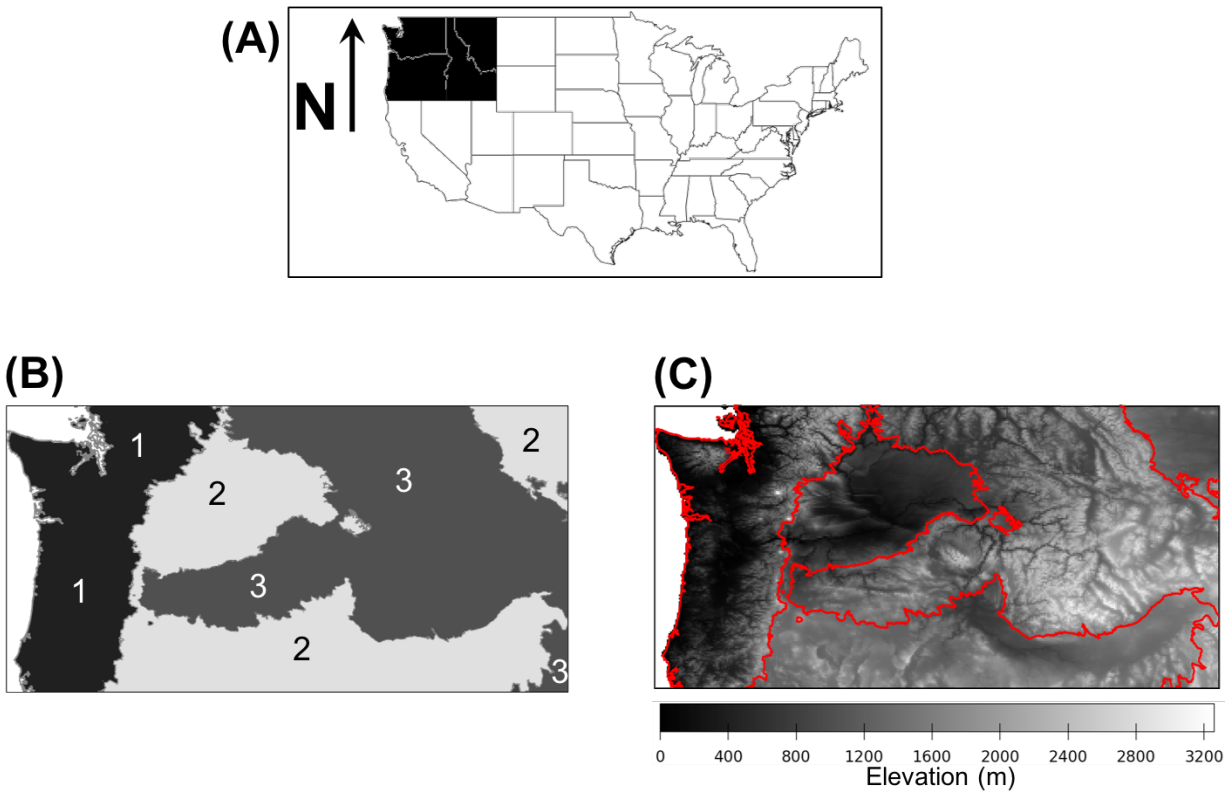

Fig. 2.1: Study area. (A) Index map of study area within the contiguous United States; (B) subregions defined for this study: 1. western Northwest (WNW); 2. Northwest plains and plateau (NWPP); and 3. eastern Northwest mountains (ENWM); and (C) elevation in meters.

2.3.2 Model Description

We used MC2, the C++ version of the MC1 dynamic global vegetation model (DGVM; Bachelet et al. 2015). While the code structure of MC2 was modified from MC1 for purposes of performance improvement and run option specification, it uses the same algorithms as MC1 and was designed to be functionally equivalent. MC1 and MC2 have been widely used at global to regional scales to simulate potential vegetation shifts, carbon (C) fluxes, and wildfires in national parks (e.g. King et al. 2013), individual states (Lenihan et al. 2008), across the conterminous United States (Bachelet et al. 2001), North America (Drapek et al. 2015), as well as globally (Gonzalez et al. 2010) for a variety of climate change scenarios. The model is run at a monthly time step on a spatial grid in which each cell is simulated independently, with no cell-to-cell communication. The model can be used to simulate land use (Bachelet et al. 2015), but for this project, we simulated the potential vegetation that would occur without direct human

intervention. However, fire suppression and the influence of increasing atmospheric CO_2 concentrations due to anthropogenic emissions were explored in this study. The model includes three modules that simulate biogeography, biogeochemistry, and wildfire interactions.

The biogeography module simulates shifts in vegetation types based on climate and biomass thresholds. The model does not simulate individual species. Woody functional types (trees and shrubs) are distinguished by leaf phenology (evergreen vs. deciduous) and morphology (needleleaf vs. broadleaf). The module uses environmental gradients of minimum monthly temperature and growing season precipitation to simulate the relative dominance of woody lifeforms. The relative dominance of C3 versus C4 grasses (including forbs, sedges, and other herbaceous vegetation) is simulated by calculating the potential production of pure C3 and pure C4 stands using soil temperature. Thresholds of carbon pool values are used to distinguish between forest, savanna, shrubland, and grassland classes. There are 36 vegetation types possible, 14 of these within the temperate zone.

The model always simulates competition for light, water and nutrients between herbaceous and woody vegetation. The biogeochemistry module is a modified version of the CENTURY model (Metherell et al. 1993) that simulates carbon and nitrogen cycles, including net primary production (plant growth) and net biological production (ecosystem carbon balance), decomposition, and soil respiration. The model simulates the allocation of carbon and nitrogen among plant parts, multiple classes of litter, and three soil organic matter pools. Woody life form and herbaceous production is limited by temperature, soil water availability, soil nitrogen, and atmospheric CO_2 (Bachelet et al. 2015). Decomposition is affected by substrate quality, soil texture and moisture, and temperature. The model also simulates actual and potential evapotranspiration (AET and PET), and soil water content in multiple soil layers. Grass and woody vegetation leaf moisture contents are calculated as functions of the ratio of available soil water to PET, and are interpreted as live fuel moisture contents affecting fire behavior.

The fire module (Lenihan et al. 1998; Conklin et al. 2015) simulates fire occurrence, area burned, and fire impacts including mortality, consumption of aboveground biomass, and nitrogen volatilization. Mortality and consumption of overstory biomass are simulated as a function of fire behavior and the canopy vertical structure. Fire occurrence is simulated as a discrete event. The module runs on a daily time step by using a randomly distributed set of daily precipitation values

derived from monthly precipitation values. To estimate fuel characteristics, the module calculates the Keetch-Byram drought index (Keetch and Byram 1968) using carbon pool values, daily precipitation, temperature, wind, potential evapotranspiration, relative humidity, and snowfall. Daily estimates for fine fuel moisture content (FFMC, Van Wagner 1987), buildup index (BUI, Canadian Forestry Service 1984), and energy release component (ERC, Cohen and Deeming 1985) are also calculated. An ignition source is always assumed and a fire is simulated the first time the daily FFMC and BUI values exceed respective thresholds for current vegetation type and the fuel load is sufficiently dense to carry a fire. The model does not support more than one fire per year in a grid cell.

To reflect a realistic geographic extent of a fire under assumed ignitions, the fire module limits the area burned with an algorithm based on fire return interval (FRI) and years since last fire. In the fire module each vegetation type is assigned both a maximum and minimum FRI (Leenhouts 1998). At each time step each grid cell's FRI is calculated starting with the maximum value for its vegetation type and adjusted as a function of BUI if the cell contains less than 70% fine fuels, or of FFMC if it contains 70% or more fine fuels. A higher BUI or FFMC reduces the FRI until it reaches the minimum FRI for that vegetation type. The maximum fraction of area burned is calculated as follows:

$$f = y/F \quad (1)$$

where f is the maximum fraction of area burned, y is the number of years since the last fire, and F is the fire return interval associated with the vegetation type and the severity of fuel conditions. For example, if a cell with an FRI of one hundred years had a fire five years previous, the maximum fraction of the area that could burn would be 0.05, or 5%.

The fire module includes a fire suppression option (Rogers et al. 2011) that limits the area burned to 0.06% of the cell unless the fire exceeds either an ERC of 60 or a 3.1 MW m^{-1} fireline intensity and a spread rate of 0.51 m s^{-1}. In that case, the full fire algorithm is used.

2.3.3 Model Calibration

In vegetation modeling, it is common practice to adjust model parameters to obtain the best match possible between results using historical input data and reference datasets (benchmarks). For this study, we calibrated MC2 for the conterminous United States (CONUS;

Bachelet et al. 2015) using Kuchler's (1975) potential vegetation map, Leenhouts' (1998) potential fire return intervals matched to Kuchler's vegetation types, and the National Biomass and Carbon Dataset (NBCD; Kellndorfer et al. 2012). Based on expert opinion, we assigned a weighted difference from 0 (full match) through 3 (full mismatch) between all possible pairs of MC2/Kuchler vegetation types. Using visual comparisons of potential vegetation departure, above ground carbon differences, and fire occurrence differences, we iteratively adjusted biogeographic parameters for vegetation type classification and BUI and FFMC thresholds for ignitions. The final parameterization produced a 47% full match (weighted difference of 0) and a 33% minimal mismatch (weighted difference of 1) between the MC2 results and Kuchler's (1975) potential vegetation, a normalized root mean square error of 0.35 for MC2 mean fire interval (MFI) versus Leenhout's (1998) FRI, and a normalized root mean square error of 0.11 versus the NBCD 2000 aboveground carbon dataset.

2.3.4 Run Protocol

MC2 is run in three phases. In the first phase, initialization, the static biogeography model, MAPSS (Neilson 1995) generates a map of potential vegetation distribution for the average climate between 1895 and 1924. This map is used by the biogeochemistry module to calculate initial values for carbon and nitrogen pools associated with each vegetation type with their prescribed fire return intervals. The initialization phase ends when the resistant soil carbon pool size changes by less than 1% from one year to the next. Its duration varies across the map from a few decades for grasslands up to 3000 years for temperate rainforests. Spinup, the second phase, is run iteratively using detrended historical climate from 1895 to 1924 to allow for readjustments of vegetation type and carbon pool sizes in response to interannual variability and simulated wildfires. The spinup phase ends when the net biological production (net ecosystem production minus carbon consumed by wildfire) reaches a value near zero. In the third, transient phase, the model is run with time series of historical and future climate.

2.3.5 Model Runs

For the historical period (1895 to 2010) and each of the 40 climate futures (2011 to 2100), we ran the model once with fire suppression (FS) and once with no fire suppression (NFS). For the historical fire suppression run, fire suppression is not started until 1950 to reflect

the realistic historical start of effective forest fire suppression in the United States (Pyne 1982; Dombeck 2001; Veblen et al. 2003). All runs used a 1/24 degree (~4 km) grid. The soils input dataset was originally provided by Jeff Kern for the VEMAP project (Kern 1994, 1995, 2000), and was rescaled to match the climate grid. It includes bulk density and depth to bedrock, as well as sand, clay and rock fragment content at three depths. Climate inputs for the historical data were upscaled to the 1/24 degree grid by taking the mean of 1/120 degree (~800 meter) PRISM (Daly et al. 2008) grid cells. Projected minimum and maximum temperature, precipitation, and mean dewpoint temperature were downscaled from 40 climate futures from 20 climate models (Table 2.2) run for representative concentration pathways (RCP) 4.5 and 8.5. Future climate was downscaled using the MACA algorithm (Abatzoglou and Brown 2012), which includes steps for bias correction, epoch adjustment, and constructed analogs. All told, we executed 2 historical (FS and NFS) and 80 future runs (RCP 4.5/RCP 8.5 x FS/NFS x 20 climate models).

2.3.6 Analyses

We summarized climate data and vegetation results over three thirty-year periods, late 20th century (1971-2000), mid 21st century (2036-2065), and late 21st century (2071-2100). Fire results were summarized over the entire 20th and 21st centuries (1901-2000 and 2001-2100, respectively). For future projections, results were summarized by RCP/fire suppression scenario (4 separate summaries: RCP 4.5/RCP 8.5 x FS/NFS). Unless otherwise noted, for continuous output variables, summary results for future runs were produced by taking the mean over time, followed by the mean over the study area for each of the climate futures, and finally by taking the ensemble mean (mean over all climate futures) for each RCP/fire suppression scenario pair. For categorical data, we used the mode instead of the mean. Several of the climate futures used as inputs to the MC2 model runs provided data only through 2099. Ensemble results for the year 2100 were calculated considering only models for which there were data.

Table 2.2. Climate models whose results were used as inputs to MC2 for this study.

#	GCM or ESM	Origin	Atmos res (degree lat x lon x vertical levels)
1	BCC-CSM1-1	Beijing Climate Center, China Meteorological Administration	2.8 x 2.8 x L26
2	BCC-CSM1-1-M	Beijing Climate Center, China Meteorological Administration	1.12 x 1.12 x L26
3	BNU-ESM	College of global change and earth system science, Beijing Normal University, China	2.8 x 1.4 x L26
4	CanESM2	Canadian Center for Climate Modelling and Analysis (Canada)	2.8 x 2.8 x L35
5	CCSM4	NCAR (USA)	1.25 x 0.94 x L26
6	CNRM-CM5	Meteo France and CNRS (France)	1.4 x 1.4 x L31
7	CSIRO-MK3-6.0	Commonwealth Scientific and Industrial Research Organization, Queensland Climate Change Center of Excellence (Australia)	1.8 x 1.8 x L18
8	GFDL-ESM2G	NOAA/GFDL (USA)	2.5 x 2.0 x L48
9	GFDL-ESM2M	NOAA/GFDL (USA)	2.5 x 2.0 x L48
10	HadGEM2-CC	Meteorological Office Hadley Center, UK	1.88 x 1.25 x L60
11	HadGEM2-ES	Meteorological Office Hadley Center, UK	1.88 x 1.25 x L38
12	INM-CM4	Institute for Numerical Mathematics (Russia)	2.0 x 1.5 x L21
13	IPSL-CM5A-LR	Institut Pierre Simon Laplace (France)	3.75 x 1.8 x L39
14	IPSL-CM5A-MR	Institut Pierre Simon Laplace (France)	2.5 x 1.25 x L39
15	IPSL-CM5B-LR	Institut Pierre Simon Laplace (France)	3.75 x 1.8 x L39
16	MIROC5	Atmosphere and Ocean Research Institute (U. Tokyo), National Institute for Environmental Studies, Japan Agency for Marine-Earth Science and Technology (Japan)	1.4 x 1.4 x L40
17	MIROC-ESM	Atmosphere and Ocean Research Institute (U. Tokyo), National Institute for Environmental Studies, Japan Agency for Marine-Earth Science and Technology (Japan)	2.8 x 2.8 x L80
18	MIROC-ESM-CHEM	Atmosphere and Ocean Research Institute (U. Tokyo), National Institute for Environmental Studies, Japan Agency for Marine-Earth Science and Technology (Japan)	2.8 x 2.8 x L80
19	MRI-CGCM3	Meteorological Research Institute (Japan)	1.1 x 1.1 x L48
20	NorESM1-M	Norwegian Climate Center	2.5 x 1.9 x L26

(GCM: global climate model; ESM: earth system model; Atmos: atmospheric; res: resolution; lat: latitude; lon: longitude)

Climate data are summarized by subregion, and monthly precipitation is displayed by subregion. We calculated the average number of years between fires for each grid cell and called it mean fire interval (MFI) to distinguish between MC2's fire intervals and Leenhouts' FRI values used as boundaries in the fire model. At the subregional level, we calculated the maximum annual area burned and the mean annual area burned, both in terms of actual area and percent of total area. MC2 vegetation types were aggregated into broad vegetation classes to simplify the results (Table 2.3).

Table 2.3. MC2 vegetation types comprising this study's vegetation classes.

Vegetation Class	MC2 Vegetation Types
Tundra	Tundra
Conifer Forest	Subalpine, Maritime Evergreen Needleleaf Forest, Temperate Evergreen Needleleaf Forest, Cool Needleleaf Forest
Cool Mixed Forest	Temperate Cool Mixed Forest
Decidous Forest	Temperate Deciduous Broadleaf Forest
Warm Mixed Forest	Temperate Warm Mixed Forest, Subtropical Mixed Forest
Woodland/Savanna	Temperate Deciduous Broadleaf Woodland, Temperate Cool Mixed Woodland, Temperate Warm Mixed Woodland, Subtropical Evergreen Broadleaf Woodland, Subtropical Mixed Woodland
Shrubland/Woodland	Temperate Evergreen Needleleaf Woodland, Temperate Shrubland, Subtropical Shrubland
Grassland	Temperate Grassland, Subtropical Grassland

2.4 Projected Climate Change

For all three regions, all climate projections show rising minimum and maximum monthly temperatures (Tmin and Tmax, respectively) compared to the historical baseline period (1971-2000) with ensemble mean changes ranging from 2.18°C for mid-century average Tmin under the RCP 4.5 scenario for WNW to 5.87°C for late century average Tmin under RCP 8.5 for ENWM (Table 2.4). Standard deviations for temperature change range from 0.54°C (Tmin, WNW, RCP 4.5 early century) to 1.19°C (Tmin and Tmax, ENWM, RCP 8.5, late century). Temperatures rise more under RCP 8.5 than under RCP 4.5. Rising temperatures are consistent across the 21st century under RCP 8.5 while under RCP 4.5 the rate of rising slows over the later part of the century.

The change in mean annual precipitation from the late 20th century baseline is generally positive, but varies across projections (Table 2.4). Standard deviations range from 3.1% (Full

Study Area, RCP 4.5, early century) to 7.5% (NWPP, RCP 8.5, late century). Ensemble means indicate increases for all subregion / RCP / time period combinations ranging from 0.12% (Full Area, RCP 4.5, early century) to 13.18% (NWPP, RCP 8.5, late century). Increases are generally largest for RCP 8.5 late century.

The change in mean summer precipitation from late 20th century is generally small but varies greatly across projections (Table 2.4). Standard deviations range from 8.7% (Full Study Area, RCP 8.5, early century) to 21.0% (NWPP, RCP 8.5, late century). Ensemble means indicate decreases for all subregion / RCP / time period combinations ranging from 33.14% (WNW, RCP 8.5, late century) to 13.82% (ENWM, RCP 4.5, early century). Increases are generally greatest for RCP 8.5 late century. Among all climate futures and subregions, changes ranged from -55.5% (WNW, RCP 8.5, early century) to 45.0% (NWPP, RCP 8.5, late century).

Compared to the late 20th century, summer precipitation is lower under the RCP 4.5 and 8.5 scenarios for the mid- and late 21st century, but for all climate futures the duration of the dry period is not longer (Fig. 2.2). During the rest of the year, especially fall (October, November, December) and spring months (March, April, and May) precipitation generally increases (Fig. 2.2).

Table 2.4. Changes in annual means of climate variables between historical (1971-200) and future periods by subregion and representative concentration pathway (RCP). Ensemble means, minimums, maxiums, and standard deviations were taken across results of runs produced using all climate futures.

	RCP 4.5								RCP 8.5							
	2036-2065				2071-2100				2036-2065				2071-2100			
	Min	Max	Ens. Mean	SD	Min	Max	Ens. Mean	SD	Min	Max	Ens. Mean	SD	Min	Max	Ens. Mean	SD
Full NW																
Tmin (°C)	1.38	3.62	2.59	0.61	1.78	4.66	3.32	0.82	1.79	4.31	3.23	0.71	3.55	7.21	5.51	1.15
Tmax (°C)	1.29	3.49	2.55	0.61	1.80	4.64	3.34	0.83	1.73	4.10	3.17	0.72	3.51	7.23	5.55	1.13
Ann ppt (% chg)	-2.13	8.25	1.76	3.11	-4.61	8.98	3.39	3.84	-5.74	7.84	2.22	3.76	0.54	18.22	8.46	4.66
Sum ppt (% chg)	-38.97	-1.10	-17.63	8.91	-42.66	-4.83	-18.47	9.62	-36.02	-4.73	-20.36	8.70	-48.30	15.35	-21.81	13.93
WNW																
Tmin (°C)	1.01	2.91	2.18	0.54	1.39	3.84	2.86	0.72	1.55	3.70	2.74	0.66	2.89	6.14	4.76	1.07
Tmax (°C)	1.05	2.94	2.21	0.54	1.66	4.10	2.93	0.70	1.56	3.68	2.77	0.64	3.09	6.24	4.84	1.01
Ann ppt (% chg)	-8.14	6.60	0.12	3.69	-4.55	7.01	1.17	3.38	-9.44	8.14	0.34	4.09	-3.00	11.53	4.77	3.80
Sum ppt (% chg)	-38.34	-0.75	-25.14	10.08	-43.84	-4.90	-24.66	10.44	-55.45	-14.67	-27.90	11.50	-50.76	-14.97	-33.14	10.57
NWPP																
Tmin (°C)	1.33	3.64	2.59	0.63	1.74	4.74	3.33	0.84	1.72	4.23	3.24	0.73	3.53	7.34	5.57	1.18
Tmax (°C)	1.34	3.69	2.61	0.65	1.92	4.92	3.43	0.88	1.73	4.28	3.25	0.75	3.61	7.65	5.71	1.17
Ann ppt (% chg)	-2.61	11.30	3.67	3.63	-3.35	13.78	5.88	5.54	-5.23	12.85	4.61	4.27	1.83	27.91	13.18	7.52
Sum ppt (% chg)	-40.81	9.81	-14.54	11.09	-47.50	6.30	-15.32	12.60	-30.23	0.53	-17.46	8.82	-49.85	45.02	-14.50	20.99
ENWM																
Tmin (°C)	1.58	3.98	2.81	0.66	2.03	5.05	3.57	0.87	2.00	4.71	3.50	0.75	3.75	7.67	5.87	1.19
Tmax (°C)	1.36	3.61	2.68	0.64	1.78	4.87	3.48	0.88	1.81	4.27	3.32	0.76	3.61	7.51	5.78	1.19
Ann ppt (% chg)	-2.08	10.84	3.29	4.07	-5.42	12.24	5.44	4.89	-4.49	11.80	3.86	4.34	2.63	24.88	11.43	6.33
Sum ppt (% chg)	-39.87	10.41	-13.82	10.46	-42.70	8.58	-15.61	11.52	-28.96	6.09	-16.45	10.52	-45.83	37.44	-17.34	18.08

(RCP: representative concentration pathway; NW: Northwest; WNW: western Northwest; NWPP: Northwest plains and plateau; ENWM: eastern Northwest mountains; Tmin: minimum monthly temperature; Tmax: maximum monthly temperature; Ann ppt: full year precipitation; Sum ppt: precipitation total for July-September; Min: minimum from the climate futures; Max: maximum from the climate futures; Ens Mean: mean over climate futures; SD standard deviation over climate futures.)

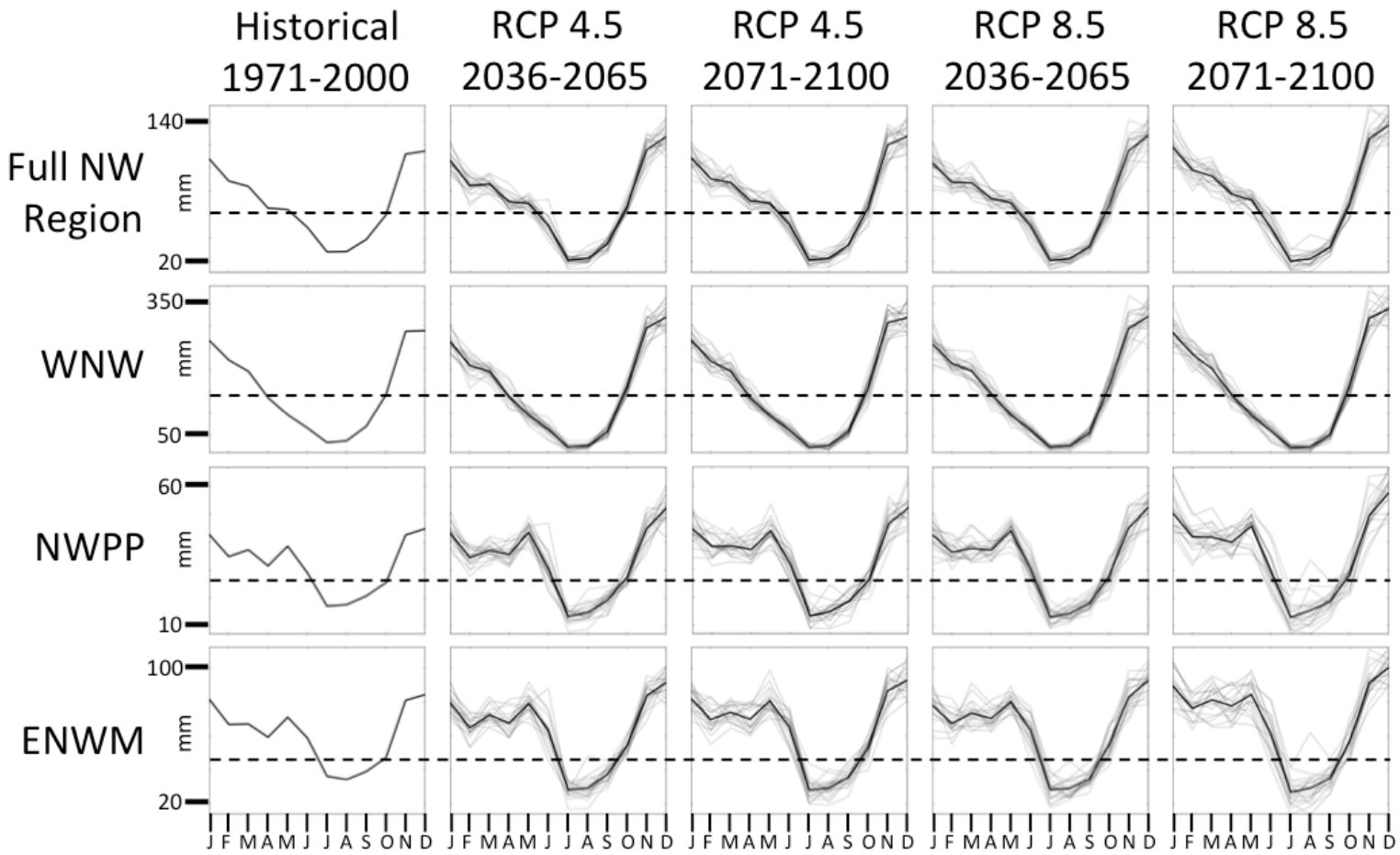

Fig. 2.2. Monthly precipitation by subregion, period, and representative concentration pathway (RCP). Heavy black line is ensemble mean over all climate futures, light grey lines are individual climate futures (WNW: western Northwest; NWPP: Northwest plains and plateau; ENWM: eastern Northwest mountains).

2.5 Subregional results

2.5.1 WNW

In the 21st century, the WNW subregion has a lower ensemble MFI, (Table 2.5), a higher ensemble annual percent area burned (PAB; Table 2.6), and a higher ensemble maximum annual PAB than in the 20th century across all emissions and fire suppression scenarios. Compared to results under the RCP 4.5 scenario, results under RCP 8.5 show a lower MFI, larger mean annual PAB, and slightly larger maximum annual PAB. Fire suppression shows a higher MFI, lower mean PAB, and slightly lower maximum annual PAB compared to no fire suppression. During the 20th century, maximum PAB exceeds 5% one time and reaches a maximum of 10% (Fig. 2.3 B) while during the 21st century, the ensemble mean for maximum annual PAB ranges from 13.45% (RCP 4.5 FS) to 16.96% (RCP 8.5 NFS). Results from individual future simulations range as high as 30% and encompass the 20th century results for maximum annual PAB (Fig. 2.3 B). All 21st century results for mean annual PAB (Fig. 2. 3 B) lie above those for the 20th century and those for MFI (Fig. 2.4 B) lie below. During the 20th century, most of the WNW experiences no fire regardless of whether fire suppression is applied or not (Fig. 2.5 B). Only southern portions of the northern Cascades and southern Klamath region experience years with large areas burned by wildfire. In sharp contrast, during the 21st century, most of the area experiences extensive wildfires with PAB approaching 100% in burned grid cells, the exceptions being the Klamath area, along the Pacific coastline, and at high elevations (Fig. 2.5 C).

Table 2.5. Simulated mean fire interval (MFI) by subregion for 20th century and 21st century by representative concentration pathway (RCP). Ensemble means and standard deviations were taken across results of runs produced using all climate futures.

Region and Fire Suppression	20th Century	RCP 4.5 21st Century		RCP 8.5 21st Century	
		Ensemble Mean	Standard Deviation	Ensemble Mean	Standard Deviation
Full NW FS	42.36	25.87	6.72	20.81	6.69
Full NW NFS	36.66	14.60	5.65	9.35	4.99
WNW FS	81.34	47.27	11.17	37.40	10.93
WNW NFS	79.93	40.92	11.37	27.15	9.75
NWPP FS	18.56	21.10	3.77	20.01	4.70
NWPP NFS	11.39	2.84	0.98	2.05	0.69
ENWM FS	44.88	19.49	9.48	13.16	8.37
ENWM NFS	38.39	12.28	8.66	7.17	7.00

(RCP: representative concentration pathway; NW: Northwest; WNW: western Northwest; NWPP: Northwest plains and plateau; ENWM: eastern Northwest mountains; FS: fire suppression; NFS: no fire suppression.)

Table 2.6. Simulated annual percent area burned (PAB) by subregion for 20th century and 21st century by representative concentration pathway (RCP). Ensemble means and standard deviations were taken across results of runs produced using all climate futures.

Region and Fire Suppression	20th Century	RCP 4.5 21st Century		RCP 8.5 21st Century	
		Ensemble Mean	Standard Deviation	Ensemble Mean	Standard Deviation
Full NW FS	1.99	2.31	0.20	2.36	0.22
Full NW NFS	3.06	3.85	0.23	3.91	0.22
WNW FS	0.53	1.12	0.19	1.27	0.17
WNW NFS	0.58	1.32	0.23	1.52	0.19
NWPP FS	2.90	2.75	0.21	2.74	0.29
NWPP NFS	4.89	5.52	0.12	5.48	0.12
ENWM FS	1.88	2.50	0.28	2.55	0.26
ENWM NFS	2.61	3.58	0.38	3.66	0.35

(RCP: representative concentration pathway; NW: Northwest; WNW: western Northwest; NWPP: Northwest plains and plateau; ENWM: eastern Northwest mountains; FS: fire suppression; NFS: no fire suppression.)

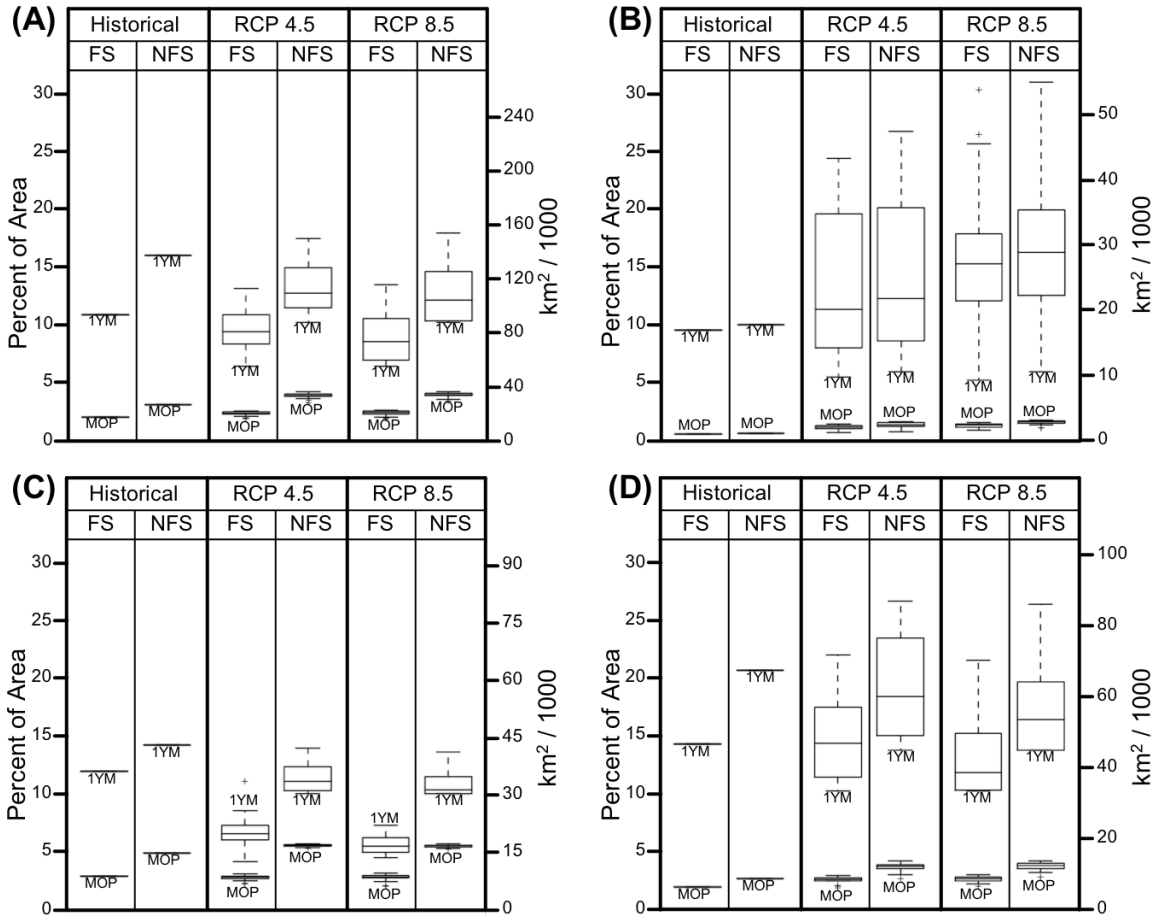

Fig. 2.3. Spread across model runs for mean annual area burned over time period (MOP) and maximum annual area burned (1YM) for 20th century and 21st century for two representative concentration pathways (RCPs). (A) full study area, (B) WNW (western Northwest), (C) NWPP (Northwest plains and plateau), and (D) ENWM (eastern Northwest mountains). Whiskers extend to a maximum of 1.5 x interquartile range (Q3 – Q1) (FS: fire suppression; NFS: no fire suppression).

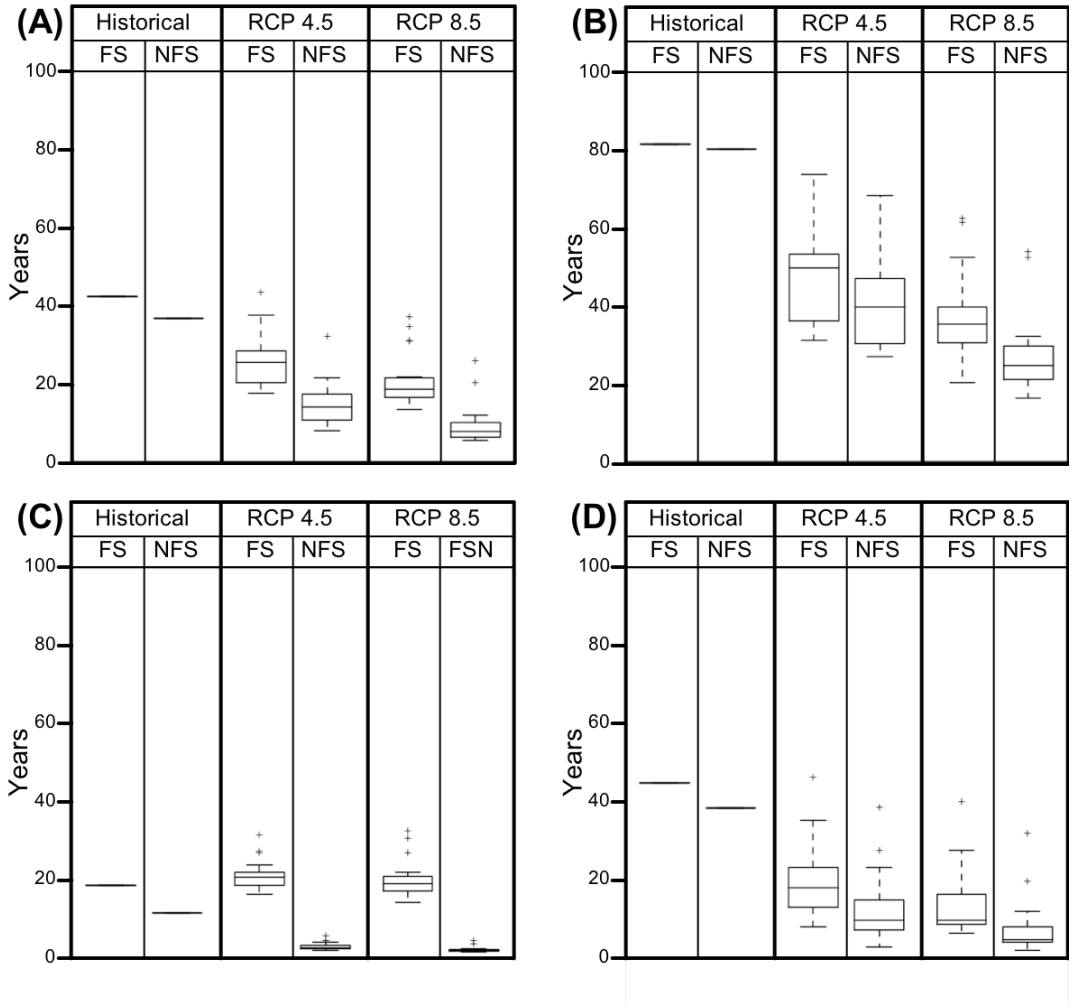

Fig. 2.4. Spread across model runs for simulated mean fire interval (MFI) for 20th century (Historical) and 21st century for two representative concentration pathways (RCPs). (A) full study area, (B) WNW (western Northwest), (C) NWPP (Northwest plains and plateau), and (D) ENWM (eastern Northwest mountains). Whiskers extend to a maximum of 1.5 x interquartile range (Q3 – Q1) (FS: fire suppression; NFS: no fire suppression).

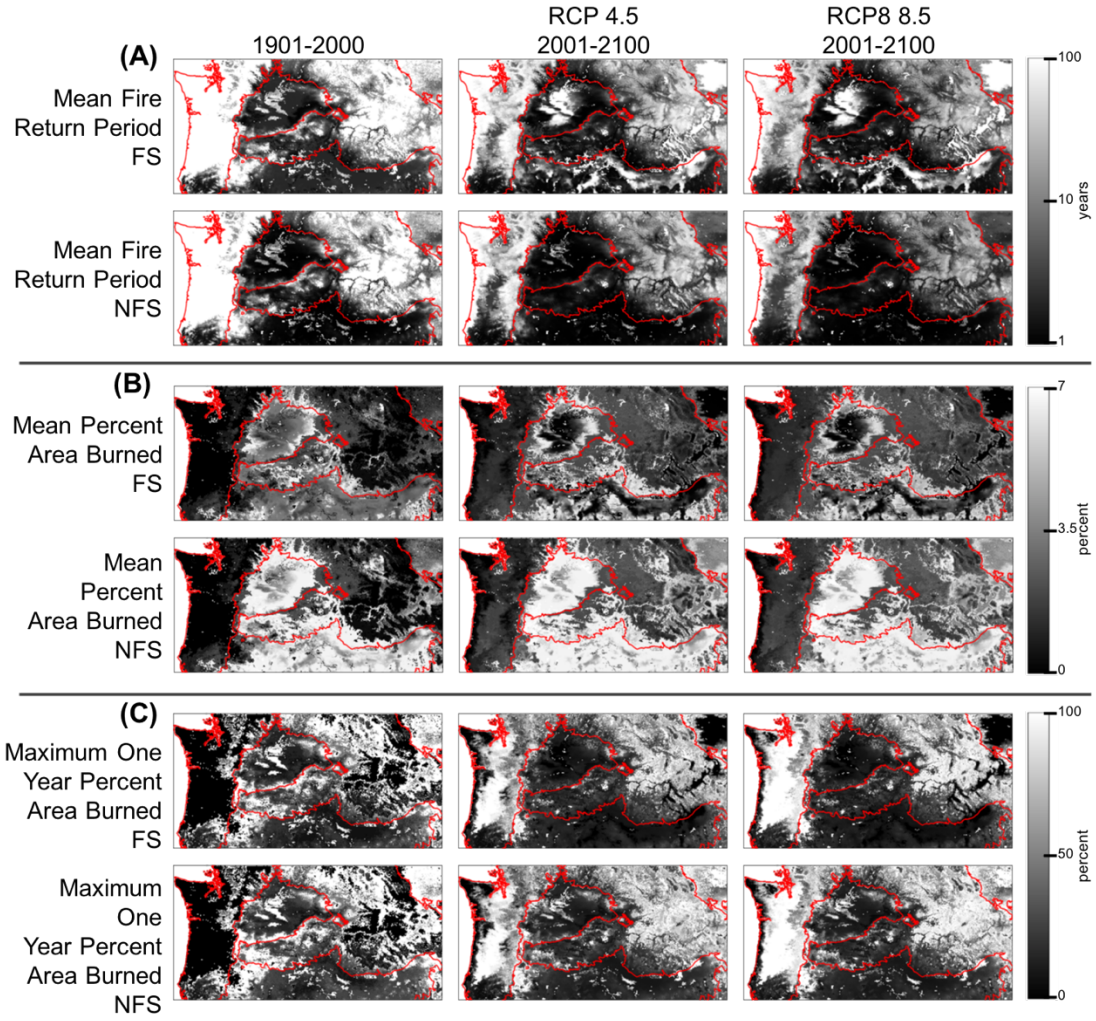

Fig. 2.5. Simulated fire results for 20th century and 21st century for two representative concentration pathways (RCPs). (A) mean fire interval (MFI), (B) mean annual percent area burned (PAB), and (C) maximum annual percent of area burned (PAB). Means and maximums taken across results of runs produced using all climate futures (Pct: percent; FS: fire suppression; NFS: no fire suppression).

Vegetation shifts from predominantly conifer to mixed forests as temperatures warm during the 21st century (Fig. 2.6, Table 2.8). The shift starts in the south, expands along the coast, and spreads northward and upslope over the Coast range and into the middle reaches of the Cascades. This shift is earlier and more extensive under the warmer RCP 8.5 scenario than under the cooler RCP 4.5 scenario. In the late 21st century under RCP 8.5, remnant conifer forests occur only in the northern Oregon Coast Range, the higher elevations of the Olympic Peninsula, and the higher elevations of the Cascades. Following the shift from conifer to mixed vegetation, warm mixed forests replace cool mixed forests, starting in the southwest, spreading north along the coast, and then inland and north into the foothills of the Cascades. This trend is most extensive under the RCP 8.5 scenario in the late 21st century.

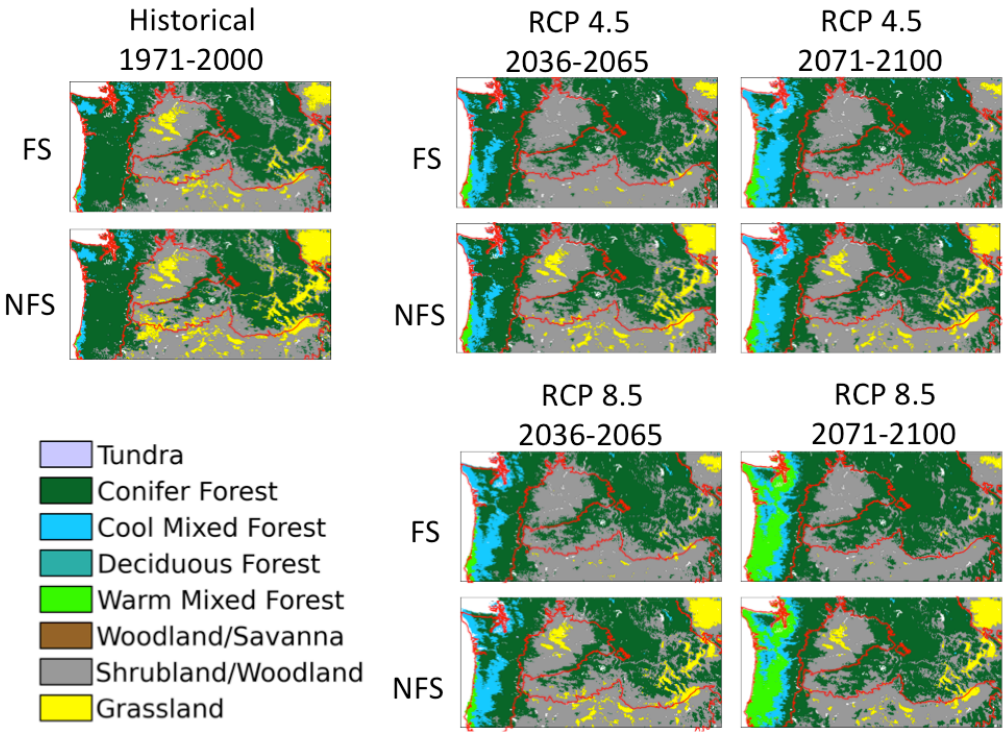

Fig. 2.6. Simulated modal vegetation classes for historical time period and across 20 climate futures for two representative concentration pathways (RCPs). Modes taken across results of runs produced using all climate futures (FS: fire suppression; NFS: no fire suppression).

2.5.2 NWPP

In the NWPP subregion, RCP scenarios have little effect on fire results (Figures 3 C, 4 C, Tables 5, 6, 7), while fire suppression has a marked effect. Even though its effect during the 20th

century is limited because suppression is not applied until 1950, fire suppression produces a longer MFI (18.56 vs 11.39 years), a lower annual mean PAB (2.90 vs 4.89%), and a lower maximum annual PAB (11.95 vs 14.18%) than no fire suppression. During the 21st century fire suppression results in a MFI up to ten times as long (~20 vs ~2 to 3 years), a mean PAB half as large (~2.75 vs ~5.5%), and a maximum annual PAB of just over half as large (6.79 vs 11.50% for RCP 4.5, 5.59 vs 10.80% for RCP 8.5) as those without fire suppression.

Table 2.7. Simulated maximum single year percent area burned (PAB) by subregion for 20th century and 21st century by representative concentration pathway (RCP). Ensemble means and standard deviations were taken across results of runs produced using all climate futures.

Region and Fire Suppression	20th Century	RCP 4.5 21st Century		RCP 8.5 21st Century	
		Ensemble Mean	Standard Deviation	Ensemble Mean	Standard Deviation
Full NW FS	10.85	9.47	1.69985	8.98	2.05752
Full NW NFS	15.97	13.25	2.24275	12.66	2.42619
WNW FS	9.55	13.45	6.33449	15.93	6.37986
WNW NFS	9.97	14.20	6.60039	16.96	6.79137
NWPP FS	11.95	6.79	1.39409	5.59	0.764454
NWPP NFS	14.18	11.50	1.40379	10.80	0.96752
ENWM FS	14.29	14.82	3.79227	13.52	3.63536
ENWM NFS	20.69	19.43	4.65294	17.88	4.58403

(RCP: representative concentration pathway; NW: Northwest; WNW: western Northwest; NWPP: Northwest plains and plateau; ENWM: eastern Northwest mountains; FS: fire suppression; NFS: no fire suppression.)

Table 2.8. Dominant simulated vegetation types and percent coverage for historical and future time periods by representative concentration pathway (RCP). Results are from modes across results of runs produced using all climate futures.

Region and Fire Suppression	Historical 1971-2000		RCP 4.5 2036-2065		RCP 4.5 2070-2100		RCP 8.5 2036-2065		RCP 8.5 2070-2100	
Full NW FS	CON	47.70	CON	49.06	CON	47.52	CON	47.55	CON	49.18
Full NW NFS	CON	46.10	CON	44.05	CON	42.96	CON	42.27	CON	44.34
WNW FS	CON	85.90	CON	71.07	MIX	49.61	MIX	60.69	MIX	64.60
WNW NFS	CON	85.42	CON	70.93	MIX	49.17	MIX	60.35	MIX	64.48
NWPP FS	FSH	89.51	FSH	97.08	FSH	98.57	FSH	97.16	FSH	98.53
NWPP NFS	FSH	80.00	FSH	84.94	FSH	87.10	FSH	84.74	FSH	88.08
ENWM FS	CON	60.50	CON	66.89	CON	70.96	CON	67.60	CON	77.18
ENWM NFS	CON	58.23	CON	58.45	CON	62.75	CON	58.72	CON	68.56

(RCP: representative concentration pathway; NW: Northwest; WNW: western Northwest; NWPP: Northwest plains and plateau; ENWM: eastern Northwest mountains; FS: fire suppression; NFS: no fire suppression; CON: conifer forest; MIX: warm mixed forest + cool mixed forest; FSH = forest + shrubs.)

Without fire suppression, during both historical and future periods, frequent fires reduce the dominance of woody vegetation (forests and shrubs) by 9.5 to 12.4% (Fig. 2.6, Table 2.8) compared to results with fire suppression. This trend is most apparent at lower elevations in the western and southern portions of the subregion where, without fire suppression, grasslands are more extensive and shrublands less. Both with and without fire suppression, the dominance of woody vegetation increases between 4.7 and 9.1% in the future period.

2.5.3 ENWM

Over the entire ENWM subregion, MFI (7.2 to 19.5 years 21st century vs 38.4 to 44.9 years 20th century) decreases, mean annual PAB (2.7 to 3.7% 21st century vs 1.9 to 2.6% 20th century) increases, and maximum annual PAB (13.5 to 19.4% 21st century vs 14.3 to 20.7% 20th century) is nearly unchanged during the 21st century as compared to the 20th century (Tables 5, 6, 7, Figures 3 D, 4 D). MFI is lower, mean annual PAB higher, and maximum annual PAB higher without fire suppression. Results differ little between RCP 4.5 and 8.5 scenarios. Lower elevation valleys and slopes within the ENWM (Fig. 2.5) show similar responses to emission scenarios and fire suppression to comparable areas in the NWPP.

Fire in the Blue Mountains (area of generally lower elevation stretching westward from the southern portion of the subregion) differs from that in the eastern portion of the subregion, with generally more frequent, smaller fires (Figures 5 A-B) resulting in a mean annual PAB similar to that of the rest of the subregion. Fire suppression effects are consistent with those across the ENWM subregion, reducing both mean annual and maximum annual PAB, and increasing MFI. In the 21st century fires are somewhat more frequent and have a somewhat higher mean annual and maximum annual PAB than those in the rest of the NWPP.

The eastern portion of the ENWM subregion exhibits different fire responses based on elevation (Fig. 2.5). Higher elevations have a higher MFI, lower mean annual PAB, and lower maximum annual PAB during the 20th century than lower elevations. During the 21st century, MFI decreases across this part of the subregion. Lower elevations have a higher MFI and a higher maximum annual PAB than higher elevations, but mean annual PAB similar to that of the rest of the subregion.

Conifer forests dominate the subregion for all historical and future simulations (Table 2.8, Fig. 2.6). Conifer dominance is greater with fire suppression than without and under RCP 8.5 versus RCP 4.5. It increases through time for all future simulations. During the late 20th century, with and without fire suppression, subalpine vegetation (not shown here, part of the conifer forest vegetation type) is present at high elevation and comprises 30% of the subregion area. By the late 21st century it is nearly absent, comprising 2% and 0.3% of the subregion area for RCP 4.5 and RCP 8.5 respectively. Other vegetation type changes are limited to shifts between more or less woody types at lower elevations with conifer forest supplanting shrubland/woodland, and shrubland/woodland supplanting grassland when fire suppression is implemented.

2.6 Discussion

In the WNW subregion, the prevalence of large fires and the change of the dominant vegetation from conifer to mixed forest are both associated with projected increases in temperature and take place under warmer, drier summer conditions. Large fires in the WNW subregion are currently limited by fuel moisture rather than fuel amount, requiring climate conditions such as drought or extreme fire weather that have rarely occurred historically (Meyn et al. 2007). These fire-conducive conditions – warmer temperatures and drier summers – become common in the future and cause large fires. Along the trajectory from historical to future climate conditions, vegetation shifts from conifer to mixed forests are facilitated by increased wildfire occurrence in much of the subregion. However, climate, rather than fire is the driving force behind the vegetation shift. Historically droughts have led to large fires in this subregion (Agee 1991), and the model simulated such large fires in several areas over the 20th century. In the case of either actual or simulated historical fires, conifer forests returned. Increased future temperatures and longer, dryer summers cause the vegetation to shift from the current conifer to less dense, more drought-tolerant mixed forest. This vegetation shift takes place even along the coast where moister conditions prevent fires in the future period (Fig. 2.6).

In MC2, the longer the period between fires, the higher the fraction of grid cell available to burn when a fire occurs. When a group of grid cells experiences a long period without burning followed by a year in which fire thresholds are exceeded, as occurs in some areas of the WNW under most climate futures, the entire area experiences a uniquely high PAB. The model is likely

overestimating the annual maximum area burned in the WNW subregion. Results are best interpreted as an indication that conditions will be conducive to large fires and that if such conditions become frequent, as they are projected to under a climate with hotter, drier summers in the WNW, then large fires are likely.

In the NWPP, the use of a fixed range of FRI for each vegetation type to limit the area burned has a very strong effect on fire behavior, in turn strongly influencing the vegetation. Without fire suppression, the assumption of unlimited ignition coupled with fixed FRI leads to very frequent, small fires in grass/shrub dominated areas. This maintains grasslands by denying woody vegetation the fire-free years needed to establish. Fire suppression in the model prevents large fire occurrence even when conditions exceed fire suppression thresholds thus limiting mortality and consumption of woody vegetation and amplifying woody encroachment. The model likely overestimates fire suppression effectiveness and underestimates the frequency of shifts between grassland and shrubland with and without fire suppression. Limiting as opposed to assuming ignitions would likely lead to greater spatial variability in fire frequency, extent, and intensity. This in turn would likely result in greater spatial and temporal variation in woody versus grass vegetation dominance (Ratajczak et al. 2014).

The more frequent fire and greater mean area burned in the ENWM subregion are primarily due to rising temperatures. Although summer precipitation is reduced, the summer dry period is not longer than during the historical period (Fig. 2.2). Consequently, the effect of the decrease in precipitation on the length of the fire season is minimal. Warmer temperatures and increased precipitation during fall, winter, and spring are not great enough to shift vegetation from conifer to mixed forest. However, along with a moderate increase in water use efficiency due to increased CO_2, these conditions result in greater conifer growth. Increased growth exceeds losses through increased fire, resulting in an overall increase in forested area. As with the WNW, assumed ignitions have led to large annual PAB in the ENWM and should be viewed in a similar manner.

Rogers et al. (2011) ran MC1 using climate data from 3 climate model projections under SRES A2 scenarios and presented results of fire suppression over the western 2/3 of the states of Oregon and Washington. For their western forest domain, which corresponds closely to our WNW subregion, the ensemble mean of their mean annual PAB (0.14%) over the historical

period (1971-2000) was lower than ours over the entire 20th century (Table 2.6; 0.58% for NFS and 0.53% for FS). The mean of their future period (2070-2099) mean annual PAB (0.71%) was lower than ours for the 100 years of the 21st century (range of 1.12% for RCP 4.5 FS to 1.52% for RCP8.5 NFS). From the Cascades west, their results show a similar trend with mixed forests in the Willamette Valley under the MIROC future, however they simulate a smaller extent of mixed forest in the historical and future periods than we did. Elsewhere in their study area, they generally simulated woodier vegetation than we did with more forest and less grassland and shrubland/woodland. They simulated woody vegetation increases over time, as we did with fire suppression.

More recently, using three downscaled CMIP5 climate futures representing low, moderate and high levels of climate change, Turner et al. (2015) simulated vegetation and land use changes in the Willamette watershed of Oregon. They found shifts in potential vegetation similar to ours for this portion of the study region, with warmer mixed forests dominating lower elevations, cooler mixed forests at intermediate elevations, and conifers remaining at high elevations. They found, as we did, that shifts to mixed and warmer mixed forest types were more extensive with the warmer drier climate scenarios. Their annual PAB for recent decades was 0.2% and they observed a 3 to 9-fold increase in annual area burned for their moderate to severe climate scenarios. We found that for the 20th century PAB in the WNW subregion was between 0.5% and 0.6% with a 2 to 3-fold increase in mean 21st century PAB. These differences are likely due to different parameterization, since they adjusted MC2 fire thresholds for each of their runs to match local historical records, while ours was adjusted once to match CONUS reference datasets using PRISM historical data.

Differences between our results and those of Rogers et al. (2011) may be due to differences in climate futures, parameterizations, or both. Given the similarity between our results and Turner et al.'s (2015) despite independent parameterizations, it is likely that the differences are attributable to differences in the future climates used to drive the model.

West of the Cascades, Rehfeldt et al. (2006) simulated the range of Oregon coastal conifer forests shrinking to the north and west of its original range. Most of the Douglas-fir forests they mapped in late 21st century were exposed to novel climate conditions. Similarly, we

simulated the near complete conversion of conifer forests to mixed forests over the same region. They also mapped a larger extent of grasslands in the NWPP than we did.

Using Rehfeldt et al.'s (2006) results for Douglas-fir as well as a similar, statistics-driven analysis for three pine species, Littell et al. (2010) projected Douglas-fir vulnerability and species richness gains and losses within Washington state and northern Oregon. They included vulnerability to pine beetle outbreaks (which we did not simulate) and fire in their analysis. There is general concurrence between their projections of Douglas-fir being at risk (present in <50% of models) or not at risk (present in ≥50% of models) by the 2060s and MC2 projections of conifer forests converting to mixed or remaining as conifer. However, they projected unforested areas on some Cascade peaks as well as at lower elevations on the east side of Puget Sound and in lower elevation areas in the northern Willamette Valley and southern Puget Trough, while MC2 simulated forests in these areas. Overall, they projected a doubling or tripling of annual area burned by the 2080s. This is lower than what MC2 simulated for the entire region, but is consistent with MC2 projections for the WNW.

Shafer et al. (2001) projected species range shifts using 3 CMIP3 futures. In the WNW, they simulated decreases in the range of Douglas-fir (*Pseudotsuga menziesii*), Pacific silver fir (*Abies amabilis*), Oregon white oak (*Quercus garryana*), and red alder (*Alnus rubra*) with increases in the ranges of valley oak (*Quercus lobata*) and ponderosa pine (*Pinus ponderosa*). This is consistent with our simulated shifts from conifer forest under cooler historical conditions to warmer mixed forests in the 21st century. They simulated the expansion of ponderosa pine within the ENWM which agrees with our simulated shifts from subalpine to warmer types at high elevations.

On a state-by-state basis for western states, McKenzie et al. (2004) used multiple regression analysis to determine the area burned as a function of summer temperature and precipitation and projected how climate change may affect area burned. Projections with the mild PCM-B2 climate projection showed increases in area burned by a factor of approximately 1.3 (Idaho) to approximately 3 (Washington) compared to the current mean. Their results are generally 20-30% greater than ours, likely as a result of their use of static vegetation while MC2 simulate shifts to more fuel-limited mixed forests over much of the study area.

Due to different modeling techniques, climate futures, and model calibrations, our results differ in specifics from those of other studies. However, they closely agree in trends towards increased fire occurrence and intensity as well as vegetation shifts. Given the uncertainties inherent in climate inputs, biogeography rules, and fire modeling, our results should be considered in the broader context of other impacts modeling work just as each general circulation model provides another projection of future climate.

2.7 Limitations

Climate projections generally agree on warmer future conditions, however, precipitation projections are more variable (e.g. Meehl et al. 2007). Seasonality, quantity, and interannual variability of precipitation have large effects on factors influencing fire occurrence and behavior. Years with greater precipitation can lead to increases in both dead and live fuels, in turn producing greater fire in fuel-limited areas. Dry years – or longer intraannual dry periods – can result in more fire in moisture-limited areas. Reliable soils data are key to projecting accurate soil water availability and drought stress (Peterman et al. 2014). Accurate vapor pressure deficit data are also important for producing meaningful vegetation modeling results.

MC2 simulates potential vegetation most adapted to the climate drivers. However, in reality vegetation is long lived and endures under suboptimal conditions, preventing better-suited vegetation from gaining a foothold. Vegetation can remain in a metastable state until disturbance or natural mortality removes this legacy vegetation.

Modeling fire also presents challenges as fire occurrence, spread, and intensity depend on inherently unpredictable factors including seasonal weather extremes, immediate weather conditions, ignition occurrence, and other factors that may affect fuel load and condition. A fire model will always be a simplification of dynamic processes and must strike a balance between realism, ease of implementation, and computational performance.

The effects of CO_2 concentration on water use efficiency and plant productivity are still not completely understood and may depend on factors such as ontogeny and site conditions (Camarero et al. 2015). While the CO_2 fertilization effect in MC2 is moderate, it does lead to greater woody plant production and fuel accumulation. Improved understanding of the CO_2 fertilization effects will undoubtedly lead to improvements in vegetation modeling.

The addition of insect attacks, disease, and invasive species to the model would allow the model to better reflect the effects of these influences on vegetation dynamics. However, these additions were beyond the scope of this project.

2.8 Conclusions

Vegetation dynamics and wildfire are inextricably linked, yet MC2 is one of the few DGVMs to include a dynamic fire model. Using MC2, we modeled future vegetation and fire for the PNW using 40 different climate futures, each with and without fire suppression. Results illustrate the range of likely future fire frequency and extent as well as the pattern of possible vegetation changes throughout the 21st century. Fire and vegetation trends were distinctly different geographically and to facilitate interpretation we summarized the results using three subregions as follows.

In the WNW, the predominant conifer forest is replaced by mixed forest under future climate scenarios. While fire is absent in most of the subregion during the 20th century, large fires are simulated during the 21st century. The metastable state of the vegetation and the potential for widespread fire indicate that this region could undergo a rapid ecological change in the coming decades. Managers will have to consider how to maintain continuity of ecosystem services and provide refugia for threatened species and communities.

Fire suppression has a significant effect in the NWPP, leading to an expansion of woody vegetation, primarily shrubs. However, the potential for periodic large fires under fire suppression is probably more likely than indicated by our results, and would likely dampen the woody expansion and possibly lead to spatial and temporal variation in grass/shrub composition. Since we do not model invasive species, their importance in changing fire regimes across the intermountain West is missing from our analysis. Managing this diverse region where invasive species and locally accumulated fuels could pose threats to existing communities presents managers with a difficult challenge.

In the ENWM, the predominant vegetation type remains conifer forest under all future climate scenarios. However, subalpine forests are supplanted by warmer forest types. The occurrence of large fires in the 21st century, especially in subalpine areas, points to the potential for sudden vegetation shifts. The possibility of rapid ecological change facilitated by sudden

large fires and other disturbances is real and might affect the effectiveness of management strategies designed to maintain ecosystem resilience and future ecosystem health.

The Pacific Northwest is an ecologically diverse region that provides many ecosystem services including timber, carbon sequestration, grazing, wildlife habitat, and recreation. In addition, it is home to a number of ecosystems under pressure from landuse, invasive species, and changing climate. There is little doubt that the last of these pressures will have an increasing influence as climate change effects increase into the future. Because of this, it is important that land managers – from national leaders to regional planners – utilize the best available projections for future climate, vegetation, and landuse. This study provides one example of actionable projections and provides a platform for further enhancements to best address ecological issues into the future.

2.9 Acknowledgments

Funding for this research was provided by the U.S. Department of the Interior via the Northwest Climate Science Center through agreement #G12AC20495 within the framework of the research project entitled “Integrated Scenarios of climate, hydrology and vegetation for the Northwest”, P. Mote (Oregon State U.) principal investigator.

We acknowledge the World Climate Research Programme's Working Group on Coupled Modelling, which is responsible for CMIP, and we thank the climate modeling groups (listed in Table 2.1 of this paper) for producing and making available their model output. For CMIP, the U.S. Department of Energy's Program for Climate Model Diagnosis and Intercomparison provides coordinating support and led development of software infrastructure in partnership with the Global Organization for Earth System Science Portals.

The authors wish to acknowledge R. Nemani (NASA) for allowing them free access to the Pleiades NASA supercomputer and John Abatzoglou and Katherine Hegewisch (both of University of Idaho) for providing the downscaled CMIP5 climate data used in this study.

We thank B. Baker and A. Syphard (CBI) for useful comments on early versions of the manuscript. We also thank the manuscript reviewers who provided thoughtful comments.

2.10 References

Agee, J. K. (1991). Fire history of Douglas-fir forests in the Pacific Northwest in *Wildlife and Vegetation of Unmanaged Douglas-fir Forests*. USDA Forest Service General Technical Report. U.S. Department of Agriculture, Forest Service, Pacific Northwest Research Station, Portland, OR.

Bachelet, D., Neilson, R. P., Lenihan, J. M., & Drapek, R. J. (2001). Climate change effects on vegetation distribution and carbon budget in the United States. *Ecosystems*, 4(3), 164-185.

Bachelet, D., Ferschweiler, K., Sheehan, T. J., Sleeter, B. M., & Zhu, Z. (2015). Projected carbon stocks in the conterminous USA with land use and variable fire regimes. *Global Change Biology*, 21(12), 4548-4560.

Bentz, B. J., Régnière, J., Fettig, C. J., Hansen, E. M., Hayes, J. L., Hicke, J. A., Kelsey, R. G., Negrón, J. F., & Seybold, S. J. (2010). Climate change and bark beetles of the western United States and Canada: direct and indirect effects. *BioScience*, 60(8), 602-613.

Camarero, J. J., Gazol, A., Galván, J. D., Sangüesa-Barreda, G., & Gutiérrez, E. (2015). Disparate effects of global-change drivers on mountain conifer forests: warming-induced growth enhancement in young trees vs. CO_2 fertilization in old trees from wet sites. *Global Change Biology*, 21(2), 738-749.

Canadian Forestry Service (1984). *Tables for the Canadian Forest Fire Weather Index System*. Forestry technical report 25, 4th ed. Environment Canada, Canadian Forest Service, Ottawa, ON, CA.

Cayan, D. R., Kammerdiener, S. A., Dettinger, M. D., Caprio, J. M., & Peterson, D. H. (2001). Changes in the onset of spring in the western United States. *Bulletin of the American Meteorological Society*, 82(3), 399-416.

Chmura, D. J., Anderson, P. D., Howe, G. T., Harrington, C. A., Halofsky, J. E., Peterson, D. L., Shaw, D. C., & Clair, J. B. S. (2011). Forest responses to climate change in the northwestern United States: ecophysiological foundations for adaptive management. *Forest Ecology and Management*, 261(7), 1121-1142.

Cohen, J. D., & Deeming, J. E. (1985). *The National Fire-danger Rating System: Basic Equations*. Gen. Tech. Rep. PSW-82. Pacific Southwest Forest and Range Experiment Station, Forest Service, US Department of Agriculture, Berkeley, CA, USA.

Conklin, D. R., Lenihan, J. M., Bachelet, D., Neilson, R. P., Kim, J. B. (2015). *MCFire Model Technical Description*. Gen. Tech. Rep. PNW-GTR-904. U.S. Department of Agriculture, Forest Service, Pacific Northwest Research Station, Portland, OR.

Coops, N. C., & Waring, R. H. (2011). Estimating the vulnerability of fifteen tree species under changing climate in Northwest North America. *Ecological Modelling*, 222(13), 2119-2129.

Coops, N. C., Waring, R. H., Beier, C., Roy-Jauvin, R., & Wang, T. (2011). Modeling the occurrence of 15 coniferous tree species throughout the Pacific Northwest of North

America using a hybrid approach of a generic process-based growth model and decision tree analysis. *Applied Vegetation Science*, 14(3), 402-414.

Creutzburg, M. K., Halofsky, J. E., Halofsky, J. S., & Christopher, T. A. (2015). Climate change and land management in the rangelands of central Oregon. *Environmental Management*, 55(1), 43-55.

Daly, C., Halbleib, M., Smith, J. I., Gibson, W. P., Doggett, M. K., Taylor, G. H., Curtis, J., & Pasteris, P. P. (2008). Physiographically sensitive mapping of climatological temperature and precipitation across the conterminous United States. *International Journal of Climatology*, 28(15), 2031-2064.

Dombeck, M. (2001). How can we reduce the fire danger in the interior West. *Fire Management Today*, 61(1), 5-13.

Drapek, R. J., Kim, J. B., & Neilson, R. P. (2015). Continent-wide Simulations of a Dynamic Global Vegetation Model over the United States and Canada under Nine AR4 Future Scenarios, in *Global Vegetation Dynamics* (pp. 73-90). American Geophysical Union (AGU).

Gonzalez, P., Neilson, R. P., Lenihan, J. M., & Drapek, R. J. (2010). Global patterns in the vulnerability of ecosystems to vegetation shifts due to climate change. *Global Ecology and Biogeography*, 19(6), 755-768.

Halofsky, J. S., Halofsky, J. E., Burcsu, T., & Hemstrom, M. A. (2014). Dry forest resilience varies under simulated climate-management scenarios in a central Oregon, USA landscape. *Ecological Applications*, 24(8), 1908-1925.

Keetch, J. J., & Byram, G. M. (1968). *A Drought Index for Forest Fire Control*. USDA Forest Service Research Paper SE-38. US Department of Agriculture, Forest Service, Southeastern Forest Experiment Station, Asheville, NC, USA.

Kellndorfer, J., Walker, W., Kirsch, K., Fiske, G., Bishop, J., LaPoint, L., Hoppus, M., & Westfall, J. (2013). *NACP Aboveground Biomass and Carbon Baseline Data, V. 2* (NBCD 2000), Oak Ridge National Laboratories, Oak Ridge, TN, USA.

Kern, J. S. (1994). Spatial patterns of soil organic carbon in the contiguous United States. *Soil Science Society of America Journal*, 58(2), 439-455.

Kern, J. S. (1995). Geographic patterns of soil water-holding capacity in the contiguous United States. *Soil Science Society of America Journal*, 59(4), 1126-1133.

Kern, J. S. (2000). Erratum for Geographic patterns of soils water-holding capacity in the contiguous United States. *Soil Science Society of America Journal* 64, 382.

King, D. A., Bachelet, D. M., & Symstad, A. J. (2013). Climate change and fire effects on a prairie–woodland ecotone: projecting species range shifts with a dynamic global vegetation model. *Ecology and Evolution*, 3(15), 5076-5097.

Kuchler, A. W. (1975). *Potential Natural Vegetation of the Conterminous United States*, *2nd ed*. American Geographical Society, New York, NY, USA.

Latta, G., Temesgen, H., & Barrett, T. M. (2009). Mapping and imputing potential productivity of Pacific Northwest forests using climate variables. *Canadian Journal of Forest Research*, 39(6), 1197-1207.

Leenhouts, B. (1998). Assessment of biomass burning in the conterminous United States. *Conservation Ecology,* 2(1), 1-18. Available at: http://www.consecol.org/vol2/iss1/

Lenihan, J. M., Daly, C., Bachelet, D., & Neilson, R. P. (1998). Simulating broad-scale fire severity in a dynamic global vegetation model. *Northwest Science*, 72(4), 91-101.

Lenihan, J. M., Bachelet, D., Neilson, R. P., & Drapek, R. (2008). Response of vegetation distribution, ecosystem productivity, and fire to climate change scenarios for California. *Climatic Change*, 87(1), 215-230.

Littell, J. S., Oneil, E. E., McKenzie, D., Hicke, J. A., Lutz, J. A., Norheim, R. A., & Elsner, M. M. (2010). Forest ecosystems, disturbance, and climatic change in Washington State, USA. *Climatic Change*, 102(1-2), 129-158.

McKenzie, D., Gedalof, Z. E., Peterson, D. L., & Mote, P. (2004). Climatic change, wildfire, and conservation. *Conservation Biology*, 18(4), 890-902.

Meehl, G. A., Covey, C., Delworth, T., Latif, M., McAvaney, B., Mitchell, J. F., Stouffer, R. J., & Taylor, K. E. (2007). The WCRP CMIP3 multimodel dataset: A new era in climate change research. *Bulletin of the American Meteorological Society*, 88(9), 1383-1394.

Metherell, A. K. (1993). *CENTURY Soil organic matter model environment*. Technical Documentation Agroecosystem. Agroecosystem version 4.0. USDA Great Plains System Research Unit Technical Report No. 4. Fort Collins, CO, U. S.

Meyn, A., White, P. S., Buhk, C., & Jentsch, A. (2007). Environmental drivers of large, infrequent wildfires: the emerging conceptual model. *Progress in Physical Geography*, 31(3), 287-312.

Millar, C. I., Stephenson, N. L., & Stephens, S. L. (2007). Climate change and forests of the future: managing in the face of uncertainty. *Ecological Applications*, 17(8), 2145-2151.

Mote, P. W., Hamlet, A. F., Clark, M. P., & Lettenmaier, D. P. (2005). Declining mountain snowpack in western North America. Bulletin of the American Meteorological Society, 86(1), 39-50.

Mote, P. W., & Salathe, E. P. (2010). Future climate in the Pacific Northwest. *Climatic Change*, 102(1-2), 29-50.

Neilson, R. P. (1995). A model for predicting continental-scale vegetation distribution and water balance. *Ecological Applications*, 5(2), 362-385.

Omernik, J. M., & Griffith, G. E. (2014). Ecoregions of the conterminous United States: evolution of a hierarchical spatial framework. *Environmental Management*, 54(6), 1249-1266.

Pyne, S. J. (2017). *Fire in America: A Cultural History of Wildland and Rural Fire*. University of Washington Press, Seattle, WA, USA.

Peterman, W., Bachelet, D., Ferschweiler, K., & Sheehan, T. (2014). Soil depth affects simulated carbon and water in the MC2 dynamic global vegetation model. *Ecological Modelling*, 294, 84-93.

Ratajczak, Z., Nippert, J. B., Briggs, J. M., & Blair, J. M. (2014). Fire dynamics distinguish grasslands, shrublands and woodlands as alternative attractors in the Central Great Plains of North America. *Journal of Ecology*, 102(6), 1374-1385.

Rehfeldt, G. E., Crookston, N. L., Sáenz-Romero, C., & Campbell, E. M. (2012). North American vegetation model for land-use planning in a changing climate: a solution to large classification problems. *Ecological Applications*, 22(1), 119-141.

Rehfeldt, G. E., Crookston, N. L., Warwell, M. V., & Evans, J. S. (2006). Empirical analyses of plant-climate relationships for the western United States. *International Journal of Plant Sciences*, 167(6), 1123-1150.

Rehfeldt, G. E., Jaquish, B. C., López-Upton, J., Sáenz-Romero, C., St Clair, J. B., Leites, L. P., & Joyce, D. G. (2014a). Comparative genetic responses to climate for the varieties of *Pinus ponderosa* and *Pseudotsuga menziesii*: Realized climate niches. *Forest Ecology and Management*, 324, 126-137.

Rehfeldt, G. E., Leites, L. P., St Clair, J. B., Jaquish, B. C., Sáenz-Romero, C., López-Upton, J., & Joyce, D. G. (2014b). Comparative genetic responses to climate in the varieties of *Pinus ponderosa* and *Pseudotsuga menziesii*: Clines in growth potential. *Forest Ecology and Management*, 324, 138-146.

Rehfeldt, G. E., Jaquish, B. C., Sáenz-Romero, C., Joyce, D. G., Leites, L. P., St Clair, J. B., & López-Upton, J. (2014c). Comparative genetic responses to climate in the varieties of *Pinus ponderosa* and *Pseudotsuga menziesii*: reforestation. *Forest Ecology and Management*, 324, 147-157.

Rogers, B. M., Neilson, R. P., Drapek, R., Lenihan, J. M., Wells, J. R., Bachelet, D., & Law, B. E. (2011). Impacts of climate change on fire regimes and carbon stocks of the US Pacific Northwest. *Journal of Geophysical Research: Biogeosciences*, 116, G03037.

Shafer, S. L., Bartlein, P. J., & Thompson, R. S. (2001). Potential changes in the distributions of western North America tree and shrub taxa under future climate scenarios. *Ecosystems*, 4(3), 200-215.

Turner, D. P., Conklin, D. R., & Bolte, J. P. (2015). Projected climate change impacts on forest land cover and land use over the Willamette River Basin, Oregon, USA. *Climatic Change*, 133(2), 335-348.

Van Wagner, C. E. (1987). *Development and Structure of the Canadian Forest Fire Weather Index System*. Technical report 35. Petawawa National Forestry Institute, Canadian Forest Service, Chalk River, Ontario, CA.

Vano, J. A., Kim, J. B., Rupp, D. E., & Mote, P. W. (2015). Selecting climate change scenarios using impact-relevant sensitivities. *Geophysical Research Letters*, 42(13), 5516-5525.

Veblen, T. T., Baker, W. L., Montenegro, G., & Swetnam, T. W. (Eds.). (2006). *Fire and Climatic Change in Temperate Ecosystems of the Western Americas* (Vol. 160). Springer Science & Business Media, Berlin, Germany.

Whitlock, C., Shafer, S. L., & Marlon, J. (2003). The role of climate and vegetation change in shaping past and future fire regimes in the northwestern US and the implications for ecosystem management. *Forest Ecology and Management*, 178(1-2), 5-21.

FIRE, CO_2, AND CLIMATE EFFECTS ON MODELED VEGETATION AND CARBON DYNAMICS IN WESTERN OREGON AND WASHINGTON

Timothy J. Sheehan, Dominique Bachelet, and Ken Ferschweiler

PLOS ONE
1160 Battery Street
Koshland Building East, Suite 225
San Francisco, CA 94111
United States
Volume 14, Issue 1

3.1 Abstract

To develop effective long-term strategies, natural resource managers need to account for the projected effects of climate change as well as the uncertainty inherent in those projections. Vegetation models are one important source of projected climate effects. We explore results and associated uncertainties from the MC2 Dynamic Global Vegetation Model for the Pacific Northwest west of the Cascade crest. We compare model results for vegetation cover and carbon dynamics over the period 1895-2100 assuming: 1) unlimited wildfire ignitions versus stochastic ignitions, 2) no fire, and 3) a moderate CO_2 fertilization effect versus no CO_2 fertilization effect. Carbon stocks decline in all scenarios, except without fire and with a moderate CO_2 fertilization effect. The greatest carbon stock loss, approximately 23% of historical levels, occurs with unlimited ignitions and no CO_2 fertilization effect. With stochastic ignitions and a CO_2 fertilization effect, carbon stocks are more stable than with unlimited ignitions. For all scenarios, the dominant vegetation type shifts from pure conifer to mixed forest, indicating that vegetation cover change is driven solely by climate and that significant mortality and vegetation shifts are likely through the 21st century regardless of fire regime changes.

3.2 Introduction

Expected ecosystem responses to climate change include altered fire regimes (e.g., Sheehan et al., 2015; Rogers et al., 2011; Westerling et al., 2006), insect outbreaks (e.g., Kurz et al., 2008), hydrologic changes (e.g., Mote PW et al., 2003), altered nutrient cycling (e.g., Fowler et al., 2015), species range shifts (e.g., Chen et al., 2011; Rehfeldt et al., 2009; Rehfeldt et al., 2006), and novel species assemblages (e.g., Lurgi et al., 2012; Williams and Jackson, 2007). Vegetation models have been used to simulate such changes and provide resource managers projections to help their decision process (Littell et al., 2011). Estimating associated uncertainty allows managers to modulate their strategies (Littell et al., 2011).

Dynamic Global Vegetation Models (DGVMs) are process-based models that simulate vegetation, carbon, nutrient, and hydrological dynamics. They are driven by historical climate data and climate projections from General Circulation Models (GCMs; e.g., Cramer et al., 2001) or Earth System Models (ESMs; Turner et al., 2015). Sources of uncertainty in DGVM projections come from both external drivers such as climate and soil characteristics, and internal

characteristics such as model structure, empirical parameter values, built-in thresholds, and inherent assumptions and simplifications.

Another source of uncertainty is the complex relationship between fire and vegetation, which takes place over a range of spatial and temporal scales (Harris et al., 2016). Shifts in fire regime cause vegetation-altering feedbacks (e.g., Batllori et al., 2015; Kitzberger et al., 2016). The type and level of complexity of fire models adequate for management-relevant vegetation modeling remains unclear (Hantson et al., 2016). Researchers have implemented a variety of models (Sullivan 2009a-c) which may or may not include fuel types, fuel moisture, ignitions sources, fire suppression, rate of spread, and energy release component calculation (Hantson et al., 2016; Rabin et al., 2017). Disturbance modeling at the landscape scale is discussed in Keane et al. (2015), and fire model limitations and uncertainties in global vegetation models are described in Hantson et al. (2016) and Rabin et al. (2017). While comparing results among DGVMs using different fire models provides one way to characterize uncertainty, modifying the assumptions within a single DGVM's fire model is another method for sensitivity analysis and the exploration of fire-related uncertainty.

An additional source of uncertainty is the assumptions of CO_2 effects on plant productivity. CO_2 concentration effects on the water use efficiency and productivity of many species is not well known (e.g., Norby and Zak 2011). Increased productivity has been attributed to the CO_2 fertilization effect, but plant responses at large scales, with complex species assemblages, and combined with concurrent warming are uncertain (Way and Kroner, 2015). Free-air CO_2 enrichment experimental results (FACE; Hendrey et al., 1999) have shown that increased CO_2 can cause an increase in water use efficiency (WUE), leaf area index (LAI) and net primary productivity (NPP), but other factors, such as nutrient availability, may constrain responses over time (e.g., Ainsworth and Long, 2005). Species-specific response can modulate plant responses (e.g., Ainsworth and Long, 2005; Brodribb et al., 2009) and increased NPP may not increase C stocks (Norby and Zak 2011) just as increased WUE may not always lead to increased growth (Van Der Sleen et al., 2015). Uncertainties in the CO_2 fertilization effect underscore the importance of testing different assumptions with DGVMs to explore vegetation response.

A previous study simulated climate change effects on fire and vegetation in the Pacific Northwest using the MC2 DGVM (Sheehan et al., 2015). That study characterized the uncertainty due to different atmospheric CO_2 concentrations, climate drivers, and anthropogenic fire suppression actions. Fire occurrence and effects were driven by fuel condition thresholds and unlimited ignition sources. That study used a modest CO_2 fertilization effect proportional to atmospheric CO_2 concentration.

In this study, we evaluate uncertainty due to model assumptions regarding fire occurrence and CO_2-driven WUE. We compare results from unlimited ignitions and fixed fuel thresholds to those with stochastic ignition occurrence and ignition propagation based on fuel conditions. We also compare results obtained with and without CO_2 fertilization effect. We address the following research questions concerning vegetation and carbon dynamics in the MC2 DGVM:

1. What are the consequences of model assumptions about wildfire ignitions on spatial and temporal fire effects, carbon dynamics, and vegetation dynamics?
2. What are the consequences of model assumptions about CO_2 fertilization effects on carbon and vegetation dynamics?

3.3 Methods

3.3.1 Study area

The study area (Fig. 3.1) consists of portions of Oregon and Washington west of the Cascade Mountain Range crest that include Coast Range, Klamath Mountains/California High North Coast Range, Willamette Valley, Puget Lowlands, Cascades, and North Cascades Level III Ecoregions (Omernik and Griffith, 2014). This area falls under strong coastal influence with mild, wet winters and dry summers.

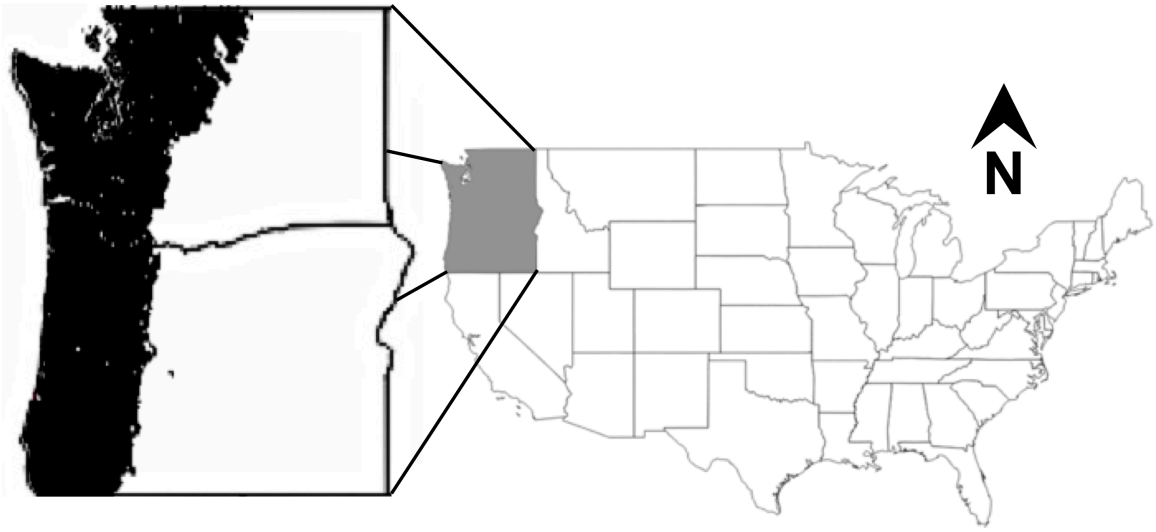

Fig. 3.1. Study area. Portions of Oregon and Washington west of the Cascade Mountain Range crest.

3.3.2 Model Description

We used the MC2 dynamic global vegetation model (DGVM; Bachelet et al., 2015) to simulate potential vegetation shifts, carbon fluxes, and wildfires. We simulated potential vegetation without land use effects, and with previously defined model parameterization and protocol for the conterminous United States (detailed in Bachelet et al., 2015).

MC2 does not simulate species, but instead simulates combinations of life forms in functional vegetation types. Woody lifeforms (trees and shrubs) are distinguished by leaf phenology (evergreen vs. deciduous) and morphology (needleleaf vs. broadleaf). The woody lifeforms and the relative dominance of C3 versus C4 grasses (including sedges and forbs) are simulated using climate thresholds. Carbon thresholds are used to distinguish broad vegetation types ranging from forest to grassland.

The fire module simulates fire occurrence and fire effects including area burned, mortality, consumption of aboveground biomass, carbon emissions, and nitrogen volatilization. Fire occurrence is simulated as a discrete event. The module runs on a pseudo-daily time step and derives a randomly distributed set of daily precipitation amounts from monthly precipitation values. Fuel types are derived from carbon stocks, and their characteristics are determined by weather effects on their moisture content (see Sheehan et al., 2015 for a detailed description). Per vegetation type fire return intervals (FRIs) and time since last fire are used to limit the maximum

portion of a grid cell burned. Fire occurrence is based on fuel condition thresholds and assumed unlimited ignitions. Fire suppression is simulated by assuming fires below empirical fuel condition thresholds can be extinguished while those above cannot.

For this study, we added an optional, three-stage stochastic ignition algorithm to MC2. Stage one uses a per-day ignition source probability and a Monte Carlo draw to determine whether a grid cell is exposed to an ignition source. Stage two checks fuel conditions for fine fuels moisture code (FFMC; Van Wagner and Forest 1987) and buildup index (BUI; Canadian Forestry Service, 1984). With unlimited ignitions, both FFMC and BUI must exceed a cell's vegetation type's threshold for a fire to be simulated. With the stochastic algorithm, they must both exceed a specified fraction of their respective thresholds. The third stage uses a Monte Carlo method to determine whether or not an ignition source initiates a fire. The probability of fire initiation is determined using the Chapman-Richards function:

$$s = (1 - e^{(-k * ffmc\_thresh\_frac)})^2 \quad (1)$$

where *ffmc_thresh_frac* is defined as the fraction of the FFMC threshold, adjusted to offset the curve so that values below the minimum threshold produce an initiation probability of zero, and values near the maximum threshold produce a initiation probability near 1.0. It is calculated as:

$$ffmc\_thresh\_frac = \max((ffmc\_min\_frac - ffmc\_max\_frac), 0) \quad (2)$$

k in (2) is the Chapman-Richards constant and is calculated as:

$$k = \frac{-\ln(1-\sqrt{0.99})}{ffmc\_max\_frac - ffmc\_min\_frac} \quad (3)$$

where *ffmc_min_frac* is the fraction of the FFMC threshold below which fire initiation approaches 0, and *ffmc_max_frac* is the fraction of the FFMC threshold where it approaches 1.

For this study, the daily ignition source probability was 0.001, the *threshold_fraction* was 0.6 and *ffmc_min_frac* and *ffmc_max_frac* were 0.6 and 0.99 respectively (Fig. 3.2).

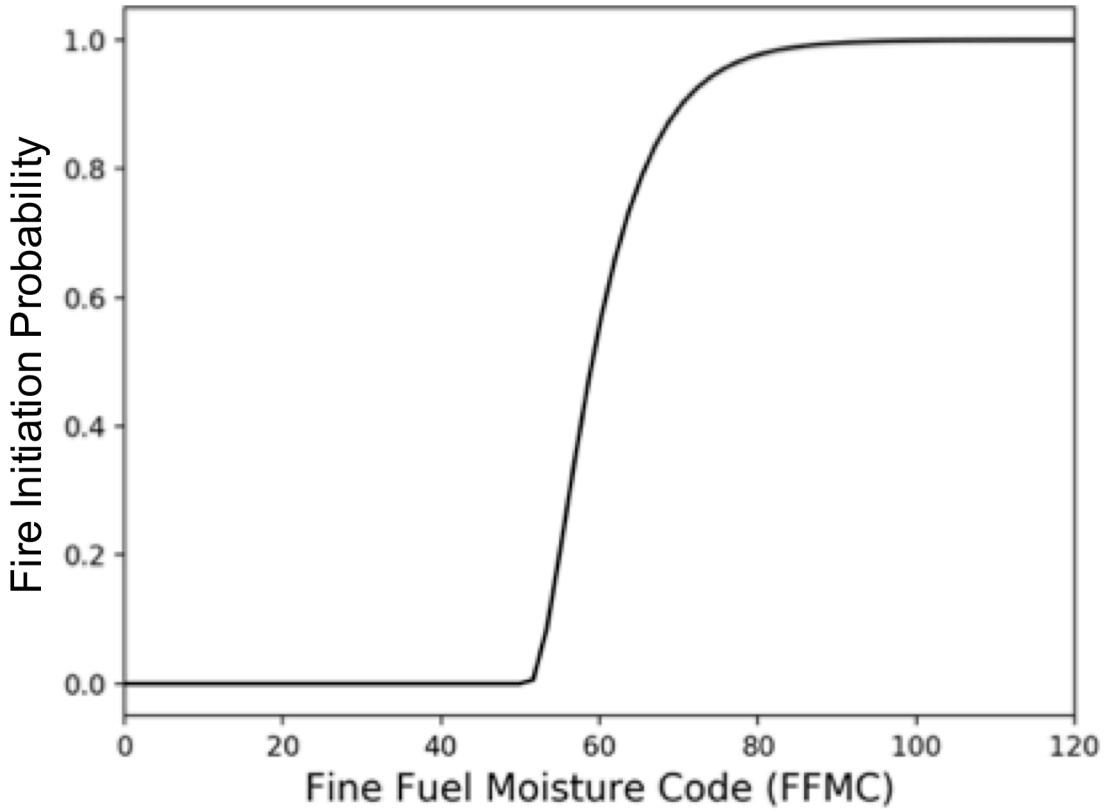

Fig. 3.2. Example fire initiation probability curve. This example is for a vegetation type with a fine fuel moisture code (FFMC) threshold of 86, an FFMC and buildup index (BUI) minimum threshold fraction of 0.6 and an FFMC maximum threshold fraction of 1.0.

To implement the CO_2 fertilization effect on WUE, MC2 uses a multiplier applied directly to production and transpiration. It is calculated as:

$$multiplier = 1 + \left(effect_{param} - 1\right) * \ log_2 \frac{current\_co2\_conc}{baseline\_co2\_conc} \qquad (4)$$

where *multiplier* is the value used to modify production, *effect_param* specifies the degree of the effect, *current_co2_conc* is the CO_2 concentration for the current model year, and *baseline_co2_conc* is the CO_2 concentration at which the multiplier is equal to 1.0 (350 ppm in this study). CO_2 concentrations above 350 ppm yield a positive effect and values below 350 yield a negative effect. The default CO_2 fertilization effect used in this study is 1.25 (Fig. 3.3).

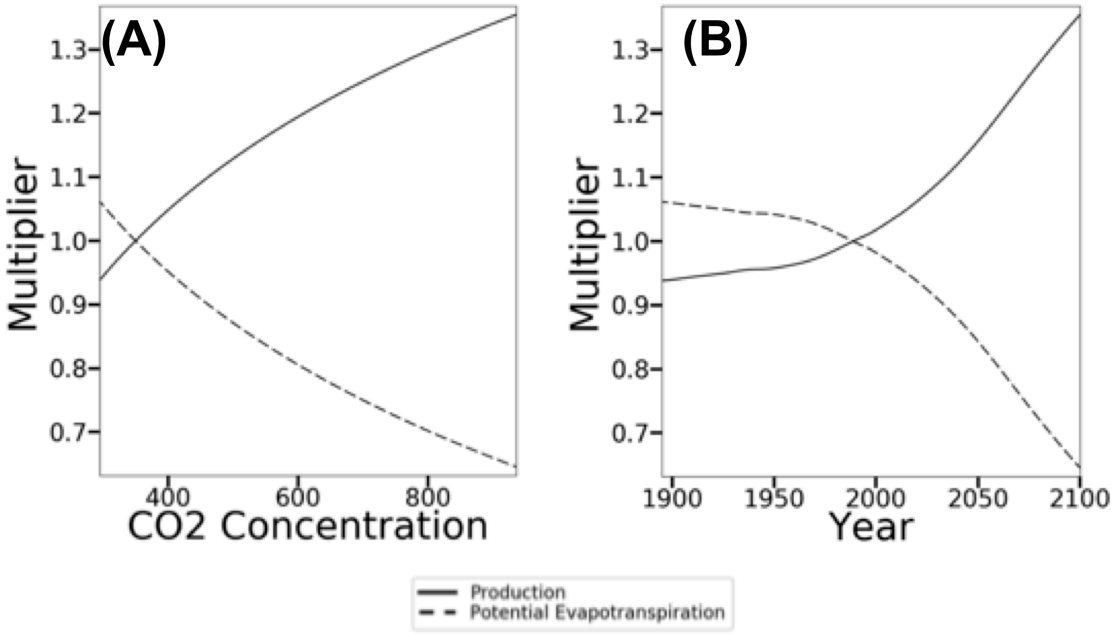

Fig. 3.3. CO_2 fertilization effect scalar. The scalar used in MC2 to calculate production and potential evapotranspiration vs (A) atmospheric CO_2 concentration and (B) year.

3.3.3 Model Runs

We ran MC2 on a 1/24 degree (~4 km) grid using PRISM (Daly et al., 2008) data for the historical period (1895-2010) and CCSM4 (National Center for Atmospheric Research) climate projections for 2011-2100 downscaled using the MACA (Abatzoglou and Brown 2012) algorithm which performs well in capturing fire danger indices across the western US. We used the CO_2 concentrations associated with RCP 8.5 ("business as usual"). We used the same CMIP5 climate, CO_2 projections, and soil data as in Sheehan et al. (2015).

3.3.4 Run Protocol

For this study, we ran the model with different combinations of fire and CO_2 fertilization effects (Table 3.1). To run without the CO_2 fertilization effect, atmospheric CO_2 concentration was held at its preindustrial value.

Table 3.1. Fire and CO_2 fertilization scenarios used for this study's MC2 runs

	With CO_2 fertilization effect (WCE for with CO_2 fertilization effect)	**Without CO_2 fertilization effect (NCE for no CO_2 fertilization effect)**
Assumed ignitions, without fire suppression (FF for full fire)	FF-WCE	FF-NCE
Assumed ignitions with fire suppression (FS)	FS-WCE	Not modeled
Stochastic fire (SF)	SF-WCE	Not modeled
No fire (NF)	NF-WCE	NF-NCE

3.3.5 Validation and comparison with other studies

For the FF-WCE and SF-WCE scenarios, we compared simulated results with the observed area burned from the Monitoring Trends in Burn Severity (MTBS; Eidenshink et al., 2009) fire perimeter dataset (https://www.mtbs.gov/) dataset. We also compared simulated results for aboveground live woody biomass (AGB), aboveground dead woody carbon (AGD), and total aboveground woody carbon (AGT) densities and pools with published modeled results based on observed Forest Inventory and Analysis (FIA) National Program (https://www.fia.fs.fed.us/) data (Hudiburg et al., 2009, hereafter, Hudiburg, available on Data Basin, http://bit.ly/2CcZ7wK; Turner et al., 2004; Turner et al., 2015; Law et al., 2004). To reflect the influence of land use, we limited our results to non human-affected (NHA) based on the LandFire US 140 EVT dataset (landfire.gov; 30m x 30m).

In the Hudiburg datasets, we set densities of carbon in human-affected (HA) cells to 0 before resampling to the 1/24 degree grid used in our simulation. We adjusted carbon densities from our simulation results by multiplying the results by the ratio of NHA area to the total grid cell area. We similarly adjusted results for validation against the MTBS (Eidenshink et al., 2009) dataset.

3.3.6 Analyses

We compared fire results, carbon dynamics, and vegetation change among modeled scenarios. For fire, we compared three results: 1) area with fire (AWF) – the total area of grid cells burned; 2) fraction area burned (FAB) – fraction of area burned in grid cells with fire; and 3) total area burned (TAB), the sum of (AWF * FAB) over all grid cells.

For carbon, we compared live and dead carbon (C) pools, total ecosystem C stocks, net primary production (NPP), net ecosystem production (NEP), net biome production (NBP), and C

consumed and emitted by fire (consumed C). Results for C pools and fluxes were summarized by taking mean values over the study area for five 30-year periods: early 20th c. (1895-1924), mid 20th c. (1936-1965), late 20th c. (1971-2000), mid 21st c. (2036-2065), and late 21st c. (2071-2100).

To more easily compare vegetation cover, we reclassified vegetation types into four categories: conifer forest; temperate mixed conifer/broadleaf forest; subtropical mixed conifer/broadleaf forest; and other which includes vegetation types dominated by grasses, forbs, and shrubs (Table S3.1). We then calculated the mode of the vegetation category for each grid cell for each time period and calculated the area-weighted distribution for each category.

3.3.7 Background climate description

Climate projections used for the future period (2011-2100) are overall hotter with decreasing summer precipitation towards the late 21st c. and increasing PET. Maximum annual and April-September average temperatures are relatively constant over the 20th c. (Fig. S3.1 A, S2 Table), with 30-year means varying by 0.2°C or less. During the 21st c. temperatures increase sharply with maximum annual temperatures 4.4°C higher, and April-September average temperatures 4.8°C higher than during the late 20th c. Annual precipitation increases by 4% from the early to late 20th c. and an additional 6% from the late 20th c. to the late 21st c. (Fig. S3.1 B, S2 Table). April-September precipitation increases 6% over the 20th c. but compared to the late 20th c., decreases by 15% during the mid 21st c. and again during the late 21st c. (Fig. S3.1 B, Table S3.2). PET (calculated by MC2) increases by 3% from the early to the late 20th c., increases by 29% from the late 20th c. to the mid 21st c. and by 52% from the early 20th c. to the late 21st c. (Fig. S3.1 C, Table S3.2).

3.4 Results

3.4.1 Validation and comparison with other studies

For simulations with fire, TAB (total area burned) is 2.3 to 2.8 times observed (Table 3.2). Burned areas for both observed and FF-WCE are concentrated across the southeastern corner of the study area, the central east edge, and the northeastern corner (Fig. 3.4 B-C). However, for FF-WCE, fire is simulated in the northernmost central portion of the area (northern Cascades) where it is not observed, and in the southeast fire is less concentrated than observed.

For SF-WCE, fire occurrence is also concentrated in the southeastern and northeast (Fig. 3.4 D), but also occurs more frequently throughout non-human-influenced areas than either for observed or FF-WCE, most commonly in the Cascade Mountains, southern Coast Range, and Puget Trough (Fig. 3.4 B-D).

Table 3.2. Area burned over the period 1985-2012 for MTBS and TAB (total area burned, AWF (area with fire) * FAB (fraction burned)) for with-fire simulations.

Scenario	Area Burned (km^2)
MTBS (km^2)	10,753
FF-WCE (km^2)	28,205
FS-WCE (km^2)	24,828
SF-WCE (km^2)	24,603
FF-NCE (km^2)	29,211

(FF-WCE: full fire, with CO_2 fertilization effect; FS-WCE: with fire suppression, with CO_2 fertilization effect; SF-WCE: with stochastic ignitions, with CO_2 fertilization effect; and FF-NCE: full fire, with no fertilization effect)

Table 3.3. Carbon values for Hudiburg and MC2 results.

Scenario	AGB Total (Pg)	AGD Total (Pg)	AGT Total (Pg)	AGB Densitiy (gCm^{-2}) (maximum)	AGD Density (gCm^{-2}) (maximum)	AGT Density (gCm^{-2}) (maximum)
Hudiburg	1.84	0.58	2.42	26900-44200 (~50000-~70000)	2600-9500 (~8000-~1700)	38100-46800 (~58000-~84000)
FF-WCE	2.31	1.11	3.43	14205	6826	21092
FS-WCE	2.32	1.12	3.44	14266	6887	21154
SF-WCE	2.05	1.04	3.09	12606	6395	19001
NF-WCE	2.89	1.19	4.07	17772	7318	25028
FF-NCE	2.26	1.09	3.35	13897	6703	20600
NF-NCE	2.82	1.17	3.99	17341	7195	24536

NHA (non-human affected) AGB (above ground live woody biomass), AGD (above ground dead woody carbon), and AGT (above ground total woody carbon). (For Hudiburg values, absolute values were calculated from Oregon and Washington maps published in Data Basin (http://bit.ly/2CcZ7wK), density values are maxima of mean trends (maxima of maximum trends in parentheses) from (Hudiburg et al., 2009) for ecoregions included in the current study; FF-WCE: full fire, with CO_2 fertilization effect; FS-WCE: with fire suppression, with CO_2 fertilization effect; SF-WCE: with stochastic ignitions, with CO_2 fertilization effect; NF-WCE: no fire, with CO_2 fertilization effect; FF-NCE: full fire, with no fertilization effect; and NF-NCE: no fire, with no CO_2 fertilization effect)

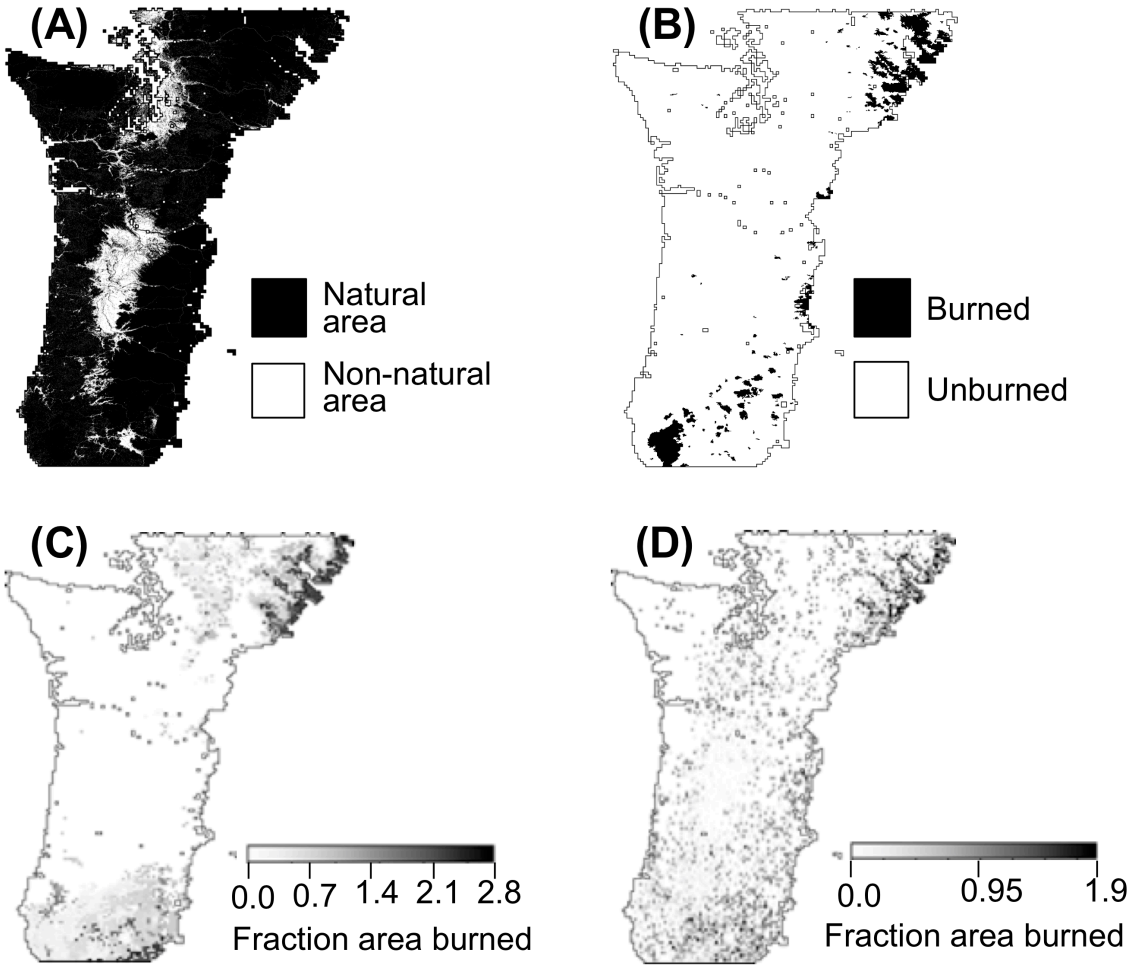

Fig. 3.4. Measures of fire on the landscape. (A) Natural and human-affected areas as determined by reclassifying LandFire vegetation classes; (B) MTBS fire perimeters for 1985-2015; (C) Total NHA (non-human affected) area burned over 1985-2015 (sum of FAB weighted by grid cells' NHA fraction over 1985-2015) for FF-WCE (full fire, with CO_2 fertilization effect); and (D) Total NHA area burned over 1985-2015 for SF-WCE (no fire suppression, with CO_2 fertilization effect).

Our simulated AGB ranges from 11 to 57% higher than that modeled by Hudiburg (Table 3.3). AGD carbon also ranges from 79 to 105% higher, and AGT carbon ranges from 28 to 68% higher. Among our simulations, AGB, AGD, and AGT are highest for NF-WCE, and lowest for SF-WCE (Table 3.3). AGB, AGD, and AGT densities are generally higher and more flatly distributed than Hudiburg's (Fig. 3.5). AGB, AGD, and AGT density distributions are flattest for SF-WCE.

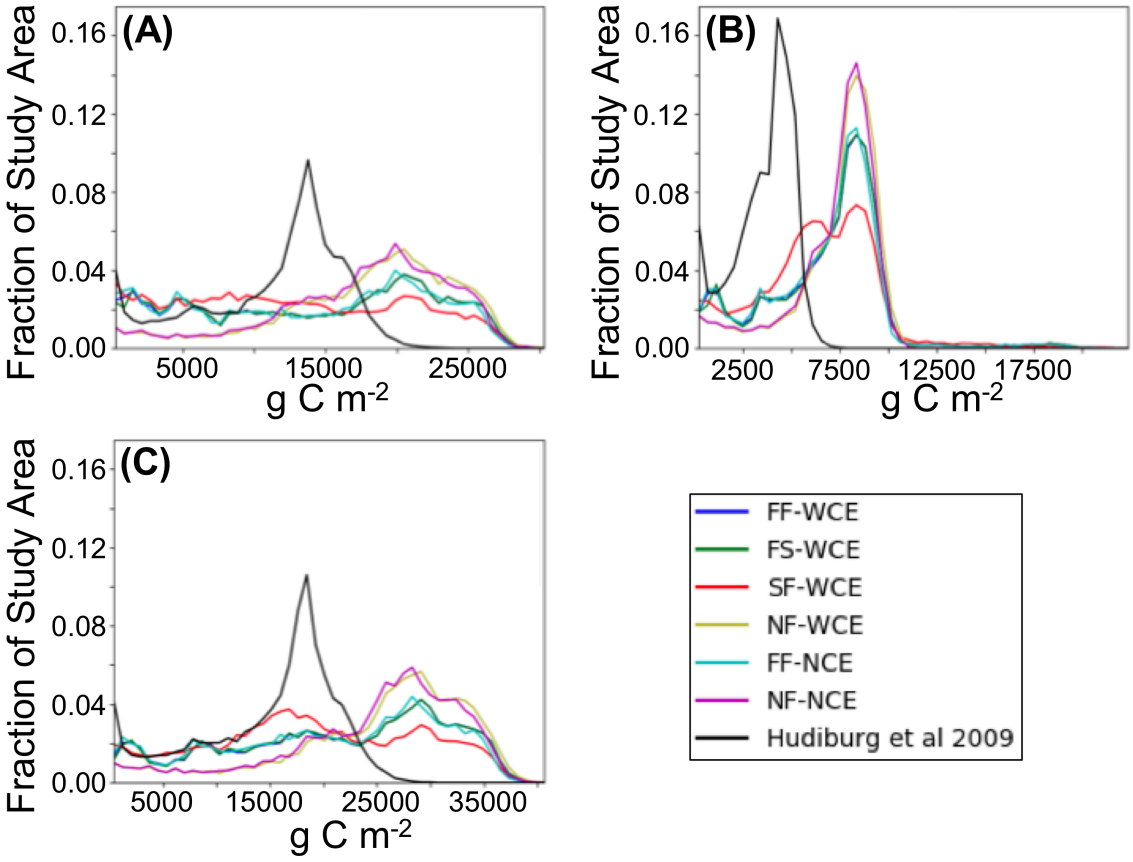

Fig. 3.5. Simulated carbon density distributions by the MC2 vegetation model for natural areas as a fraction of the entire study area. (A) AGB (above ground live woody biomass), (B) AGD (above ground dead woody carbon), and (C) AGT (above ground total woody carbon).

Our simulated AGB and AGT values fall below Hudiburg's mean trend maxima for those ecoregions in our study area (Coast Range, West Cascades, and Klamath mountains; Table 3.3). Our simulated AGD values fall between Hudiburg's lowest and highest mean trend maxima and below their largest mean trend maxima (Table 3.3).

Our simulated AGT carbon density (Fig. 3.6 C-E) is lowest in highly human affected (HA) areas (Fig. 3.6 A) such as in the Willamette Valley and surrounding Puget Sound. In these areas, there is little difference among values for our simulations or between our simulations and Hudiburg's (Fig. 3.6 B).

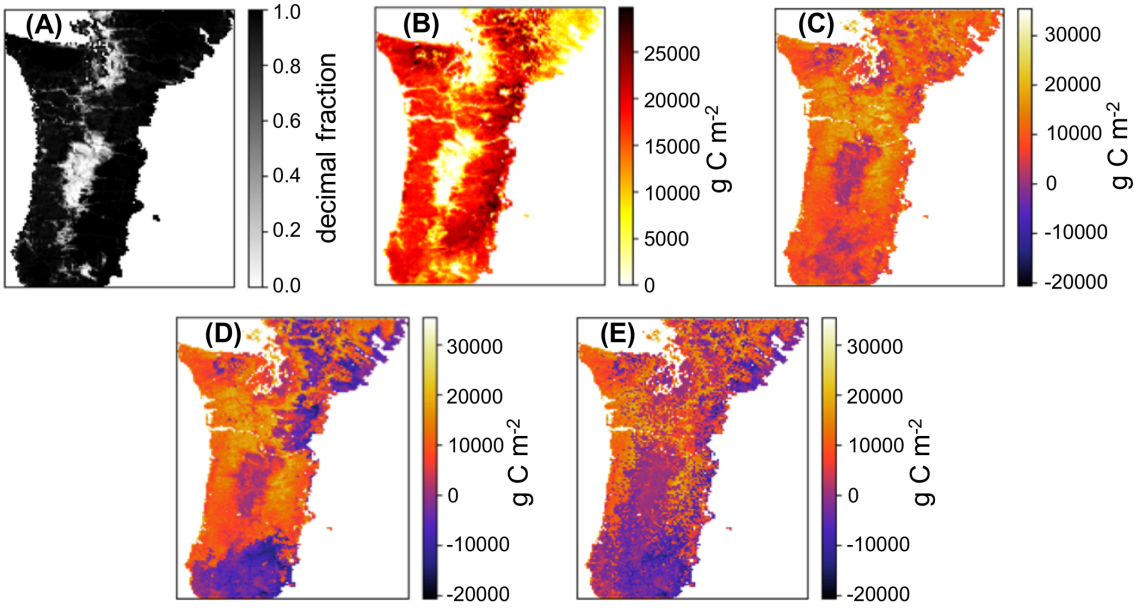

Fig. 3.6. Human affected areas and carbon measures over the study area. (A) Density of NHA (non-human-affected) area used to calculate carbon densities. (B) AGT (aboveground total woody biomass) densities derived from (Hudiburg et al., 2009) for 1991-1999. (C-E) Differences in carbon densities calculated by subtracting Hudiburg's results from simulation results for 1991-1999: (C) NF-WCE (no fire, with CO_2 fertilization effect); (D) FF-WCE (full fire, with CO_2 fertilization effect) (D) SF-WCE (stochastic fire, with CO_2 fertilization effect).

For NF-WCE (Fig. 3.6 C) our simulated AGT carbon density is higher than Hudiburg's over most of the study area. For FF-WCE (Fig. 3.6 D) our simulated AGT carbon density is generally lower in areas that have experienced fire and higher in areas that have not. Similarly, for SF-WCE, our simulated carbon density is lower in areas having experienced fire, but those areas are greater due to the spatially broader simulated fire occurrence (Fig. 3.6 D). Compared to other studies (Turner et al., 2004; Turner et al., 2015; Law et al., 2004) in the same region, our values for NPP, NEP, and NBP are generally lower, while our values for carbon stocks are higher (Table 3.4).

3.4.2 Fire

AWF is identical for FF-NCE and FF-WCE throughout the simulation (Fig. 3.7 A, Table 3.5). FAB for FF-NCE is very similar to that for FF-WCE during the early 20th c. but is higher through the rest of the simulation with a peak difference of 1.08 % of cell area during the late 21st c. (Fig. 3.7 B, Table 3.5). TAB for FF-NCE is similar to that for FF-WCE through the

20th c., but is higher during the 21st c. with a maximum difference of 0.28 % during the late 21st c. (Fig. 3.7 C, Table 3.5).

AWF for FS-WCE is virtually identical to that for FF-WCE during the early 20th c. but is less during the remainder of the simulation with the largest difference (11.28% of area) during the mid 21st c. (Fig. 3.7 A, Table 3.5). FAB for FS-WCE is similar to that for FF-WCE through the 20th c., but is greater during the 21st c, with the largest difference (2.79% of cell area) during the mid 21st c. (Fig. 3.7 B, Table 3.5). TAB for FS-WCE is identical to that for FF-WCE during the early 20th c., but lower during all other periods, with the largest difference (0.29% of area) during the mid 21st c. (Fig. 3.7 C, Table 3.5).

AWF is consistently lower for SF-WCE than for FF-WCE during the entire simulation with the greatest difference (24.34% of area) during the late 21st c. (Fig. 3.7 A, Table 3.5). FAB is consistently higher for SF-WCE than for FF-WCE throughout the simulation with the greatest difference (49.71% of area) occurring in the early 20th c. (Fig. 3.7 B, Table 3.5). TAB is initially higher for SF-WCE than for FF-WCE during the early and mid 20th c. (largest difference of 0.28% of area during mid 20th c.) but is lower for the remainder of the simulation (largest difference of 0.60% of area during the mid 21st c.; Fig. 3.7 B, Table 3.5).

For WCE scenarios, NPP increases by approximately 5% over the 20th c. and an additional 18% over the 21st c. (Fig. 3.8 A, Table 3.6). NPP varies by less than 3% across all WCE scenarios within any time period. For FF-NCE, NPP does not vary over the 20th c. but decreases by 10% over the 21st c. (Fig. 3.8 A, Table 3.6). NPP for NF-NCE increases by 1% over the 20th c. and decreases by 8% over the 21st c. (Fig. 3.8 A, Table 3.6).

Table 3.4. Carbon flux and pool values from other studies and the current study.

Source	Period	Method	NPP ($gCm^{-2}yr^{-1}$)	NEP ($gCm^{-2}yr^{-1}$)	NBP or NECB ($gCm^{-2}yr^{-1}$)	C stocks (gCm^{-2})	Comments
(Turner et al., 2004)[1]	1986-2010	Biome BGC informed by field and remote sensing observations		~100 to ~200			Includes harvest, fire, and land cover
(Turner et al., 2015)[2]	1986-2010	Biome BGC informed by field and remote sensing observations	~600 to ~800	~0 to ~-600	~22 to ~67		West Cascades ecoregion only; study includes fire, timber harvest, land use, and pests
(Law et al., 2004)[3]	1980-1997	Biome BGC informed by field and remote sensing observations	640 to 700	190 to 226	1684	32810 to 38810	Forested areas within western OR; includes fire and harvest
(Hudiburg et al., 2009)[5]	1991-1999	Biome BGC informed by field observations	540 to 820 (~1200 to ~1500)			32810 to 46800 (~58000 to 84000)	OR and Northern CA, C Stocks are for above ground live and dead carbon including only trees and shrubs.
FF-WCE	1971-2000		1198	52	19	54400	
FS-WCE	1971-2000		1198	52	21	54500	
SF-WCE	1971-2000		1199	65	20	50900	
NF-WCE	1971-2000		1214	29	29	59700	
FF-NCE	1971-2000		1136	19	-13	53300	
NF-NCE	1971-2000		1152	-2	-3	58500	

(FF-WCE: full fire, with CO_2 fertilization effect; FS-WCE: with fire suppression, with CO_2 fertilization effect; SF-WCE: with stochastic ignitions, with CO_2 fertilization effect; NF-WCE: no fire, with CO_2 fertilization effect; FF-NCE: full fire, with no fertilization effect; and NF-NCE: no fire, with no CO_2 fertilization effect. [1]NEP values included for only for those ecoregions within our study area; [2]NECB listed in table, calculated as NEP minus fire emissions minus simulated harvest removals; [3]Values included for only forested lands in areas falling within our study area; [4]Value is for all of forested western Oregon, reported as NBP; [5]Oregon and northern California, values are the maximum versus stand age, values are from central trend line of data with maximum values in parentheses.)

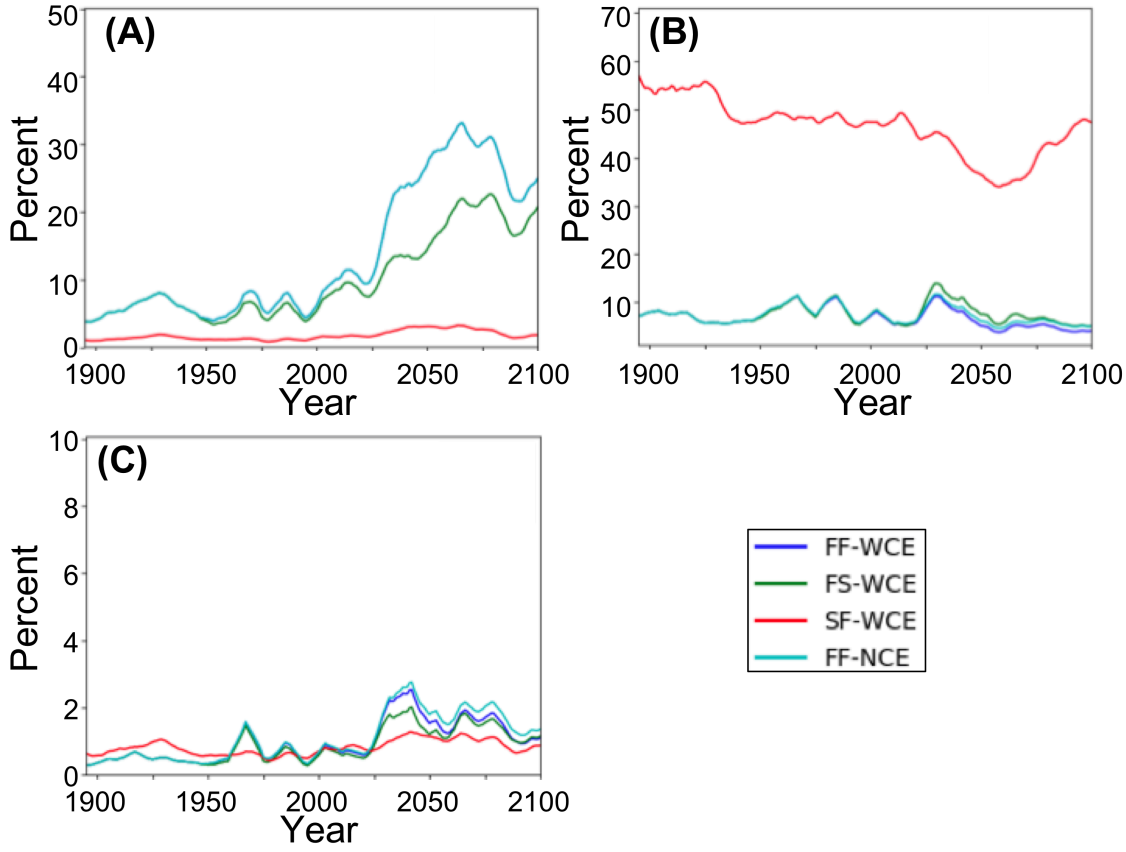

Fig. 3.7. Fire results by scenario as a percentage of total area. (A) AWF (Area with fire; the area of all grid cells experiencing any fire); (B) FAB (Fraction area burned; the fraction of are burned in grid cells with fire); and (C) TAB (Total area burned; the sum of (AWF * FAB) over all grid cells). (FF-WCE: full fire, with CO_2 fertilization effect; FS-WCE: with fire suppression, with CO_2 fertilization effect; SF-WCE: with stochastic ignitions, with CO_2 fertilization effect; and FF-NCE: full fire, with no fertilization effect. Results smoothed using triangle smoothing +/- 8 years.)

Table 3.5. Summaries of fire characteristics over the study area.

1895-1924	**AWF (%)**	**FAB (%)**	**TAB (%)**
FF-WCE	5.31	8.95	0.48
FS-WCE	5.31	8.95	0.48
SF-WCE	1.25	58.66	0.73
FF-NCE	5.31	8.95	0.48
1936-1965	**AWF (%)**	**FAB (%)**	**TAB (%)**
FF-WCE	4.62	8.12	0.38
FS-WCE	4.27	7.99	0.34
SF-WCE	1.21	49.44	0.60
FF-NCE	4.62	8.19	0.38
1971-2000	**AWF (%)**	**FAB (%)**	**TAB (%)**
FF-WCE	5.94	9.43	0.56
FS-WCE	4.88	9.70	0.47
SF-WCE	1.08	49.46	0.53
FF-NCE	5.94	9.64	0.57
2036-2065	**AWF (%)**	**FAB (%)**	**TAB (%)**
FF-WCE	26.93	6.47	1.74
FS-WCE	15.65	9.26	1.45
SF-WCE	2.97	38.26	1.14
FF-NCE	26.93	7.38	1.99
2071-2100	**AWF (%)**	**FAB (%)**	**TAB (%)**
FF-WCE	26.36	5.03	1.33
FS-WCE	19.90	6.37	1.27
SF-WCE	2.02	43.88	0.89
FF-NCE	26.36	6.11	1.61

Mean annual percentage of AWF (area with fire; area of gridcells in which fire occurred); FAB (fraction area burned; area weighted mean of the fraction of burning in burned grid cells); and TAB (total area burned; AWF * FAB). (FF-WCE: full fire, with CO_2 fertilization effect; FS-WCE: with fire suppression, with CO_2 fertilization effect; SF-WCE: with stochastic ignitions, with CO_2 fertilization effect; and FF-NCE: full fire, with no fertilization effect)

3.4.3 Carbon fluxes

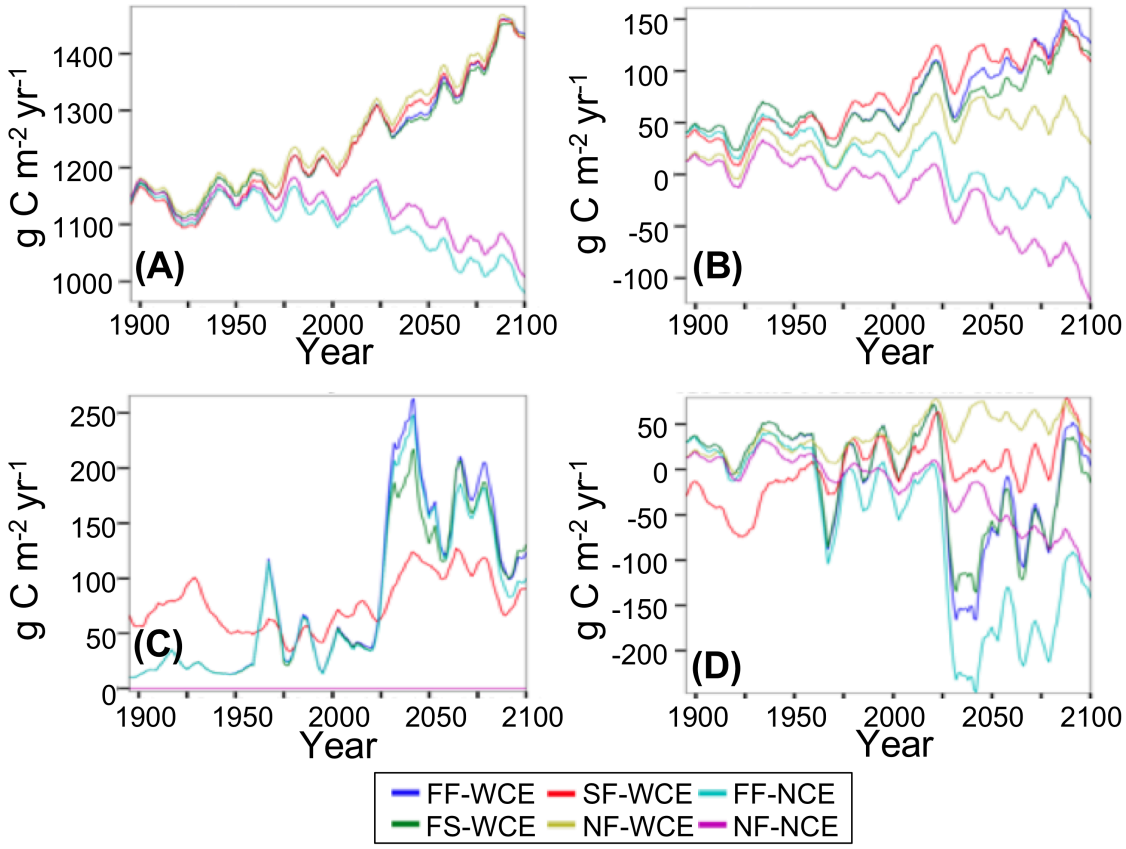

Fig. 3.8. Carbon fluxes simulated by the MC2 vegetation model. (A) NPP (net primary production), (B) NEP (net ecosystem production), (C) C consumed by fire, and (D) NBP (net biome production). (FF-WCE: full fire, with CO_2 fertilization effect; FS-WCE: with fire suppression, with CO_2 fertilization effect; SF-WCE: with stochastic ignitions, with CO_2 fertilization effect; NF-WCE: no fire, with CO_2 fertilization effect; FF-NCE: full fire, with no fertilization effect; and NF-NCE: no fire, with no CO_2 fertilization effect. Results smoothed using triangle smoothing +/- 8 years.)

Table 3.6. Mean (standard deviation in parentheses) carbon fluxes by time period for simulation scenarios.

NPP (g C m^{-2} yr^{-1})					
	1895 - 1924	**1936-1965**	**1971 - 2000**	**2036 - 2065**	**2071 - 2100**
FF-WCE	1143 (79)	1173 (94)	1198 (87)	1315 (132)	1422 (136)
FS-WCE	1143 (79)	1173 (94)	1198 (87)	1307 (130)	1413 (134)
SF-WCE	1131 (79)	1156 (92)	1199 (87)	1329 (133)	1420 (133)
NF-WCE	1150 (80)	1179 (94)	1214 (87)	1344 (131)	1430 (130)
FF-NCE	1136 (80)	1149 (93)	1136 (81)	1072 (122)	1024 (109)
NF-NCE	1143 (80)	1155 (93)	1152 (81)	1111 (126)	1060 (114)
NEP (g C m^{-2} yr^{-1})					
	1895 - 1924	**1936 - 1965**	**1971 - 2000**	**2036 - 2065**	**2071 - 2100**
FF-WCE	37 (46)	55 (50)	52 (49)	99 (66)	136 (100)
FS-WCE	37 (46)	55 (50)	52 (49)	82 (63)	121 (97)
SF-WCE	27 (46)	48 (49)	65 (50)	115 (67)	126 (96)
NF-WCE	10 (46)	27 (49)	29 (49)	62 (62)	54 (92)
FF-NCE	32 (46)	42 (49)	19 (44)	-12 (61)	-19 (76)
NF-NCE	5 (46)	14 (48)	-3 (44)	-40 (63)	-82 (80)
Consumed (g C m^{-2} yr^{-1})					
	1895 - 1924	**1936 - 1965**	**1971 - 2000**	**2036 - 2065**	**2071 - 2100**
FF-WCE	20 (32)	15 (19)	34 (55)	177 (217)	145 (139)
FS-WCE	20 (32)	15 (18)	31 (52)	155 (199)	139 (132)
SF-WCE	71 (51)	53 (36)	45 (30)	112 (72)	92 (48)
NF-WCE	0 (0)	0 (0)	0 (0)	0 (0)	0 (0)
FF-NCE	20 (32)	15 (18)	33 (54)	169 (200)	126 (124)
NF-NCE	0 (0)	0 (0)	0 (0)	0 (0)	0 (0)
NBP (g C m^{-2} yr^{-1})					
	1895 - 1924	**1936 - 1965**	**1971 - 2000**	**2036 - 2065**	**2071 - 2100**
FF-WCE	17 (61)	40 (56)	19 (87)	-77 (257)	-7.9 (214)
FS-WCE	17 (61)	40 (56)	21 (85)	-73 (238)	-18 (207)
SF-WCE	-44 (71)	-5 (70)	20 (64)	3 (126)	34 (122)
NF-WCE	10 (46)	27 (49)	29 (49)	62 (62)	54 (92)
FF-NCE	12 (61)	27 (55)	-13 (81)	-181 (233)	-144 (174)
NF-NCE	5 (46)	14 (48)	-3 (43)	-40 (63)	-82 (80)

(NPP: net primary production; NEP: net ecosystem production; NBP: net biome production; FF-WCE: full fire, with CO_2 fertilization effect; FS-WCE: with fire suppression, with CO_2 fertilization effect; SF-WCE: with stochastic ignitions, with CO_2 fertilization effect; NF-WCE: no fire, with CO_2 fertilization effect; FF-NCE: full fire, with no fertilization effect; and NF-NCE: no fire, with no CO_2 fertilization effect)

Over the simulation period, NEP increases for WCE scenarios and decreases for both NCE scenarios (Fig. 3.8 B, Table 3.6). Throughout the simulation period, for FF-WCE and FF-NCE, NEP increases more than for their no-fire counterparts (Fig. 3.8 B, Table 3.6).

Consumed C for with-fire scenarios (FF-WCE, FS-WCE, FF-NCE) is nearly identical during the 20th c. (Fig. 3.8 C, Table 3.6). For these scenarios, consumed C triples from the late 20th c. to the late 21st c. The pattern of consumed C is similar among these scenarios throughout the 21st c., but the range of values increases by the end of the 21st c. For SF-WCE, consumed C is higher than that for FF-WCE over the 20th c. but lower during the 21st c. The standard deviation of SF-WCE consumed C is higher than that for FF-WCE during the early and mid 20th c. but lower during the late 20th c. and the mid 21st c. (Table 3.6).

During the early and mid 20th c. NBP is lower for SF-WCE than that for all other scenarios but becomes higher than that for all scenarios except NF-WCE by the end of the 21st c. (Fig. 3.8 D, Table 3.6). NBP for SF-WCE shows much less variability than FF-WCE in the mid and late 21st c. NBP for FF-WCE and FS-WCE falls sharply from the late 20th c. to the mid 21st c. but rises during the late 21st c. NBP for FF-NCE decreases more abruptly from the late 20th c. to the mid 21st c. and increases less during the late 21st c. NBP for NF-WCE increases from the late 20th to the mid 21st c. then decreases during the late 21st c. NBP for NF-NCE decreases from the late 20th c. through the mid and late 21st c.

3.4.4 Carbon pools

Live C (C in live plants), dead C (standing dead trees, litter, and soil C), and total ecosystem C (ecosystem C hereafter) for NF-WCE increase throughout the simulation by 4, 6, and 10% respectively, with the live to dead C ratio decreasing from 0.65 to 0.61 (Fig. 3.9 A-D, Table 3.7). For FF-WCE and FS-WCE live C decreases 7.5% from the late 20th c. to the late 21st c. (Fig. 3.9 A, Table 3.7). Over the same period dead C pools increase 4 and 6% for FF-WCE and FS-WCE respectively, and ecosystem C decreases 7% for both scenarios, and live to dead ratios decrease from 0.56 to 0.39 and 0.56 to 0.38 for FF-WCE and NF-WCE respectively (Fig. 3.9 A-D, Table 3.7). For FF-NCE, live, dead C, and ecosystem C decrease by 41, 12, and 22% respectively from the late 20th c. through the late 21st c. and the live to dead C ratio decreases (from 0.56 to 0.38; Fig. 3.9 A-D, Table 3.7).

For SF-WCE, live C decreases by 16% from the early 20th c. to the mid 20th c., dead C increases 7% from the late 20th to the late 21st c., and ecosystem C decreases by 2% from the

early 20th to the late 21st c. (Fig. 3.9 A-C, Table 3.7). Over the same period, the live to dead C ratio decreases from 0.55 to 0.42 (Fig. 3.9 D, Table 3.7).

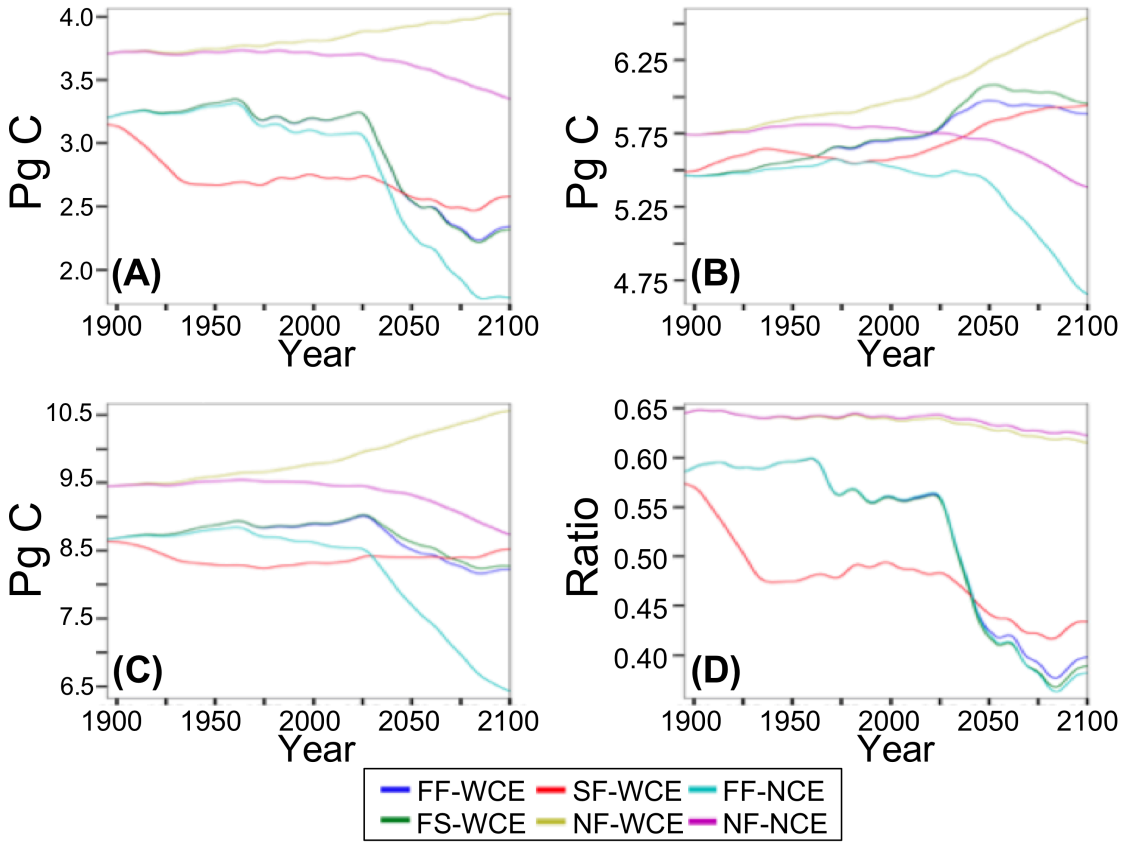

Fig. 3.9. Carbon pools and live/dead ratios. (A) live C, (B) dead C, (C) ecosystem C, and (d) ratio of live C to dead C. (FF-WCE: full fire, with CO_2 fertilization effect; FS-WCE: with fire suppression, with CO_2 fertilization effect; SF-WCE: with stochastic ignitions, with CO_2 fertilization effect; NF-WCE: no fire, with CO_2 fertilization effect; FF-NCE: full fire, with no fertilization effect; and NF-NCE: no fire, with no CO_2 fertilization effect. Results smoothed using triangle smoothing +/- 8 years.)

Table 3.7. Mean (standard deviation in parentheses) carbon pool values and live to dead C ratios by time period.

Live Carbon (Pg)					
	1895 - 1924	**1936 - 1965**	**1971 - 2000**	**2036 - 2065**	**2071 - 2100**
FF-WCE	3.24 (0.025)	3.32 (0.033)	3.18 (0.032)	2.60 (0.149)	2.30 (0.059)
FS-WCE	3.24 (0.025)	3.32 (0.033)	3.18 (0.032)	2.60 (0.151)	2.28 (0.058)
SF-WCE	3.03 (0.104)	2.66 (0.017)	2.72 (0.037)	2.59 (0.053)	2.52 (0.048)
NF-WCE	3.72 (0.014)	3.75 (0.019)	3.79 (0.020)	3.93 (0.025)	4.00 (0.024)
FF-NCE	3.23 (0.024)	3.29 (0.027)	3.12 (0.036)	2.33 (0.186)	1.83 (0.078)
NF-NCE	3.72 (0.014)	3.72 (0.014)	3.72 (0.011)	3.61 (0.037)	3.43 (0.053)
Dead Carbon (Pg)					
	1895 - 1924	**1936 - 1965**	**1971 - 2000**	**2036 - 2065**	**2071 - 2100**
FF-WCE	5.47 (0.015)	5.56 (0.019)	5.67 (0.024)	5.95 (0.037)	5.91 (0.024)
FS-WCE	5.47 (0.015)	5.56 (0.019)	5.68 (0.026)	6.04 (0.050)	6.00 (0.033)
SF-WCE	5.54 (0.042)	5.62 (0.022)	5.56 (0.015)	5.81 (0.049)	5.92 (0.015)
NF-WCE	5.75 (0.014)	5.85 (0.018)	5.92 (0.027)	6.24 (0.063)	6.46 (0.052)
FF-NCE	5.47 (0.012)	5.52 (0.009)	5.55 (0.020)	5.38 (0.100)	4.87 (0.150)
NF-NCE	5.75 (0.011)	5.80 (0.008)	5.79 (0.010)	5.67 (0.030)	5.48 (0.069)
Total Ecosystem Carbon (Pg)					
	1895 - 1924	**1936 - 1965**	**1971 - 2000**	**2036 - 2065**	**2071 - 2100**
FF-WCE	8.70 (0.028)	8.88 (0.049)	8.85 (0.026)	8.54 (0.124)	8.21 (0.052)
FS-WCE	8.71 (0.028)	8.88 (0.050)	8.87 (0.027)	8.64 (0.110)	8.28 (0.052)
SF-WCE	8.57 (0.064)	8.29 (0.016)	8.28 (0.032)	8.40 (0.017)	8.44 (0.054)
NF-WCE	9.47 (0.017)	9.60 (0.033)	9.71 (0.042)	10.2 (0.083)	10.5 (0.072)
FF-NCE	8.70 (0.023)	8.81 (0.032)	8.67 (0.033)	7.71 (0.263)	6.69 (0.213)
NF-NCE	9.46 (0.013)	9.52 (0.016)	9.51 (0.007)	9.30 (0.063)	8.91 (0.120)
Live / Dead (ratio)					
	1895 - 1924	**1936 - 1965**	**1971 - 2000**	**2036 - 2065**	**2071 - 2100**
FF-WCE	0.59 (0.005)	0.60 (0.004)	0.56 (0.007)	0.44 (0.027)	0.39 (0.011)
FS-WCE	0.59 (0.005)	0.60 (0.004)	0.56 (0.008)	0.43 (0.028)	0.38 (0.011)
SF-WCE	0.55 (0.023)	0.48 (0.005)	0.49 (0.008)	0.45 (0.013)	0.42 (0.008)
NF-WCE	0.65 (0.003)	0.64 (0.003)	0.64 (0.003)	0.63 (0.004)	0.61 (0.003)
FF-NCE	0.59 (0.005)	0.60 (0.005)	0.56 (0.007)	0.43 (0.030)	0.38 (0.011)
NF-NCE	0.65 (0.003)	0.64 (0.003)	0.64 (0.003)	0.64 (0.005)	0.63 (0.003)

(Pg: petagram; FF-WCE: full fire, with CO_2 fertilization effect; FS-WCE: with fire suppression, with CO_2 fertilization effect; SF-WCE: with stochastic ignitions, with CO_2 fertilization effect; NF-WCE: no fire, with CO_2 fertilization effect; FF-NCE: full fire, with no fertilization effect; and NF-NCE: no fire, with no CO_2 fertilization effect)

3.4.5 Vegetation

Vegetation composition is consistent across all scenarios, with the differences of 3% or less for all categories in each time period (Fig. 3.10, Table 3.8). The *other* category (non-forest) comprises two percent or less of the area from the early 20th c. through the late 21st c. Through the 20th c., conifer covers between 88% to 94% of the area with temperate mixed forest

accounting for the remainder of the forested area. From the late 20th to mid 21st c. conifer forest extent decreases to 53 to 55% of the area, temperate mixed forest increases to 39 to 40%, and subtropical mixed forest increases to 5% of the area. During the late 21st c. conifer forest extent decreases to 34 to 35%, temperate mixed forest decreases to 32%, and subtropical mixed forest increases to 33% of the area.

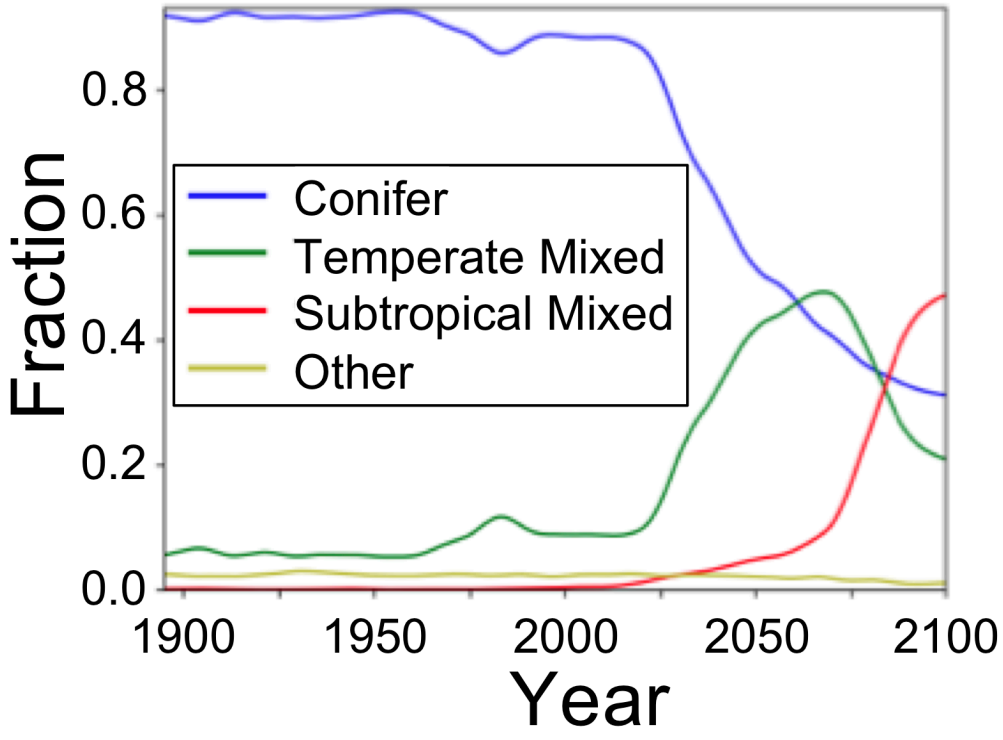

Fig. 3.10. Vegetation class mix over time for FF-WCE (full fire with CO_2 fertilization) scenario. All other scenarios yield virtually identical results.

Table 3.8. Simulated vegetation composition (%) of study area.

1895-1924	Con	T Mix	S Mix	Oth
FF-WCE	92	6	0	2
FS-WCE	92	6	0	2
SF-WCE	92	6	0	2
NF-WCE	94	6	0	0
FF-NCE	92	6	0	2
NF-NCE	94	6	0	0
1936-1965	**Con**	**T Mix**	**S Mix**	**Oth**
FF-WCE	93	5	0	2
FS-WCE	93	5	0	1
SF-WCE	92	5	0	2
NF-WCE	94	5	0	0
FF-NCE	93	5	0	2
NF-NCE	94	5	0	0
1971-2000	**Con**	**T Mix**	**S Mix**	**Oth**
FF-WCE	88	10	0	2
FS-WCE	88	10	0	2
SF-WCE	88	10	0	2
NF-WCE	90	10	0	0
FF-NCE	87	10	0	3
NF-NCE	90	10	0	0
2036-2065	**Con**	**T Mix**	**S Mix**	**Oth**
FF-WCE	54	40	5	2
FS-WCE	53	40	5	3
SF-WCE	53	40	5	2
NF-WCE	55	40	5	0
FF-NCE	53	39	5	3
NF-NCE	55	40	5	0
2071-2100	**Con**	**T Mix**	**S Mix**	**Oth**
FF-WCE	35	32	33	0
FS-WCE	34	32	33	1
SF-WCE	34	32	33	1
NF-WCE	35	32	33	0
FF-NCE	34	32	33	1
NF-NCE	35	32	33	0

(Con: conifer; T Mix: temperate mixed conifer and broadleaf; S Mix: subtropical mixed conifer and broadleaf; Oth: other; Veg: vegetation; FF-WCE: full fire, with CO_2 fertilization effect; FS-WCE: with fire suppression, with CO_2 fertilization effect; SF-WCE: with stochastic ignitions, with CO_2 fertilization effect; NF-WCE: no fire, with CO_2 fertilization effect; FF-NCE: full fire, with no fertilization effect; and NF-NCE: no fire, with no CO_2 fertilization effect)

3.5 Discussion

3.5.1 Validation, comparison with other studies, and limitations

For unlimited ignition scenarios versus observed fires there is general agreement between areas where area burned is greatest. The lack of concentrated modeled TAB in the southwest corner of the region versus observed (Fig. 3.4 C vs 3.4 B) may be due to the use of a dataset with deeper soils than are actually present. In the model, shallower soils retain less water, potentially leading to drier fuel conditions and greater fire. In this part of the study area, the STATSGO dataset used in the simulation has soil depths two to four times as deep as the more recent SSURGO dataset (Peterman et al., 2014).

The overall higher simulated TAB and the higher simulated TAB east of Puget Sound – primarily due to simulated fires in 1987 and 2003 – underscore the importance of modeling wildfire ignition limitations in addition to fuel limitations. Stochastic fire (SF) mitigates the overall higher TAB, but simulates more fires than observed in areas that are commonly fuel limited (Cascades and Coast range). The stochastic ignitions algorithm used in the SF-WCE scenario was implemented as a proof of concept with a random algorithm to locate ignition sources. An algorithm using a probability surface based on factors affecting ignition sources such as human presence and infrastructure (e.g., Pew and Larsen, 2001; Syphard et al., 2007) and lightning strikes (e.g., Rorig and Ferguson, 1999; Dorado et al., 2011) would likely produce more realistic results but this kind of data is lacking both for the beginning of 20th century and for the 21st century. Secondly, informing the algorithm with known relationships between fuel conditions and fire initiation would likely also improve results. Additionally, considering conditions more or less conducive to fire initiation, such as slope and other topographic characteristics could also contribute to higher quality fire modeling. Multiple model runs with stochastic ignition sources and success should also be considered to generate a statistics-based projection of fire on the landscape.

Differences between our results and those of other studies (Table 3.4) are due to a number of factors. First, observation-based models generally only consider aboveground stocks, while MC2 models above- and belowground carbon, including soils and litter. Second, other studies include disturbances that MC2 does not, for example logging, insect infestations, and disease, which would account for some of the higher carbon stock value in our results. Third, the

mapping of human-affected (HA) areas reduces differences due to land use, but HA areas can only be considered a first approximation of human influences on the landscape, including historical logging in areas now recovering and fires not accounted for in the simulation, (e.g., the Tillamook fire; Rienstra et al., 1991).

Our results contrast with (Law et al., 2018), which projects increasing forest carbon stocks in Oregon forests through the 21st c. That study assumes a CO_2 fertilization effect. However, unlike ours, that study includes mortality from forest harvest and beetles and also assumes the same vegetation that is lost regrows at its maximum potential.

MC2 simulates potential vegetation most adapted to climate inputs. However, vegetation can endure under suboptimal conditions, slowing the replacement of one vegetation type by another, remaining until a sudden disturbance or mortality due to crossing a physiological threshold allows for rapid change. Moreover, MC2 does not simulate seed production, seedling establishment, or natural succession. These factors should be accounted for when using model projections for management decisions.

Land use, insects, pathogens, and invasive species are important disturbances that may be amplified or mitigated by climate change (e.g., Dale, 1997; Dale et al., 2001; Bentz et al., 2010). Including them in the DGVM is desirable, but would require a better understanding of a wide variety of pests' and invasive species' response to climate change as well as calibration datasets that are still often lacking.

Soil data are critical for projecting accurate soil water availability and drought stress (Peterman et al., 2014). More accurate soil data would improve the reliability of growth, mortality, and fire simulation results. More recent MC2 simulations have used SSURGO data but at the time of this project, the dataset was still incomplete for large portions of our study area.

3.5.2 Effects of model assumptions on vegetation

The simulated transition from conifer to temperate mixed conifer/broadleaf to subtropical mixed conifer/broadleaf takes place at a similar rate and with a similar pattern regardless of fire and CO_2 fertilization and can be attributed solely to climate change. Other studies using MC2 and its predecessor, MC1, project vegetation shifts in this region towards warmer and mixed forests (Sheehan et al., 2015; Rogers et al., 2011; Turner et al., 2015; Gonzalez et al., 2010),

however, to our knowledge, ours is the first study to show that this shift is purely climate driven. This result stands in contrast to the simulated fire regime-driven vegetation shifts in other regions found in other studies using MC2 (e.g., Sheehan et al., 2015; Bachelet et al., 2015)

3.5.3 Effects of model assumptions on fire

With or without fire suppression, unlimited ignitions cause a sharp increase in AWF as climate conditions drive fuel conditions over ignition thresholds on a yearly basis during the early and mid 21st c. This is consistent with recent observed increases in wildfire across the western US, including the PNW, due to warming climate (Westerling et al., 2006; Westerling, 2016) and specifically in the Western Cascades due to decreased May through September precipitation (Turner et al., 2015). The initial decrease in FAB and TAB as AWF remains high is due to the dependency of FAB on the combination of time since last fire and fire return interval (FRI) in addition to fuel conditions. The longer a cell does not burn, the greater the fraction of that cell that can burn. With the initial transition to more frequent fires, the first fire in a cell burns a greater cell portion than subsequent fires in the same cell. The vegetation shift to subtropical mixed forest, which has a higher ignition threshold, contributes to decreased AWF, FAB, and TAB towards the end of the 21st c. The higher fuel thresholds of fire suppression reduce AWF and TAB due to fuel conditions reaching ignition thresholds less frequently. Less frequent fires, however, account for the greater TAB under fire suppression.

Stochastic fire responds to the same drivers as the unlimited ignitions but in different ways. First, the use of an ignition probability function instead of a single fuel threshold allows fires to occur even under fuel conditions less severe than those at unlimited ignition threshold levels. Thus, during the early 20th c. some cells not experiencing fire under unlimited ignitions do experience fire under stochastic ignitions leading to a greater TAB under stochastic fire. Second, the probabilistic nature of ignition sources and fire initiation limits fire occurrence under fuel conditions exceeding thresholds, as during the early to late 21st c. when fire occurrence is more common across the entire study area under unlimited ignitions than under stochastic fire. During this period, TAB is lower under stochastic fire than under unlimited ignitions scenarios due to less frequent fire occurrence. The overall less frequent fires due to stochastic fire result in a lower AWF and higher FAB. Stochastic fire occurring below the thresholds set for unlimited

ignitions accounts for the higher FAB at the end of the 21st c., when stochastic fire initiates fires in subtropical mixed forest while unlimited ignitions does not.

Fire effects due to CO_2 fertilization assumptions are generally small. However, even though AWF is identical for FF-NCE and FF-WCE, FAB and TAB are slightly higher for FF-NCE. We attribute this to dryer fuel conditions as a result of lower water use efficiency (WUE) for FF-NCE.

3.5.4 Effects of model assumptions on carbon

Separate from fire, CO_2 fertilization under climate change increases productivity and C in all pools through time. Conversely the lack of CO_2 fertilization under climate change decreases productivity C in all pools. The smooth changes in C pools and ratio of live to dead C for both no-fire scenarios indicate little change in carbon dynamics. The continuing increases in all C pools for NF-WCE and decreases for NF-NCE indicate that climate continues to influence production through the end of the 21st c.

CO_2 fertilization is the strongest driver of NPP as shown by the similar increases in NPP across all scenarios with CO_2 fertilization versus the similar decrease for scenarios without CO_2 fertilization. Consumed C is very similar for all scenarios with unlimited ignitions. Increased carbon storage in young forests recovering from fire as well as to the reduction of dead material available for decomposition due to burning drive higher NEP for all scenarios with CO_2 fertilization and unlimited ignitions. However, for FF-NCE, NEP decreases due to decreasing NPP.

For scenarios with unlimited ignitions, consumed C directly reflects TAB increasing sharply in the mid 20th c. and then decreasing. This pattern is further reflected in NBP which decreases and increases with TAB. By the end of the 21st c., NBP is close to 0 g C m^{-2} yr^{-1} for scenarios with unlimited ignitions and with CO_2 fertilization, indicating a possible equilibrium in carbon dynamics. However, for FF-NCE, NBP remains negative, indicating further C losses. For SF-WCE, consumed C and NBP also reflect TAB, with consumed C greater than that for unlimited-ignitions scenarios in the early 20th c. and less during the mid and late 21st c.

More live C is lost due to fire than is added due to CO_2 fertilization. For unlimited ignitions, losses are greatest during the mid to late 21st c. when fuel thresholds are exceeded. For

stochastic fire, the greatest losses are in the early 20th c. due to fires occurring where they cannot under unlimited ignitions. CO_2 fertilization, however, may provide enough productivity to maintain a new equilibrium with increased dead C and limited decreases in ecosystem C. For all with-CO_2 fertilization, with-fire scenarios, at the end of the 21st c., the steady values of all C stocks and live to dead C ratios indicate the possibility of a new equilibrium. This is consistent with the near 0 g C m^{-2} yr^{-1} NBP for these scenarios at the end of the 21st c.

The largest decreases in all C stocks are for the with-fire, without-CO_2 fertilization. In addition, while live vegetation C becomes steady for this scenario at the end of the 21st c., dead C, and ecosystem C continue to decrease, indicating that equilibrium has not been reached. This is consistent with the negative NBP for this scenario at the end of the 21st c.

3.5.5 Implications

The sharp, climate-driven increases in area with fire and total area burned during the first half of the 21st suggest this region will be susceptible to climate-driven trend towards "large," "very large," or "extreme" wildfire events or fires (Tedim et al., 2018) observed in the United States (Barbero et al., 2015; Dennison et al., 2014), Europe (Parente et al., 2018; Senf and Seidl, 2018), and globally (Sommerfeld et al., 2018). The increases also indicate that this region will experience the associated increases in infrastructure loss, suppression costs, and natural resource loss (Thomas et al., 2017), and underscore the importance of understanding the effects of alternative management scenarios in fire-prone landscapes (Spies et al., 2017).

The live C lost in all with-fire scenarios indicates fire will cause mortality through the 21st c. Another indication of future vegetation mortality is the climate-driven transition from needleleaf to temperate mixed to warm mixed forest. MC2 does not simulate mortality, seeding, sprouting, recruitment, and succession associated with forest type change driven by climate alone. So, for example, under a warming climate, the model could shift a forest dominated by needleleaf lifeforms to one dominated by mixed conifer and hardwood lifeforms without simulating mortality and succession. Thus, model results should be interpreted as a suggestion that vegetation will come under stress due to a changing climate. Mortality and vegetation type change would not necessarily be sudden. However, stressed vegetation would be more susceptible to disturbances (Dale et al., 2001) such as drought, fire, insects (Bentz BJ et al.,

2010; Preisler et al., 2012), and disease, with the resulting mortality providing opportunity for vegetation to change from legacy to a more suited type.

Shorter FRIs combined with reduced recruitment due to changed climate conditions has the potential to extirpate species locally (Enright et al., 2015). Furthermore, climate change velocity, especially in combination with pest outbreaks, could outpace species' migration rates (Malcolm et al., 2002), leaving portions of the area depauperate. The subtropical mixed forests projected to occupy much of the area by the end of the 21st c. are characterized by both needleleaf and broadleaf evergreens and would be similar to northern Californian forests which contain evergreen California live oaks (*Quercus agrifolia*). However, the decline of oak populations due to sudden oak death syndrome (*Phytophthora ramorum)* in California and Oregon (Gruenwald et al., 2008) challenges any assumption of a northward migration of this evergreen broadleaf species.

Ecosystem C decreases in all with-fire scenarios indicate that this region will become a carbon source in the future. Decreases may be more pronounced beyond 2100 if the increased C in the dead pool decays at a greater rate than dead C is produced. This is possible as the simulated increase in dead C is due to a sudden increase in fire in forests that had been highly productive, and the live to dead C ratios increase towards previous equilibrium values at the end of the simulation. If the CO_2 effect is lower than projected or is temporary, with plants adapting to the new CO_2 concentrations, carbon losses may be higher than projected under the WCE scenarios, for example, 1.69 Pg C (20%) greater for the FF-NCE than for the FF-WCE. However black carbon accumulation from more frequent fire and the possible slowing of decomposition due to higher evaporative demand in soils may mitigate losses of soil C.

Under our projections, a variety of ecosystem services could be impacted. As previously stated, carbon sequestration could be reduced. Widespread mortality would reduce timber available for harvest, and rapid change of vegetation types could result in a lack of mature trees for harvest. The implied negative impacts on forests could affect fresh water supplies (Neary et al., 2009), wildlife habitat quality, and recreation.

3.6 Conclusions

For the area west of the Cascade Crest in Oregon and Washington, we found assumptions about CO_2 fertilization effects and fire occurrence in the MC2 DVGM have substantial effects on

simulated carbon dynamics. Without fire, CO_2 fertilization increases C stocks, while the lack of CO_2 fertilization leads to decreases in C stocks. For scenarios with fire, CO_2 fertilization mitigates projected C losses due to fire, limiting decreases over the 20th and 21st centuries by a factor of 4 versus scenarios without CO_2 fertilization.

Stochastic fire occurrence dampens the sudden increases in area with fire, and total area burned simulated under unlimited ignitions. As a result, C pools are more stable through time under stochastic fire occurrence than under unlimited ignitions. The stark differences between results for unlimited ignitions and those for stochastic fire occurrence point to the need for further research regarding fire occurrence algorithms in DGVMs. Areas for further research include: the addition of ignition source probabilities to guide the location of fire occurrence; fire spread which would allow modeling large fires across grid cells; inclusion of land use and land cover to shape both the occurrence and spread of fire; and the elimination of fire return intervals from fire algorithms in order to model fire occurrence and extent from physical parameters and stochastic events without imposed limitations.

Vegetation is projected to change from predominantly conifer to predominantly mixed conifer and hardwood forests, regardless of CO_2 fertilization and fire effects. With climate, not fire, driving vegetation change, much of the current vegetation can be expected to experience mortality. It is reasonable to anticipate that climate stress will make forests more susceptible disease and pests, which are not modeled by MC2.

These projections underscore ongoing challenges for resource managers who must balance the possibly competing concerns of wildfire, forest condition, wildlife management, carbon sequestration, high potential for vegetation change, and a variety of ecosystem services including clean water and air. Nonetheless, this study and its conclusions should be taken in a broader context. MC2 is one of many models suitable to explore the possible futures of this region. Given the region's ecological and economic importance, extensive monitoring is warranted to provide insight into the state of the forests, possibly confirming or refuting signs of stress, vegetation change, and ecological threshold exceedance.

3.7 Acknowledgments

Funding for this research was provided by the U.S. Department of the Interior via the Northwest Climate Science Center through agreement #G12AC20495 within the framework of

the research project entitled “Integrated Scenarios of climate, hydrology and vegetation for the Northwest”, P. Mote (Oregon State University) principal investigator.

We acknowledge the World Climate Research Programme’s Working Group on Coupled Modelling, which is responsible for CMIP, and we thank the climate modeling groups for producing and making available their model output. For CMIP, the U.S. Department of Energy’s Program for Climate Model Diagnosis and Intercomparison provides coordinating support and led development of software infrastructure in partnership with the Global Organization for Earth System Science Portals.

The authors wish to acknowledge R. Nemani (NASA) for allowing them free access to the Pleiades NASA supercomputer and John Abatzoglou and Katherine Hegewisch (both of University of Idaho) for providing the downscaled CMIP5 climate data used in this study.

3.8 References

Abatzoglou, J. T., & Brown, T. J. (2012). A comparison of statistical downscaling methods suited for wildfire applications. *International Journal of Climatology*, 32(5), 772-780.

Ainsworth, E. A., & Long, S. P. (2005). What have we learned from 15 years of free-air CO_2 enrichment (FACE)? A meta-analytic review of the responses of photosynthesis, canopy properties and plant production to rising CO_2. *New Phytologist*, 165(2), 351-372.

Bachelet, D., Ferschweiler, K., Sheehan, T. J., Sleeter, B. M., & Zhu, Z. (2015). Projected carbon stocks in the conterminous USA with land use and variable fire regimes. *Global Change Biology*, 21(12), 4548-4560.

Barbero, R., Abatzoglou, J. T., Larkin, N. K., Kolden, C. A., & Stocks, B. (2015). Climate change presents increased potential for very large fires in the contiguous United States. *International Journal of Wildland Fire*, 24(7), 892-899.

Batllori, E., Ackerly, D. D., & Moritz, M. A. (2015). A minimal model of fire-vegetation feedbacks and disturbance stochasticity generates alternative stable states in grassland–shrubland–woodland systems. *Environmental Research Letters*, 10(3), 034018.

Bentz, B. J., Régnière, J., Fettig, C. J., Hansen, E. M., Hayes, J. L., Hicke, J. A., Kelsey, R. G., Negrón, J. F., & Seybold, S. J. (2010). Climate change and bark beetles of the western United States and Canada: direct and indirect effects. *BioScience*, 60(8), 602-613.

Brodribb, T. J., McAdam, S. A., Jordan, G. J., & Feild, T. S. (2009). Evolution of stomatal responsiveness to CO_2 and optimization of water-use efficiency among land plants. *New Phytologist*, 183(3), 839-847.

Canadian Forestry Service (1984). *Tables for the Canadian Forest Fire Weather Index System*. Forestry technical report 25, 4th ed. Environment Canada, Canadian Forest Service, Ottawa, ON, CA.

Chen, I. C., Hill, J. K., Ohlemüller, R., Roy, D. B., & Thomas, C. D. (2011). Rapid range shifts of species associated with high levels of climate warming. *Science*, 333(6045), 1024-1026.

Cramer, W., Bondeau, A., Woodward, F. I., Prentice, I. C., Betts, R. A., Brovkin, V., Cox, P. M., Fisher, V., Foley, J. A., Friend, A. D., & Kucharik, C. (2001). Global response of terrestrial ecosystem structure and function to CO_2 and climate change: results from six dynamic global vegetation models. *Global Change Biology*, 7(4), 357-373.

Dale, V. H. (1997). The relationship between land-use change and climate change. *Ecological Applications*, 7(3), 753-769.

Dale, V. H., Joyce, L. A., McNulty, S., Neilson, R. P., Ayres, M. P., Flannigan, M. D., Hanson, P. J., Irland, L. C., Lugo, A. E., Peterson, C. J., & Simberloff, D. (2001). Climate change and forest disturbances: climate change can affect forests by altering the frequency, intensity, duration, and timing of fire, drought, introduced species, insect and pathogen outbreaks, hurricanes, windstorms, ice storms, or landslides. *BioScience*, 51(9), 723-734.

Daly, C., Halbleib, M., Smith, J. I., Gibson, W. P., Doggett, M. K., Taylor, G. H., Curtis, J., & Pasteris, P. P. (2008). Physiographically sensitive mapping of climatological temperature and precipitation across the conterminous United States. *International Journal of Climatology*, 28(15), 2031-2064.

Dennison, P. E., Brewer, S. C., Arnold, J. D., & Moritz, M. A. (2014). Large wildfire trends in the western United States, 1984–2011. *Geophysical Research Letters*, 41(8), 2928-2933.

Castedo-Dorado, F., Rodríguez-Pérez, J. R., Marcos-Menéndez, J. L., & Álvarez-Taboada, M. F. (2011). Modelling the probability of lightning-induced forest fire occurrence in the province of León (NW Spain). *Forest Systems*, 20(1), 95-107.

Eidenshink, J., Schwind, B., Brewer, K., Zhu, Z., Quayle, B., & Howard, S. (2007). A project for monitoring trends in burn severity. Fire Ecology 3 (1): 3-21. *Fire Ecology Special Issue* Vol, 3(1), 3-21.

Enright, N. J., Fontaine, J. B., Bowman, D. M., Bradstock, R. A., & Williams, R. J. (2015). Interval squeeze: altered fire regimes and demographic responses interact to threaten woody species persistence as climate changes. *Frontiers in Ecology and the Environment*, 13(5), 265-272.

Fowler, D., Steadman, C. E., Stevenson, D., Coyle, M., Rees, R. M., Skiba, U. M., Sutton, M. A., Cape, J. N., Dore, A. J., Vieno, M., & Simpson, D. (2015). Effects of global change during the 21st century on the nitrogen cycle. *Atmospheric Chemistry and Physics*, 15(24), 13849-13893.

Gonzalez, P., Neilson, R. P., Lenihan, J. M., & Drapek, R. J. (2010). Global patterns in the vulnerability of ecosystems to vegetation shifts due to climate change. *Global Ecology and Biogeography*, 19(6), 755-768.

Gruenwald, N. J., Goss, E. M., & Press, C. M. (2008). *Phytophthora ramorum*: a pathogen with a remarkably wide host range causing sudden oak death on oaks and ramorum blight on woody ornamentals. *Molecular Plant Pathology*, 9(6), 729-740.

Hantson, S., Arneth, A., Harrison, S. P., Kelley, D. I., Prentice, I. C., Rabin, S. S., Archibald, S., Mouillot, F., Arnold, S. R., Artaxo, P., & Bachelet, D. (2016). The status and challenge of global fire modelling. *Biogeosciences*, 13(11), 3359-3375.

Harris, R., Remenyi, T. A., Williamson, G. J., Bindoff, N. L., & Bowman, D. M. (2016). Climate–vegetation–fire interactions and feedbacks: trivial detail or major barrier to projecting the future of the Earth system? *Wiley Interdisciplinary Reviews: Climate Change*, 7(6), 910-931.

Hendrey, G. R., Ellsworth, D. S., Lewin, K. F., & Nagy, J. (1999). A free-air enrichment system for exposing tall forest vegetation to elevated atmospheric CO_2. *Global Change Biology*, 5(3), 293-309.

Hudiburg, T., Law, B., Turner, D. P., Campbell, J., Donato, D., & Duane, M. (2009). Carbon dynamics of Oregon and Northern California forests and potential land-based carbon storage. *Ecological Applications*, 19(1), 163-180.

Kitzberger, T., Perry, G. L. W., Paritsis, J., Gowda, J. H., Tepley, A. J., Holz, A., & Veblen, T. T. (2016). Fire–vegetation feedbacks and alternative states: common mechanisms of temperate forest vulnerability to fire in southern South America and New Zealand. New *Zealand Journal of Botany*, 54(2), 247-272.

Keane, R. E., McKenzie, D., Falk, D. A., Smithwick, E. A., Miller, C., & Kellogg, L. K. B. (2015). Representing climate, disturbance, and vegetation interactions in landscape models. *Ecological Modelling*, 309, 33-47.

Kurz, W. A., Dymond, C. C., Stinson, G., Rampley, G. J., Neilson, E. T., Carroll, A. L., Ebata, T., & Safranyik, L. (2008). Mountain pine beetle and forest carbon feedback to climate change. *Nature*, 452(7190), 987-990.

Law, B. E., Hudiburg, T. W., Berner, L. T., Kent, J. J., Buotte, P. C., & Harmon, M. E. (2018). Land use strategies to mitigate climate change in carbon dense temperate forests. *Proceedings of the National Academy of Sciences*, 115(14), 3663-3668.

Law, B. E., Turner, D., Campbell, J., Sun, O. J., Van Tuyl, S., Ritts, W. D., & Cohen, W. B. (2004). Disturbance and climate effects on carbon stocks and fluxes across Western Oregon USA. *Global Change Biology*, 10(9), 1429-1444.

Littell, J. S., McKenzie, D., Kerns, B. K., Cushman, S., & Shaw, C. G. (2011). Managing uncertainty in climate-driven ecological models to inform adaptation to climate change. *Ecosphere*, 2(9), 1-19.

Lurgi, M., López, B. C., & Montoya, J. M. (2012). Novel communities from climate change. *Philosophical Transactions of the Royal Society of London B: Biological Sciences*, 367(1605), 2913-2922.

Malcolm, J. R., Markham, A., Neilson, R. P., & Garaci, M. (2002). Estimated migration rates under scenarios of global climate change. *Journal of Biogeography*, *29*(7), 835-849.

Mote, P. W., Parson, E. A., Hamlet, A. F., Keeton, W. S., Lettenmaier, D., Mantua, N., Miles, E. L., Peterson, D. W., Peterson, D. L., Slaughter, R., & Snover, A. K. (2003). Preparing for climatic change: the water, salmon, and forests of the Pacific Northwest. *Climatic Change*, 61(1), 45-88.

Neary, D. G., Ice, G. G., & Jackson, C. R. (2009). Linkages between forest soils and water quality and quantity. *Forest Ecology and Management*, 258(10), 2269-2281.

Norby, R. J., & Zak, D. R. (2011). Ecological lessons from free-air CO_2 enrichment (FACE) experiments. *Annual Review of Ecology, Evolution, and Systematics*, 42, 181-203.

Omernik, J. M., & Griffith, G. E. (2014). Ecoregions of the conterminous United States: evolution of a hierarchical spatial framework. *Environmental management*, *54*(6), 1249-1266.

Parente, J., Pereira, M. G., Amraoui, M., & Fischer, E. M. (2018). Heat waves in Portugal: Current regime, changes in future climate and impacts on extreme wildfires. *Science of the Total Environment*, 631, 534-549.

Peterman, W., Bachelet, D., Ferschweiler, K., & Sheehan, T. (2014). Soil depth affects simulated carbon and water in the MC2 dynamic global vegetation model. *Ecological Modelling*, 294, 84-93.

Pew, K. L., & Larsen, C. P. S. (2001). GIS analysis of spatial and temporal patterns of human-caused wildfires in the temperate rain forest of Vancouver Island, Canada. *Forest Ecology and Management*, 140(1), 1-18.

Preisler, H. K., Hicke, J. A., Ager, A. A., & Hayes, J. L. (2012). Climate and weather influences on spatial temporal patterns of mountain pine beetle populations in Washington and Oregon. *Ecology*, 93(11), 2421-2434.

Rabin, S. S., Melton, J. R., Lasslop, G., Bachelet, D., Forrest, M., Hantson, S., Li, F., Mangeon, S., Yue, C., Arora, V. K., & Hickler, T. (2017). The Fire Modeling Intercomparison Project (FireMIP), phase 1: experimental and analytical protocols with detailed model descriptions. *Geoscientific Model Development*, 10(3), 1175.

Rehfeldt, G. E., Crookston, N. L., Warwell, M. V., & Evans, J. S. (2006). Empirical analyses of plant-climate relationships for the western United States. *International Journal of Plant Sciences*, 167(6), 1123-1150.

Rehfeldt, G. E., Ferguson, D. E., & Crookston, N. L. (2009). Aspen, climate, and sudden decline in western USA. *Forest Ecology and Management*, 258(11), 2353-2364.

Rienstra, J. T., Teensma, P. D. A., & Yeiter, M. A. (1991). *Preliminary Reconstruction and Analysis of Change in Forest Stand Age Classes of the Oregon Coast Range from 1850 to 1940*. United States Department of the Interior Bureau of Land Management technical note T/N OR-9. Portland, OR, USA

Rogers, B. M., Neilson, R. P., Drapek, R., Lenihan, J. M., Wells, J. R., Bachelet, D., & Law, B. E. (2011). Impacts of climate change on fire regimes and carbon stocks of the US Pacific Northwest. *Journal of Geophysical Research: Biogeosciences*, 116, G03037.

Rorig, M. L., & Ferguson, S. A. (1999). Characteristics of lightning and wildland fire ignition in the Pacific Northwest. *Journal of Applied Meteorology*, 38(11), 1565-1575.

Senf, C., & Seidl, R. (2018). Natural disturbances are spatially diverse but temporally synchronized across temperate forest landscapes in Europe. *Global change Biology*, 24(3), 1201-1211.

Sheehan, T., Bachelet, D., & Ferschweiler, K. (2015). Projected major fire and vegetation changes in the Pacific Northwest of the conterminous United States under selected CMIP5 climate futures. *Ecological Modelling*, 317, 16-29.

Sommerfeld, A., Senf, C., Buma, B., D'Amato, A. W., Després, T., Díaz-Hormazábal, I., Fraver, S., Frelich, L. E., Gutiérrez, Á. G., Hart, S. J. and Harvey, B. J. (2018). Patterns and drivers of recent disturbances across the temperate forest biome. *Nature Communications*, 9(1), 4355.

Spies, T., White, E., Ager, A., Kline, J., Bolte, J., Platt, E., Olsen, K., Pabst, R., Barros, A., Bailey, J., & Charnley, S. (2017). Using an agent-based model to examine forest management outcomes in a fire-prone landscape in Oregon, USA. *Ecology and Society*, 22(1).

Sullivan, A. L. (2009a). Wildland surface fire spread modelling, 1990–2007. 1: Physical and quasi-physical models. *International Journal of Wildland Fire*, 18(4), 349-368.

Sullivan, A. L. (2009b). Wildland surface fire spread modelling, 1990–2007. 2: Empirical and quasi-empirical models. *International Journal of Wildland Fire*, 18(4), 369-386.

Sullivan, A. L. (2009c). Wildland surface fire spread modelling, 1990–2007. 3: Simulation and mathematical analogue models. *International Journal of Wildland Fire*, 18(4), 387-403.

Syphard, A. D., Radeloff, V. C., Keeley, J. E., Hawbaker, T. J., Clayton, M. K., Stewart, S. I., & Hammer, R. B. (2007). Human influence on California fire regimes. *Ecological Applications*, 17(5), 1388-1402.

Tedim, F., Leone, V., Amraoui, M., Bouillon, C., Coughlan, M., Delogu, G., Fernandes, P., Ferreira, C., McCaffrey, S., McGee, T., & Parente, J. (2018). Defining extreme wildfire events: difficulties, challenges, and impacts. *Fire*, 1(1), 9.

Thomas, D., Butry, D., Gilbert, S., Webb, D., & Fung, J. (2017). *The Costs and Losses of Wildfires*: *A Literature Review*. NIST Special Publication 1215. National Institute of Standards and Technology, Washington, D. C., USA.

Turner, D. P., Conklin, D. R., & Bolte, J. P. (2015). Projected climate change impacts on forest land cover and land use over the Willamette River Basin, Oregon, USA. *Climatic Change*, 133(2), 335-348.

Turner, D. P., Ritts, W. D., Kennedy, R. E., Gray, A. N., & Yang, Z. (2015). Effects of harvest, fire, and pest/pathogen disturbances on the West Cascades ecoregion carbon balance. *Carbon Balance and Management*, 10(1), 12.

Turner, D. P., Ritts, W. D., Kennedy, R. E., Gray, A. N., & Yang, Z. (2016). Regional carbon cycle responses to 25 years of variation in climate and disturbance in the US Pacific Northwest. *Regional Environmental Change*, 16(8), 2345-2355.

Van Der Sleen, P., Groenendijk, P., Vlam, M., Anten, N. P., Boom, A., Bongers, F., Pons, T. L., Terburg, G., & Zuidema, P. A. (2015). No growth stimulation of tropical trees by 150 years of CO_2 fertilization but water-use efficiency increased. *Nature Geoscience*, 8(1), 24-28.

Van Wagner, C. E. (1987). *Development and Structure of the Canadian Forest Fire Weather Index System*. Technical report 35. Petawawa National Forestry Institute, Canadian Forest Service, Chalk River, Ontario, CA.

Way, D. A., Oren, R. A. M., & Kroner, Y. (2015). The space-time continuum: the effects of elevated CO_2 and temperature on trees and the importance of scaling. *Plant, Cell & Environment*, 38(6), 991-1007.

Westerling, A. L. (2016). Increasing western US forest wildfire activity: sensitivity to changes in the timing of spring. *Philosophical Transactions of the Royal Society B: Biological Sciences*, 371(1696), 20150178.

Westerling, A. L., Hidalgo, H. G., Cayan, D. R., & Swetnam, T. W. (2006). Warming and earlier spring increase western US forest wildfire activity. *Science*, 313(5789), 940-943.

Williams, J. W., & Jackson, S. T. (2007). Novel climates, no-analog communities, and ecological surprises. *Frontiers in Ecology and the Environment*, 5(9), 475-482.

3.9 Supporting information

Table S3.1. Reclassifications of MC2 vegetation types.

Reclassified vegetation type	MC2 vegetation types
Conifer forest	Subalpine, Maritime Evergreen Needleleaf Forest, Temperate Evergreen Needleleaf Forest, Temperate Evergreen Needleleaf Woodland, Subtropical Evergreen Needleleaf Forest, Cool Needleleaf Forest
Temperate mixed forest	Temperate Cool Mixed Forest, Temperate Warm Mixed Forest, Temperate Cool Mixed Woodland, Temperate Warm Mixed Woodland
Subtropical mixed forest	Subtropical Mixed Forest, Subtropical Mixed Woodland
Other	Temperate Grassland, Subtropical Grassland, Temperate Shrubland, Subtropical Shrubland

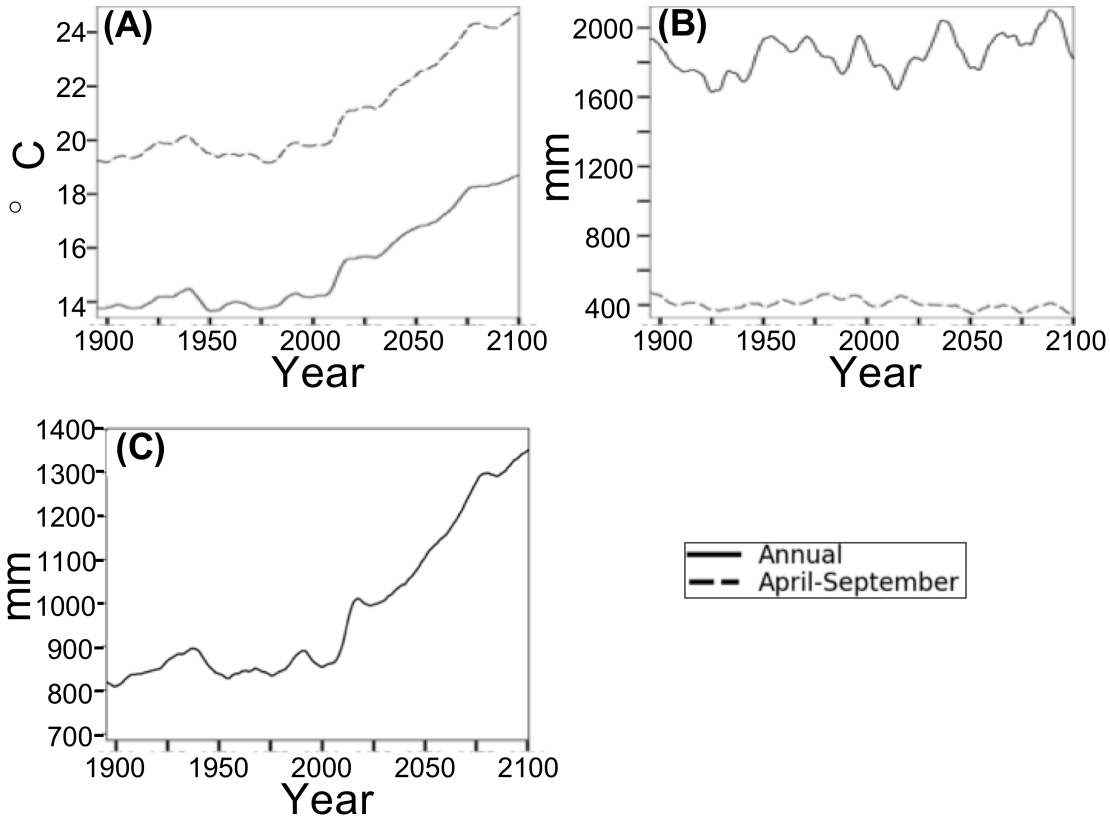

Fig. S3.1. Selected climate results for this study. (A) CCSM4 RCP 8.5 annual and April-September maximum temperature, (B) CCSM4 RCP 8.5 annual and April-September precipitation, and (C) Annual PET calculated by MC2. All results smoothed using triangle smoothing +/- 8 years.

Table S3.2. Mean (standard deviation in parentheses) over study region for selected climate variables by time period.

	1895 - 2024	1936 - 1965	1971 - 2000	2036 - 2065	2071 - 2100
Annual Tmax (degC)	13.8 (0.45)	14.0 (0.70)	14.0 (0.54)	16.7 (0.57)	18.4 (0.52)
Apr.-Sep. Tmax (degC)	19.4 (0.68)	19.6 (0.93)	19.5 (0.66)	22.4 (0.78)	24.3 (0.59)
Annual Tmin (degC)	3.1 (0.45)	3.3 (0.56)	3.5 (0.50)	6.0 (0.56)	7.5 (0.56)
Apr.-Sep. Tmin (degC)	6.2 (0.42)	6.5 (0.50)	6.8 (0.51)	9.0 (0.62)	10.7 (0.65)
Annual Ppt (mm)	1795 (208)	1838 (275)	1874 (307)	1906 (304)	1978 (343)
April-Sep. ppt(mm)	418 (83)	410 (95)	445 (86)	378 (114)	377 (84)
Annual PET (cm)	832 (47)	85 (72)	855 (56)	1107 (66)	1305 (57)

Temperature and precipitation are from PRISM and CCSM4 results used to drive the MC2 simulation, potential evapotranspiration was calculated by MC2. (Tmax: mean of monthly maximum temperature; Ppt: total precipitation; PET: potential evapotranspiration)

4 A fuzzy logic decision support model for climate-driven biomass loss risk in western Oregon and Washington

4.1 Abstract

Managing wildlands to protect species and ecosystem services in response to climate change is challenging. Future projections from dynamic global vegetation models (DGVMs) are often put forth as valuable data to aid resource managers in decision making. However, interpreting model results in a meaningful way to support landscape level and policy decisions can be difficult. Uncertainty in results may come from factors including embedded assumptions about atmospheric CO_2 levels, uncertain climate projections driving DGVMs, and DGVM algorithm selection.

We created a decision support model to interpret results from MC2 DGVM results and express them in a straightforward manner more suitable for decision makers. For western Oregon and Washington, we implemented an Environmental Evaluation Modeling System (EEMS) decision support model using MC2 DGVM results to characterize biomass loss risk, defined as the combination of likelihood of a factor leading to biomass loss and a high concentration of biomass. MC2 results were driven by climate projections from 20 global climate models (GCMs) and earth system models (ESMs), under representative concentration pathways (RCPs) 4.5 and 8.5, with and without assumed fire suppression, for three different time periods. We produced maps of mean, minimum, and maximum biomass loss risk and uncertainty for each RCP / +/- fire suppression / time period. We characterized the uncertainty due to RCP, fire suppression, and climate projection choice. Finally, we evaluated whether fire or climate maladaptation mortality was the dominant driver of risk for each model run.

The risk of biomass loss generally increases in current high biomass areas within the study region through time. The pattern of increased risk is generally south to north and upslope into the Coast and Cascade mountain ranges and along the coast. Uncertainty from climate future choice is greater than that attributable to RCP or +/- fire suppression. Fire dominates as the driving factor for biomass loss risk in more model runs than mortality.

This method of interpreting DGVM results and the associated uncertainty provides data in a clear format and may be directly applicable to adaptive management planning.

4.2 Introduction

Anthropogenic emissions have caused oceanic and atmospheric warming, diminished snow and ice, and rising sea level (Pachauri et al., 2014). The effects of climate change vary regionally (Pachauri et al., 2014) and have already affected crop yields (e.g., Urban et al., 2012), biodiversity (e.g., Thom et al., 2017), and wildfire risk (Jolly et al., 2015). In the Pacific Northwest of the conterminous United States (PNW), anthropogenic influences are the leading contributor to observed warming (May et al., 2018; Abatzoglou et al., 2014), with impacts including lower winter snowpack and increased wildfire risk (May et al., 2018). Expected future warming in the PNW is projected to cause continued snowpack loss, increased risk of insect infestations (Kolb et al., 2016), increased risk of wildfires, and changes in vegetation (May et al., 2018; Sheehan et al., 2015).

Numerous studies within or including the PNW have projected climate-driven changes in vegetation, fire regime, pests, and forest productivity (Sheehan et al., 2015; Rehfeldt et al., 2006; Rehfeldt et al., 2014a; Rehfeldt et al., 2014b; Rehfeldt et al., 2014c; Littell et al., 2010; Rogers et al., 2011; Coops et al., 2011; Creutzburg et al., 2014; Whitlock et al., 2003; Latta et al., 2009; Sheehan et al., 2019). These studies have used a variety of methods and models, including Dynamic Global Vegetation Models (DGVMs; Sheehan et al., 2015; Rogers et al., 2011; Sheehan et al., 2019), statistical models (Rehfeldt et al., 2006; Rehfeldt et al., 2014a-c; Littell et al., 2010), reconstruction of relationships between past climate, fire, and vegetation (Whitlock et al., 2003), observation and imputation (Latta et al., 2009), hybrid process and statistical models (Coops et al., 2011), and hybrid state and transition models (Creutzburg et al., 2014). While these studies present both spatial and regional model results, and in many cases, uncertainty associated with those results, the implications for higher level management decisions require interpretation.

Climate impacts have been a steadily growing research topic for over thirty years, and the focus on climate adaptation has seen a marked increase over the last decade (Keenan, 2015). Uncertainty in future climate includes the unknown trend of CO_2 concentrations, which in turn depend on political and economic decisions, and the wide range of future projections from GCMs and ESMs (Pachauri et al., 2014; Pianosi et al., 2016; Littell et al., 2011). The uncertainty in vegetation modeling results is due to the range of climate futures driving them (Pianosi et al.,

2016; Littell et al., 2011), soil representation (Luo et al., 2016), parameter values based on 20th century records (Pianosi et al., 2016; Littell et al., 2011), and model choice (Littell et al., 2011). A common solution for resource managers faced with uncertainty is adaptive management (Williams, 2011; Millar et al., 2007), the "flexible decision making that can be adjusted in the face of uncertainties as outcomes from management actions and other events become better understood (National Research Council, 2004 in Williams, 2011)." Accounting for and characterizing uncertainty are important aspects of adaptive management (Littell et al., 2011; Williams, 2011; Millar et al., 2007).

In this study we report on a fuzzy logic model for assessing the risk of biomass loss due to climate change in western Oregon and Washington. We evaluate the ability of our model to: 1) interpret vegetation modeling results and express risk over time in a format quantified on a 0 to 1 scale; 2) provide upper and lower bounds of that risk; 3) quantify uncertainty in a straightforward manner; 4) attribute uncertainty to its source; and 5) attribute risk to its underlying drivers.

4.3 Methods

4.3.1 Introduction

We focused our modeling effort on the region west of the Cascade Mountain Range crest in Oregon and Washington (Fig. 4.1). We created a decision support model (DSM) to evaluate the risk of losing biomass under climate change projections. In the DSM we included results from 80 runs of the MC2 Dynamic Global Vegetation Model (DGVM; Bachelet et al., 2015) as well as carbon stocks from Hudiburg et al. (2009). We characterized uncertainty due to the diverse climate futures driving MC2 runs, and MC2 assumptions about fire suppression.

4.3.2 Study area

The study area (Fig. 4.1) consists of the region of Oregon and Washington west of the Cascade Mountain Range crest that includes Coast Range, Klamath Mountains/California High North Coast Range, Willamette Valley, Puget Lowlands, Cascades, and North Cascades Level III Ecoregions (Omernik and Griffith, 2014). This region is subject to strong coastal influence with mild, wet winters and warm dry summers.

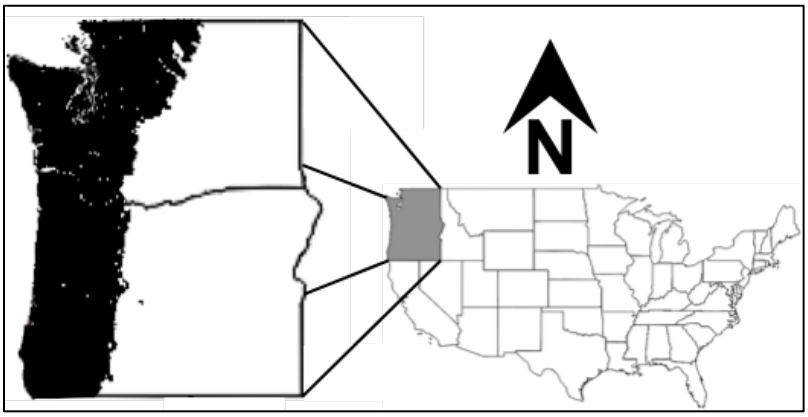

Fig. 4.1. Study area. Portions of Oregon and Washington west of the Cascade Mountain Range crest.

4.3.3 MC2 results used in this study

The protocol used to generate the MC2 results presented here was designed for an earlier project (Sheehan et al., 2015). In this case, MC2 did not account for historical or future land use, nor past disturbances (pest outbreaks, diseases, or windthrow). Historical results (1895-2010) were obtained using PRISM (Daily et al., 2008) data and observed atmospheric CO_2 concentrations as drivers. Our baseline period was 1971-2000. The vegetation model was run twice, once with fire suppression (FS) and once without (NFS - no fire suppression).

Our future scenarios included either FS or NFS, with either Representative Concentration Pathway (RCP) 4.5 or 8.5 CO_2 concentrations. For each of those scenarios, MC2 was run with 20 different climate futures from different CMIP5 General Circulation Models (GCMs) or Earth System Models (ESMs; Fig. 4.2). MC2 results were summarized over three time periods: early 21st c. (2011-2030), mid 21st c. (2036-2065), and late 21st c. (2071-2099). We refer to one set of 20 MC2 results for one scenario and one future time period as an *ensemble* of results.

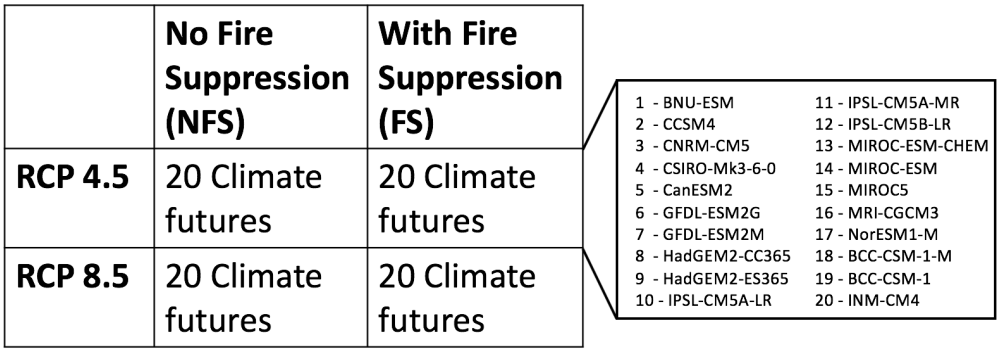

Fig. 4.2. Model scenarios. Schematic of scenario and GCM/ESM climate driver combinations used to produce MC2 results used in this study.

4.3.4 EEMS fuzzy logic modeling

The Environmental Evaluation Modeling System (EEMS; Sheehan and Gough, 2016) is a fuzzy logic (Zadeh, 1973; Giles, 1976) modeling platform designed to inform answers to management questions. A model is represented by a logic tree (e.g. Fig. 4.3), with each node corresponding to a displayable spatial layer or map. The bottom-most nodes in the tree represent input data layers. Each input layer is first normalized (0 to 1 for this study) to produce a node representing its level of agreement with a user-defined statement. For example, a fuel load metric might be mapped to the statement *Simulated Live Biomass is High* using user-defined thresholds to characterize *High*. Normalized values are combined into higher level nodes using fuzzy logic operators that evaluate the relationship between two or more datasets to another statement. For example, data for *Simulated Live Biomass is High* might be combined with data for *Vegetation Stress is High* to create a resulting node for *Mortality Risk is High.* In a complete model, nodes are repeatedly combined to produce a final, top-level node that informs the original management question.

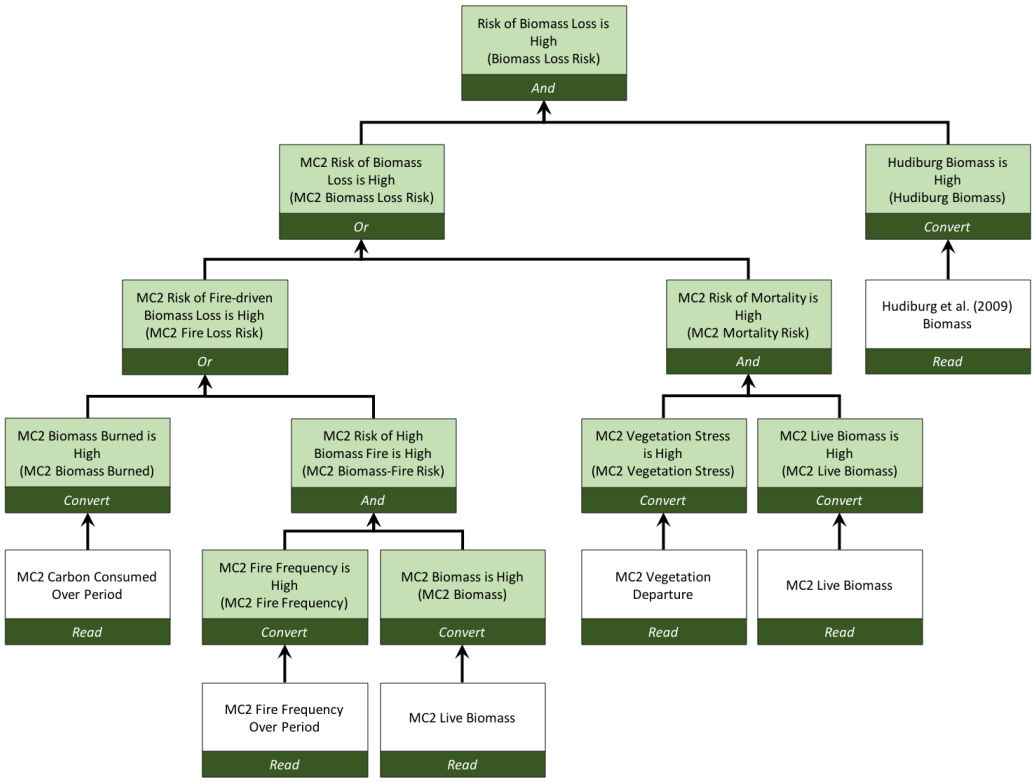

Fig. 4.3. Logic tree for *Biomass Loss Risk* (formally *Risk of Biomass Loss is High*) EEMS model. Each model node (box) represents a spatial data layer (map). Unshaded nodes represent input data layers. Shaded nodes represent data layers with normalized variable values. Labels are formal fuzzy logic statements with informal index labels in parentheses.

Formally, each node in a fuzzy logic model corresponds to a factual statement, and the values for the node (the normalized values described above) are the values for the statement's *fuzzy truth*. Fuzzy truths range from 0 for *fully false* to 1 for *fully true*. Values between 0.0 and 0.5 are considered *partially false*, 0.5 is *neither true nor false*, and values between 0.5 and 1.0 are *partially true*. Informally, values in the nodes are considered as indices for the attribute associated with the factual statement. For example, a fuzzy value for *Vegetation Stress is High* might be referred to simply as the level of *Vegetation Stress* from low (0) to high (1). We use the informal node labels hereafter.

The spatial datasets used in an EEMS model must share the same extent, projection, and reporting units (normally either polygons, or grid cells as in this study). Operations are performed using corresponding reporting units from different data layers (Fig. 4.4 A). Reporting

units within layers are treated independently of one another and do not influence each other's values.

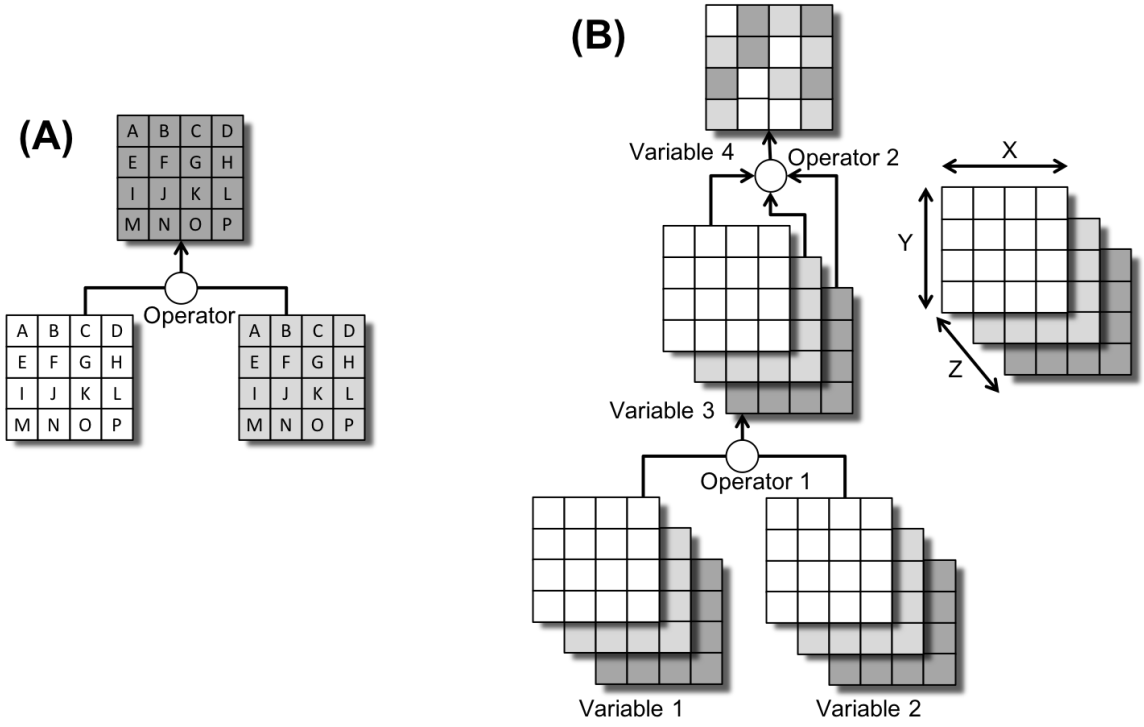

Fig. 4.4. Operations in EEMS. (A) Reporting units (grid cells in this example) in all data layers must correspond to one another. Fuzzy logic operators use the content of matching reporting units in different layers, but not between reporting units within the same layer. (B) Two methods of applying fuzzy logic operations in the extended version of EEMS. Three-dimensional variables 1 and 2 are combined by operator 1 to produce the three-dimensional variable 3. Operator 2 uses values across the Z dimension of variable 3 to produce two-dimensional variable 4. In this study, the Z dimension corresponds to the 20 members of an ensemble.

The EEMS fuzzy logic operators used in this project are *And* (minimum value of the inputs), *Or* (maximum value of the inputs), and *Union* (mean value of the inputs). With the *And* and *Or* operators a reporting unit's result value comes from only of the input values (unless multiple input values yield the same minimum value (for *And*) or maximum value (for *Or*)). For example, if corresponding cells from nodes A and B have values of 0.3 and 0.5, and these nodes are inputs to the *And* operator to produce node C, C's value for the corresponding cell would be 0.3 and would come from only the cell in node A. A result of this is that the values in cells of a node produced by *And* or *Or* can be attributed to their source node.

4.3.5 Decision support modeling

We created an EEMS decision support model (Fig. 4.3) to evaluate the combined *Biomass Loss Risk* (formally, *Risk of Biomass Loss is High*) from fire and climate maladaptation using MC2 ensemble results and aboveground biomass simulated by Hudiburg et al. (2009) (hereafter, Hudiburg). For modeled risk to be considered high, the threat to a cell's biomass – either from fire or modeled vegetation type departure from baseline vegetation type – must be high, and the biomass in the cell must also be high. High modeled biomass is insured by input variables in the *MC2 Biomass Loss Risk* branch of the model. Hudiburg's biomass values are based on observed biomass measurements and their inclusion in the EEMS model serves to adjust *Biomass Loss Risk* down due to the legacy effects of disturbance and harvest.

Normalization of the datasets to obtain fuzzy values was done by establishing minimum (*fully false*) and maximum (*fully true*) thresholds and applying linear interpolation between thresholds, such that

$$fuzzyval = 0$$

where *inputval* < *minthresh* (1)

$$fuzzyval = \frac{(inputval - minthresh)}{(maxthresh - minthresh)}$$

where *minthresh* <= *inputval* <= *maxthresh* (2)

$$fuzzyval = 1$$

where *inputval* > *maxthresh* (3)

where *fuzzyval* is the normalized fuzzy value, *inputval* is the input (raw) data value, *minthresh* is the minimum threshold corresponding to the formal node statement, and *maxthresh* is the maximum threshold.

To normalize MC2 biomass and fire frequency values, we used the distribution of each variable over the study area during the baseline period. The 10th percentile value for each variable was used as the minimum threshold and the 90th percentile was used for the maximum threshold (Table 4.1). Similarly, we normalized Hudiburg's biomass values and used the 10th and 90th percentile values from that data set. We calculated MC2 vegetation departure (a shift from the original modeled vegetation type to a new type) by comparing the cell's modal vegetation type for a future period to its vegetation type for the baseline period. A departure value

quantifying the level of disparity between past and future vegetation types was obtained from a lookup table based on expert opinion (Table S4.1). To normalize the departure values and produce a data layer representing the overall vegetation stress level (*MC2 Vegetation Stress*) we used departure values of 0 and 3 for minimum and maximum thresholds respectively.

Table 4.1. EEMS conversion thresholds. Conversion thresholds used in the EEMS model to evaluate *Biomass Loss Risk*. Threshold values are based on the distribution of each variable except for vegetation type departures.

Variable	***Fully false*** **or minimum threshold**	***Fully true*** **or maximum threshold**	**Comments**
MC2 Biomass Burned	0 (g C m^{-2})	110 (g C m^{-2})	Threshold values from historical period distribution. False threshold 10^{th} percentile, True threshold 90^{th} percentile.
MC2 Fire Frequency	0.0 (decimal fraction)	1.0 (decimal fraction)	Fraction of years with fire. False threshold 10^{th} percentile, True threshold 90^{th} percentile.
MC2 Biomass	31572 (g C m^{-2})	73148 (g C m^{-2})	Threshold values from historical period distribution. False threshold 10^{th} percentile, True threshold 90^{th} percentile.
MC2 Live Biomass	5839 (g C m^{-2})	29387 (g C m^{-2})	Threshold values from historical period distribution. False threshold 10^{th} percentile, True threshold 90^{th} percentile.
Hudiburg Biomass	4053 (g C m^{-2})	21844 (g C m^{-2})	False threshold 10^{th} percentile, True threshold 90^{th} percentile.
MC2 Vegetation Stress	0 (departure value)	3 (departure value)	Level of vegetation departure from historical based on expert opinion (Table S4.1).

(g: gram; C: carbon; m: meter)

4.3.6 Uncertainty Analysis

We characterized uncertainty by first calculating the variability of *Biomass Loss Risk* values spatially across each ensemble of results. Results from each ensemble of 20 MC2 runs were combined into 3-dimensional datasets with ensemble members comprising the third dimension (Fig. 4.4 B). *Biomass Loss Risk* was calculated independently for each ensemble member. An extended version of EEMS was used to produce a data layer for each of the minimum, maximum, and mean fuzzy values (Fig. 4.4 B), bracketing the variability. The fuzzy value *High Variability* (formally, *Variability is High*) was calculated for each cell in each ensemble by converting standard deviations into fuzzy space using the minimum possible

standard deviation (0) as the false threshold and the maximum possible standard deviation (0.5) as the true threshold.

We characterized the non-spatial uncertainty between members of each ensemble using box and whisker plots of their area-weighted means for *Biomass Loss Risk.* Plots for all scenarios within a time period are displayed together for inter-scenario comparison.

To determine whether climate futures' annual temperature and/or precipitation are tightly coupled with *MC2 Biomass Loss Risk*, we evaluated the relationships between those 3 variables. First, we compared each ensemble member's area-weighted mean change in temperature from the baseline period against its change in precipitation. Secondly, we compared each ensemble member's contribution to an ensemble's fraction of area matching the maximum *MC2 Biomass Loss Risk* vs its fraction of area matching the minimum. A visual comparison of an ensemble member's position in the first graph to its position in the second graph illustrates the strength of relationship between these two measures.

4.3.7 Drivers of Biomass Loss Risk

The *Or* operator in the model node *MC2 Biomass Loss Risk* (Fig. 4.3) takes the maximum values of the two inputs, one corresponding to the simulated biomass lost by fire from the MC2 model, the other corresponding to the risk of mortality due to vegetation shift (not due to fire) as simulated by MC2. For each ensemble, we took the ensemble mean for each of *MC2 Fire Loss Risk*, *MC2 Mortality Risk*, and *MC2 Fire Loss Risk* minus *MC2 Mortality Risk* to show which factor most strongly drives *MC2 Biomass Loss Risk*. Absolute difference values are greatest where one factor produces a high risk and the other produces a low risk. These results reflect the contribution to *Biomass Loss Risk* from MC2 results without the contribution from *Hudiburg Biomass*.

We characterized the influence of fire versus that of vegetation shift over the study area. For each ensemble member, we compared the fraction of the area for which mortality due to vegetation shift was the dominant driver of the risk to lose biomass vs the fraction of area where fire was the main driver of risk. Grid cells with a zero risk value were not considered.

4.3.8 Results presented

In this manuscript, we present detailed results for the RCP 8.5 / NFS / 2071-2099 time period ensemble and summary results from other ensembles. Detailed results from other ensembles are in supplemental materials.

4.4 Results

4.4.1 Decision support modeling

We used normalized biomass values from Hudiburg (Fig. 4.5) for all our EEMS model runs. Biomass is highest in the Cascade Mountains and in the Olympic Peninsula, and lowest around Puget Sound, on the east side of the Northern Cascades, throughout the Willamette Valley, and in southern Oregon around the cities of Roseburg, Medford, and Ashland. Eleven percent of the study area is assumed to have zero biomass.

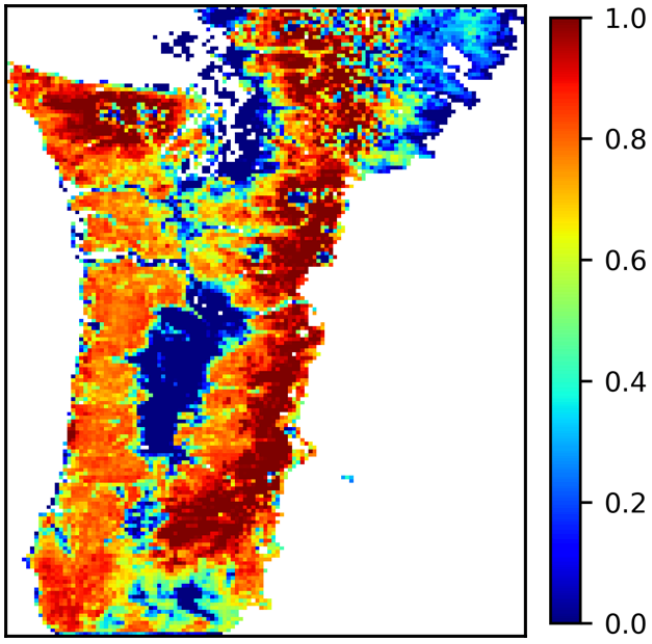

Fig. 4.5. *Hudiburg Biomass*. 11% of the area has a value of 0.

Biomass Loss Risk is low in areas where *Hudiburg Biomass* is low (Fig. 4.5-4.6, S4.1-4.3). For RCP 8.5 with or without fire suppression, mean and minimum values of *Biomass Loss Risk* are highest during the mid 21st c. in the southern portion of the study area (Fig. 4.6, S4.3. A, B, E, F, I, J). For RCP 4.5, the trend is similar, but less pronounced (Fig. S4.1-4.2 A, B, E, F, I, J), and less apparent or absent for maximum values across all scenarios (Fig. 4.6, S4.1-4.3 C, E,

K). Overall, the risk of biomass loss is higher in the southern portion of the study area and the Coast Range than in the Cascade Range (Fig. 4.6, S4.1-4.3 A, B, C, E, F, G, I, J, K).

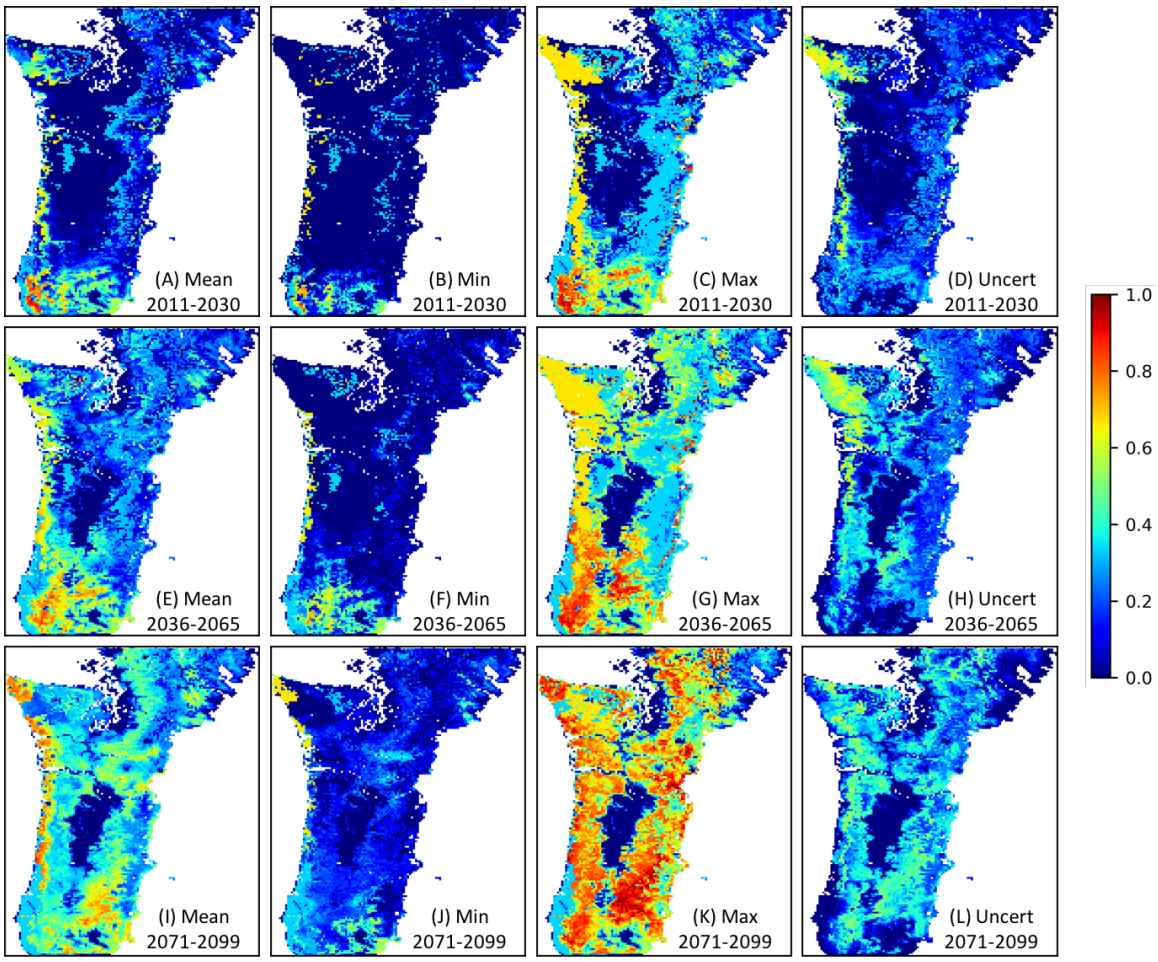

Fig. 4.6. Maps of *Biomass Loss Risk* from EEMS model for the RCP 8.5 NFS scenario. Figure rows include the mean, minimum, maximum, and uncertainty representation for one time period. (min: minimum; max: maximum; uncert: uncertainty)

The area weighted mean of *Biomass Loss Risk* increases with time, is lower for RCP 4.5 than for RCP 8.5, and is slightly higher for NFS scenarios than for FS (Fig. 4.7, Table 4.2). The range of values increases for all scenarios through time (Fig. 4.7, Table 4.2).

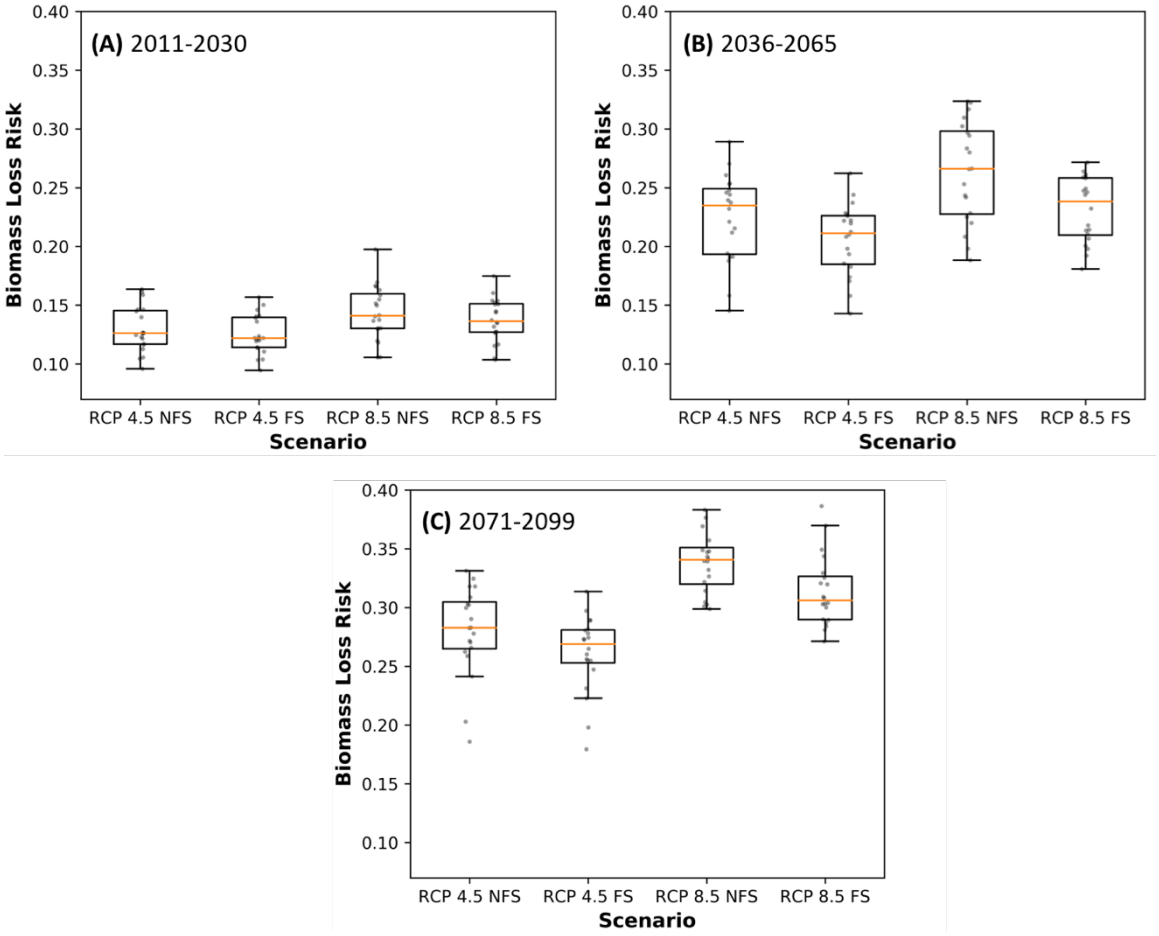

Fig. 4.7. Distribution of area weighted mean values *Biomass Loss Risk* from EEMS model. Each point represents the area weighted mean of one ensemble member.

Table 4.2. Regional values for *Biomass Loss Risk.* Mean, minimum, maximum, and uncertainty for area weighted mean of *Biomass Loss Risk* EEMS model.

	2011-2030			**2036-2065**			**2071-2099**		
	Mean	**Range (min-max)**	**Uncert**	**Mean**	**Range (min-max)**	**Uncert**	**Mean**	**Range (min-max)**	**Uncert**
RCP 4.5, FS	0.13	0.05-0.22	0.11	0.21	0.07-0.36	0.19	0.26	0.09-0.43	0.21
RCP 4.5, NFS	0.13	0.05-0.23	0.11	0.23	0.07-0.38	0.20	0.28	0.09-0.45	0.22
RCP 8.5, FS	0.14	0.05-0.24	0.12	0.23	0.08-0.39	0.19	0.32	0.12-0.51	0.22
RCP 8.5 NFS	0.15	0.06-0.27	0.14	0.27	0.09-0.42	0.20	0.34	0.14-0.53	0.23

(min: minimum; max: maximum; Uncert: Uncertainty)

4.4.2 Uncertainty

Uncertainty is 0 where *Hudiburg Biomass* is 0, and is generally lower or higher corresponding to lower and higher values for *Biomass Loss Risk* (Fig. 4.6, S4.1-4.3 D, H, L). In the Olympic Peninsula, uncertainty is generally higher overall except near the end of the century

for the RCP 8.5 scenarios. In the southeastern portion of the study area, uncertainty is low across all scenarios. Area weighted mean uncertainty is similar overall and increases with time (Table 4.2).

Between RCP 4.5 and RCP 8.5, uncertainty ranges from 0.01 to 0.09, increasing through time (Table 4.3). Between FS and NFS, uncertainty ranges from 0.00 to 0.03, with the lowest values for the early 21st c. (Table 4.3).

Table 4.3. Area weighted mean of uncertainty for RCP 4.5 vs RCP 8.5 and FS vs NFS.

	2011-2030	2036-2065	2071-2099
RCP 4.5 vs RCP 8.5, FS	0.02	0.04	0.09
RCP 4.5 vs RCP 8.5, NFS	0.02	0.05	0.10
FS vs NFS, RCP 4.5	0.00	0.02	0.02
FS vs NFS, RCP 8.5	0.01	0.03	0.03

4.4.3 Drivers of results

MC2 Fire Loss Risk (Fig. 4.8, S4.4-4.6 A, D, F) is greatest in the southern portion of the study region and generally expands through time north through the Willamette Valley and Puget Trough in the center of the region, east and west from the center into the foothills of the Coast and Cascade mountain ranges, and also on the northeast edge of the study region. The expansion into the Coast and Cascade ranges is greater under NFS than FS and markedly greater under RCP 8.5 than under RCP 4.5, with expansion towards the Cascade crest in the late 21st c. (Fig. 4.8, S4.6. G). *MC2 Fire Loss Risk* falls in the southern and eastern portions of the study area under RCP 8.5 in the late 21st c. (Fig. 4.8, S4.6. G).

MC2 Mortality Risk (Fig. 4.8, S4.4-4.6 B, E, H) is greatest along the coast, somewhat high in the Olympic Peninsula of northwestern Washington, and expands into the foothills of the Cascades and the central portion of the study region through time. It is greater under RCP 8.5 than RCP 4.5, and is virtually unaffected by +/- fire suppression.

The general spatial separation of high *MC2 Fire Loss Risk* from high *MC2 Mortality Risk* (Fig. 4.8, S4.4-4.6 A, B, D, E, G, H) is reflected in the driver difference maps (Fig. 4.8, S4.4-4.6 C, F, I). The southern portion and northeastern corner of the study area are driven by fire, whereas the coast and Olympic Peninsula are driven by mortality. Under RCP 4.5, mortality drives *MC2 Biomass Loss Risk* more strongly in the Cascades (Fig. S4.4-4.5 C, F, I). However,

under RCP 8.5, the stronger driver shifts from mortality to fire in the Cascades in the late 21st c. (Fig. 4.8, S4.6 C, F, I).

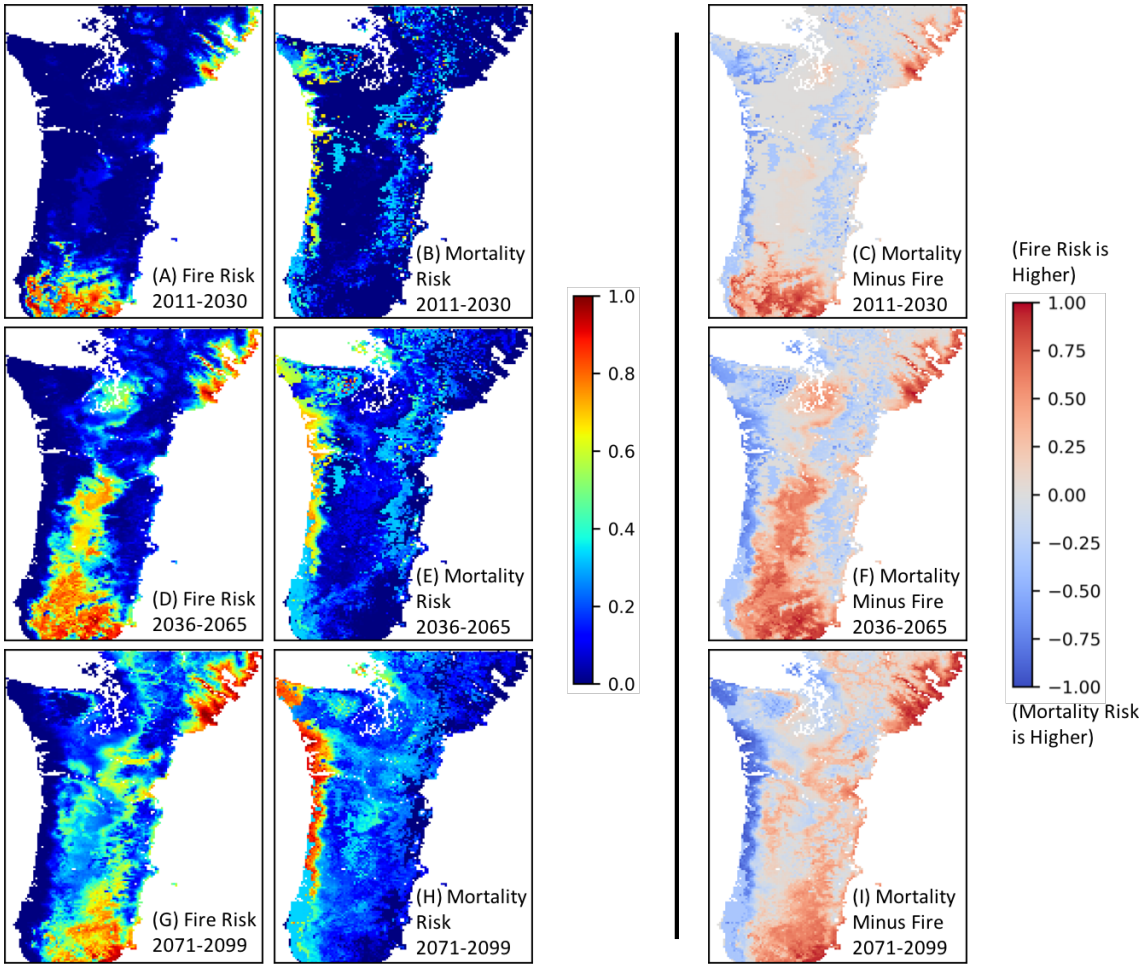

Fig. 4.8. Drivers of *MC2 Mortality Risk.* Maps of *MC2 Fire Loss Risk* (A, D, G), *MC2 Mortality Risk* (B, E, H), and *MC2 Fire Loss Risk* minus *MC2 Mortality Risk* (C, F, I) from the EEMS model for the RCP 8.5 NFS scenario. Figure rows represent time periods.

The fraction of area with 0 *MC2 Biomass Loss Risk* is somewhat greater for RCP 4.5 scenarios than for RCP 8.5, and declines through time, with a minimum of 11% for any ensemble member (Table 4.4). Fire (*MC2 Fire Loss Risk*) contributes more to the risk of losing biomass (*Biomass Loss Risk)* than does vegetation shift (*Mortality Risk*) for all ensembles with the exception of RCP 8.5, FS, 2071-2099 (Table 4.5, Fig. 4.9). The difference is generally smaller for FS scenarios than for NFS scenarios.

Table 4.4. Area-weighted summary of *MC2 Biomass Loss Risk* drivers. Fraction of area with no risk of losing biomass, risk driven by either fire (*MC2 Fire Loss Risk*) or vegetation shift (*MC2 Mortality Risk*) in the EEMS *MC2 Biomass Loss Risk* model node.

	2011-2030			**2036-2065**			**2071-2099**		
	Zero risk (min-max (mean))	**Fire-dominated (min-max (mean))**	**Mortality-dominated (min-max (mean))**	**Zero risk (min-max (mean))**	**Fire-dominated (min-max (mean))**	**Mortality-dominated (min-max (mean))**	**Zero risk (min-max (mean))**	**Fire-dominated (min-max (mean))**	**Mortality-dominated (min-max (mean))**
RCP 4.5 FS	0.43-0.69 (0.58)	0.15-0.40 (0.24)	0.15-0.24 (0.18)	0.13-0.57 (0.30)	0.19-0.47 (0.36)	0.24-0.47 (0.34)	0.11-0.42 (0.20)	0.27-0.57 (0.43)	0.28-0.49 (0.37)
RCP 4.5 NFS	0.42-0.69 (0.58)	0.15-0.40 (0.24)	0.15-0.23 (0.18)	0.13-0.57 (0.29)	0.19-0.52 (0.38)	0.23-0.45 (0.32)	0.11-0.42 (0.20)	0.28-0.58 (0.46)	0.27-0.46 (0.34)
RCP 8.5 FS	0.40-0.67 (0.54)	0.14-0.38 (0.25)	0.16-0.27 (0.20)	0.11-0.45 (0.21)	0.22-0.64 (0.42)	0.21-0.48 (0.36)	0.10-0.18 (0.12)	0.28-0.63 (0.45)	0.26-0.62 (0.43)
RCP 8.5 NFS	0.40-0.67 (0.54)	0.15-0.38 (0.26)	0.16-0.26 (0.20)	0.11-0.45 (0.21)	0.24-0.65 (0.47)	0.21-0.41 (0.32)	0.10-0.18 (0.12)	0.31-0.67 (0.50)	0.23-0.58 (0.39)

(min: minimum; max: maximum)

Table 4.5. Per ensemble drivers of *MC2 Biomass Loss Risk*. Driving factor of the risk of losing biomass illustrated by the number of ensemble members for which either fire (*MC2 Fire Loss Risk)* or simulated vegetation shifts (*MC2 Mortality Risk*) drive the risk of biomass loss for *MC2 Biomass Loss Risk*.

	2011-2030		**2036-2065**		**2071-2099**	
	Fire dominated (count)	**Mortality dominated (count)**	**Fire dominated (count)**	**Mortality dominated (count)**	**Fire dominated (count)**	**Mortality dominated (count)**
RCP 4.5 FS	16	4	11	9	13	7
RCP 4.5 NFS	17	3	13	7	15	5
RCP 8.5 FS	13	7	11	9	9	11
RCP 8.5 NFS	13	7	17	3	13	7

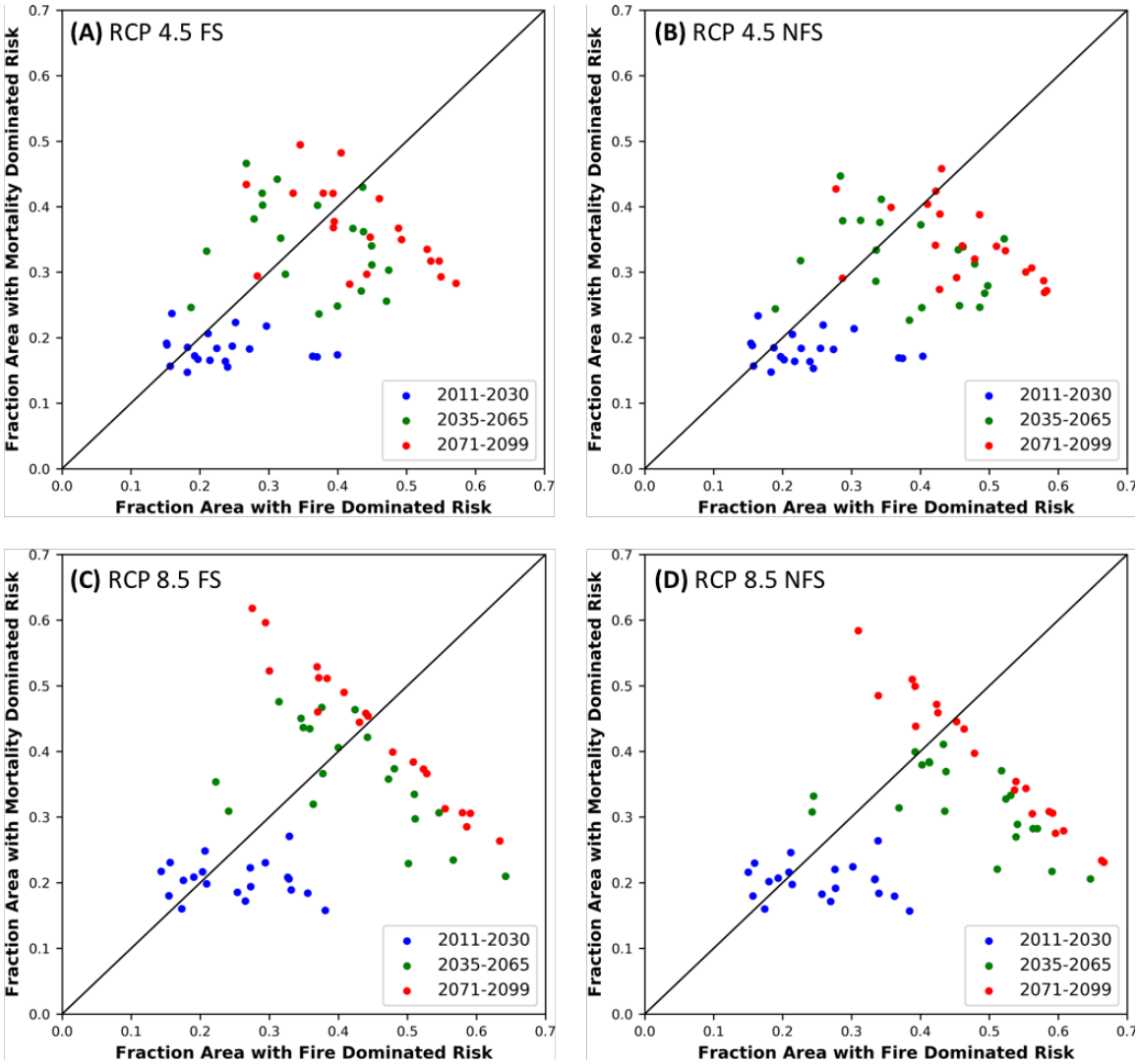

Fig. 4.9. Drivers of *MC2 Biomass Loss Risk*. Fraction of the study area at risk driven by vegetation shifts (*MC2 Mortality Risk*) versus driven by fire (*MC2 Fire Loss Risk*) in the EEMS node *MC2 Biomass Loss Risk*.

Ensemble members with the greatest (or least) change in annual temperature generally do not correspond to climate futures responsible for the largest area of maximum (minimum) risk of biomass loss (Fig. 4.10, S4.7.). One exception is under HadGEM2-ES365 (model 9) which drives the greatest change in temperature for 2071-2099 under both RCP 4.5 and RCP 8.5 and causes the greatest simulated area at risk in the node *Maximum Biomass Loss Risk*. Over time, the ratio of the number of climate models causing the largest vs the smallest areas at risk of losing biomass (*Biomass Loss Risk)* increases substantially (2-5 models for 2011-2030 to 17-19 models for 2071-2099).

4.5 Discussion

4.5.1 Context

We compared our method of expressing results with those from seven studies covering our study area using inputs from climate models. Climate-based uncertainty was handled in a variety of ways. Rehfeldt et al. (2006) used the average results from two GCMs, predicating their results on the correctness of those GCMs and the CO_2 projections driving them. Rehfeldt et al. (2014a) used an ensemble mean of results from 17 GCMs as a means of defining a consensus future climate before using that climate in their model. Many studies presented graphs and/or tables of region-summarized values of selected drivers and results (Sheehan et al., 2015; Littell et al., 2010; Rogers et al., 2011; Creutzburg et al., 2014; Sheehan et al., 2019; Bachelet et al., 2015). Several presented sets of maps allowing visual comparisons of result variation (Sheehan et al., 2015; Littell et al., 2010; Rogers et al., 2011; Sheehan et al., 2019; Bachelet et al., 2015), but only two presented spatial uncertainty. Littell et al. (2010) classified risk to Douglas-fir in terms of the percentage of models agreeing or disagreeing on its occurrence, and Rogers et al. (2011) mapped the number of models agreeing on the direction of change in ecosystem carbon, burn area, and vegetation type. To our knowledge, ours is the first study in this region to provide a detailed, quantified, spatial measure of climate-based uncertainty for modeled future vegetation. With the simplified manner of expressing risk and uncertainty, our results could be more suitable for adaptive management scenario planning.

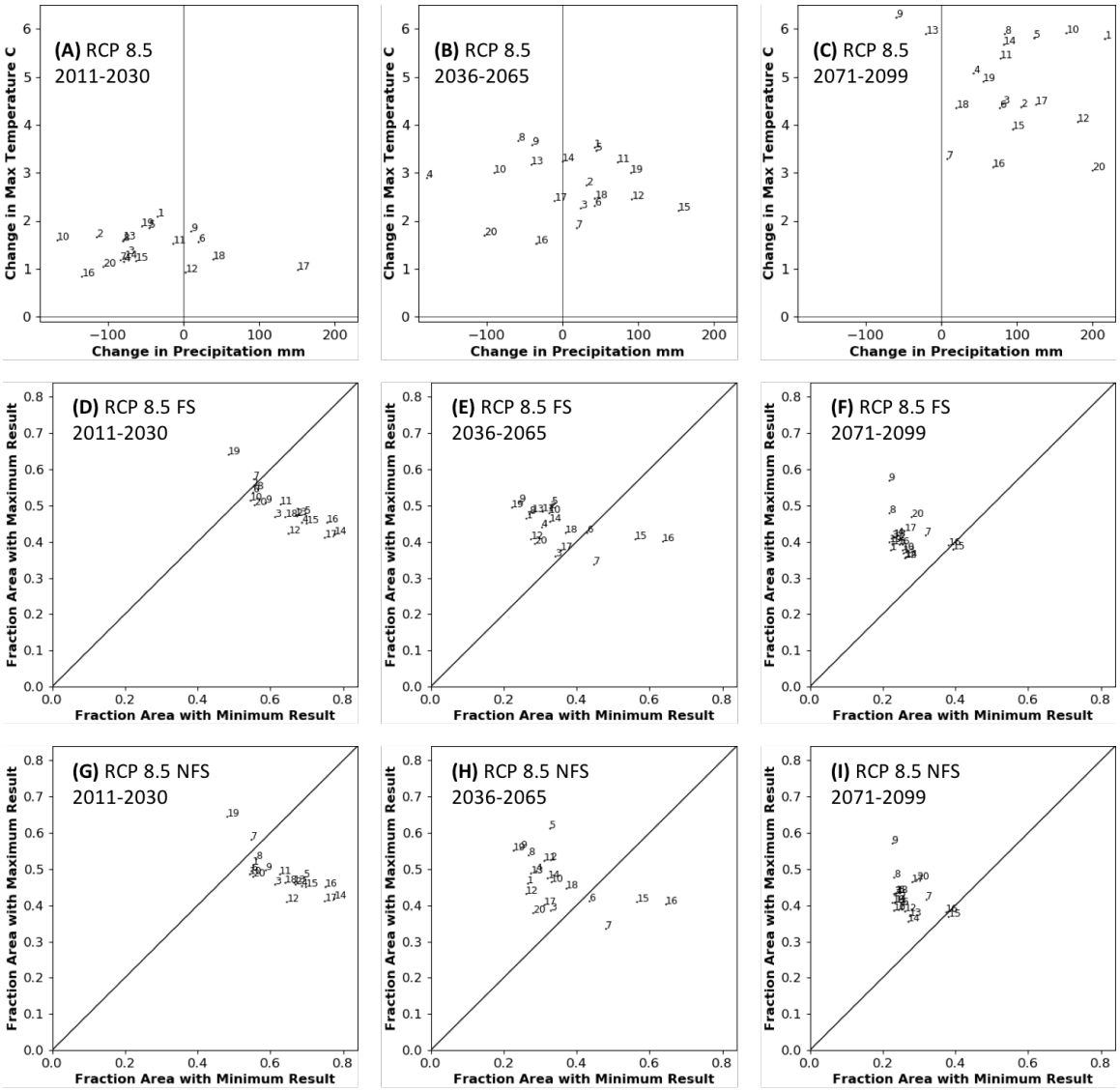

Fig. 4.10. Relationship between climate change summary and MC2 Biomass Loss Risk. Change (1971-2000 vs future time period) in average maximum temperature vs change in average annual precipitation for each of the 20 RCP 8.5 climate futures (A-C), and fraction of the simulated area with maximum and minimum values *MC2 Biomass Loss Risk* for the RCP 8.5 FS scenario (D-F) and the NFS scenario (G-I). In graphs D-I, a point above the 45° line indicates that the results of the MC2 run driven by that climate future showed a greater number of high vs low values of *MC2 Biomass Loss Risk* over more of the study area. Points below the 45° line indicate that MC2 results showed a greater number of low vs high values over more of the area. (mm: millimeters)

4.5.2 Limitations

An ensemble mean provides a single measure of risk for the ensemble, however climate models driving the results may not be completely independent of one another (Masson and Knutti, 2011). Weighting results based on the similarities of the underlying climate models could adjust for this but understanding the provenance of many climate models can be onerous. We did not account for the uncertainty resulting from assumed ignitions or the built-in CO_2 fertilization effect in MC2. The consequences of these assumptions on MC2 fire and carbon dynamics results were found to be substantial (Sheehan et al., 2019), but including those uncertainties was beyond the goal of this study. Likewise, we did not incorporate the uncertainty in Hudiburg's (Hudiburg et al., 2009) data due to the study's limited scope.

4.5.3 General Implications

Our results show the risk of biomass loss generally increasing with time in current high biomass areas within the study region. The pattern of increased fire-driven risk through time is generally south to north and upslope as fires become more frequent due to increasing temperatures. Mortality-driven risk increases along the coast where vegetation becomes maladapted to warming and where coastal climate influences reduce fire risk.

Changes in biomass are directly related to ecosystem services such as timber production, carbon sequestration, wildlife habitat provision, recreational opportunities, and fresh water quality (Neary et al., 2009). Thinning, prescribed fire, and suppression can mitigate fire risk, however each of these actions has associated economic and other costs (Hurteau et al., 2008; Fischer et al., 2016). Thinning may increase forest resistance and resilience to drought, however, it may make forests less resistant and resilient as forests age (D'Amato et al., 2013). When physiological processes cannot be buffered against environmental variability, maladaptation leads to mortality (Rehfeldt et al., 2014c). Maintaining biomass in forested areas under climate change-induced maladaptation may depend on management strategies such as sourcing seeds and species from better climatically suited sources (i.e. assisted migration; Bradley St. Clair and Howe, 2007; Chmura et al., 2011). Tools to help mangers implement such strategies have been developed (e.g. Seedlot Selection Tool, https://seedlotselectiontool.org/sst/).

4.5.4 Management and planning

Our results provide managers with spatial datasets representing three aspects of the *Biomass Loss Risk* metric. The mean value of biomass lost across all climate futures provides an overall idea of potential magnitude of loss, while minimum and maximum values bracket the range, suggesting limits for management alternatives. Uncertainty quantifies the variability of the model results. Land management takes place at multiple scales, with planning and assessment at the national or regional level and implementation at more local levels (Hann and Bunnell, 2001). Using terminology appropriate for managers such as *risk* and *uncertainty*, as well as using a spatial scale appropriate for local information makes our results appropriate for local planning.

Environmental models are often found to be insufficiently accurate to use as forecasts (Millar et al., 2007). However, they provide insights and scenarios useful for scenario planning (Millar et al., 2007) and are useful for decreasing uncertainty rather than making predictions (Littell et al., 2011). Our work is intended to be viewed within this context, providing one set of results with as much clarity as possible regarding uncertainty, sources of uncertainty, and drivers of risk.

Process-based models, such as MC2, are considered more limited than empirical models in quantifying uncertainty (Littell et al., 2011), thus limiting their usefulness in management planning. Our method, which quantifies uncertainty in MC2 results, alleviates this limitation, likely making it easier for managers to use process-based models in their decision making.

It has been suggested that when a range of future possibilities is needed for planning, selecting the most extreme climate projections (e.g. warmest, coolest, wettest, driest) as inputs to ecological models provides brackets for the needed answers (Littell et al., 2011). The lack of correspondence we found between the most extreme climate futures and their influence on minimum or maximum risk indicates that simple metrics for climate extremes are not sufficient for bracketing our model results. In a process-based model such as MC2, seasonal patterns and extreme events that are not reflected in annual values or averages over multi-year time periods have the potential to strongly affect fire and vegetation trajectories. Finding climate metrics that predict the most extreme results would be challenging, if not impossible, due to complex interactions within the model. While culling input datasets from GCMs and ESMs that perform

poorly in the region may be required to reduce uncertainty (Rupp et al., 2013), culling less extreme climate futures may inadvertently reduce the desired range of results.

4.5.5 Further opportunities and challenges

Fuzzy logic modeling has been used in a variety of ecological modeling applications (Adriaenssens et al., 2004), including species distribution (e.g., Barbosa and Real 201), habitat mapping (e.g., Petrou et al., 2014), water quality (e.g., Forio et al., 2017), wildfire risk (e.g., Soto, 2012), and the human valuation of natural elements (e.g., Smith et al., 2016). Managing forests in light of climate change requires understanding climate's potential effects on not only forests, but also industries and communities (Keenan, 2015).

Our model may prove useful to managers by itself, but it has the potential to provide greater utility when combined with other metrics reflecting landscape condition, status, and value. The modular nature of the EEMS framework would allow our model to be easily combined into new models. Ignition probabilities, fire spread probabilities, and fire refugia data (Meigs et al., 2018; Meddens et al., 2018; Krawchuk et al., 2016) could be added to provide greater detail for fire risk. Submodels of climate refugia related to microclimate and enduring landscape features (Morelli et al., 2016; Theobald et al., 2015) could provide more realism for mortality-based risk. Combining our risk model with submodels for current habitat quality (e.g., Zabihi et al., 2017), connectivity corridors (Krosby et al., 2015), and species presence or absence could help guide management conservation decisions. Similarly, incorporating risk with submodels for economic, social, and cultural values could help managers with biocultural approaches to conservation (Gavin et al., 2015). Stakeholder input and expert opinion can be used to parameterize these models so that they precisely reflect management concerns. It is our hope that this model and this methodology can contribute to sound decision making for a wide variety of purposes in our study region and beyond.

4.6 References

Abatzoglou, J. T., Rupp, D. E., & Mote, P. W. (2014). Seasonal climate variability and change in the Pacific Northwest of the United States. *Journal of Climate*, 27(5), 2125-2142.

Adriaenssens, V., De Baets, B., Goethals, P. L., & De Pauw, N. (2004). Fuzzy rule-based models for decision support in ecosystem management. *Science of the Total Environment*, 319(1-3), 1-12.

Bachelet, D., Ferschweiler, K., Sheehan, T. J., Sleeter, B. M., & Zhu, Z. (2015). Projected carbon stocks in the conterminous USA with land use and variable fire regimes. *Global Change Biology*, 21(12), 4548-4560.

Barbosa, A. M., & Real, R. (2012). Applying fuzzy logic to comparative distribution modelling: a case study with two sympatric amphibians. *The Scientific World Journal*, 2012, 428206.

Bradley St. Clair, J., & Howe, G. T. (2007). Genetic maladaptation of coastal Douglas-fir seedlings to future climates. *Global Change Biology*, 13(7), 1441-1454.

Chmura, D. J., Anderson, P. D., Howe, G. T., Harrington, C. A., Halofsky, J. E., Peterson, D. L., Shaw, D. C., & Clair, J. B. S. (2011). Forest responses to climate change in the northwestern United States: ecophysiological foundations for adaptive management. *Forest Ecology and Management*, 261(7), 1121-1142.

Coops, N. C., Waring, R. H., Beier, C., Roy-Jauvin, R., & Wang, T. (2011). Modeling the occurrence of 15 coniferous tree species throughout the Pacific Northwest of North America using a hybrid approach of a generic process-based growth model and decision tree analysis. *Applied Vegetation Science*, 14(3), 402-414.

Creutzburg, M. K., Halofsky, J. E., Halofsky, J. S., & Christopher, T. A. (2014). Climate change and land management in the rangelands of central Oregon. *Environmental Management*, 55(1), 43-55.

D'Amato, A. W., Bradford, J. B., Fraver, S., & Palik, B. J. (2013). Effects of thinning on drought vulnerability and climate response in north temperate forest ecosystems. *Ecological Applications*, 23(8), 1735-1742.

Daly, C., Halbleib, M., Smith, J. I., Gibson, W. P., Doggett, M. K., Taylor, G. H., Curtis, J., & Pasteris, P. P. (2008). Physiographically sensitive mapping of climatological temperature and precipitation across the conterminous United States. *International Journal of Climatology*, 28(15), 2031-2064.

Fischer, A. P., Spies, T. A., Steelman, T. A., Moseley, C., Johnson, B. R., Bailey, J. D., Ager, A. A., Bourgeron, P., Charnley, S., Collins, B. M., & Kline, J. D. (2016). Wildfire risk as a socioecological pathology. *Frontiers in Ecology and the Environment*, 14(5), 276-284.

Forio, M. A. E., Mouton, A., Lock, K., Boets, P., Nguyen, T. H. T., Ambarita, M. N. D., Musonge, P. L. S., Dominguez-Granda, L., & Goethals, P. L. (2017). Fuzzy modelling to identify key drivers of ecological water quality to support decision and policy making. *Environmental Science & Policy*, 68, 58-68.

Gavin, M. C., McCarter, J., Mead, A., Berkes, F., Stepp, J. R., Peterson, D., & Tang, R. (2015). Defining biocultural approaches to conservation. *Trends in Ecology & Evolution*, 30(3), 140-145.

Giles, R. (1976). Łukasiewicz logic and fuzzy set theory. *International Journal of Man-Machine Studies*, 8(3), 313-327.

Hann, W. J., & Bunnell, D. L. (2001). Fire and land management planning and implementation across multiple scales. *International Journal of Wildland Fire*, 10(4), 389-403.

Hudiburg, T., Law, B., Turner, D. P., Campbell, J., Donato, D., & Duane, M. (2009). Carbon dynamics of Oregon and Northern California forests and potential land-based carbon storage. *Ecological Applications*, 19(1), 163-180.

Hurteau, M. D., Koch, G. W., & Hungate, B. A. (2008). Carbon protection and fire risk reduction: toward a full accounting of forest carbon offsets. *Frontiers in Ecology* and *the Environment*, 6(9), 493-498.

Jolly, W. M., Cochrane, M. A., Freeborn, P. H., Holden, Z. A., Brown, T. J., Williamson, G. J., & Bowman, D. M. (2015). Climate-induced variations in global wildfire danger from 1979 to 2013. *Nature Communications*, 6, 7537.

Keenan, R. J. (2015). Climate change impacts and adaptation in forest management: a review. *Annals of Forest Science*, 72(2), 145-167.

Kolb, T. E., Fettig, C. J., Ayres, M. P., Bentz, B. J., Hicke, J. A., Mathiasen, R., Stewart, J. E., & Weed, A. S. (2016). Observed and anticipated impacts of drought on forest insects and diseases in the United States. *Forest Ecology and Management*, 380, 321-334.

Krawchuk, M. A., Haire, S. L., Coop, J., Parisien, M. A., Whitman, E., Chong, G., & Miller, C. (2016). Topographic and fire weather controls of fire refugia in forested ecosystems of northwestern North America. *Ecosphere*, 7(12), e01632.

Krosby, M., Breckheimer, I., Pierce, D. J., Singleton, P. H., Hall, S. A., Halupka, K. C., Gaines, W. L., Long, R. A., McRae, B. H., Cosentino, B. L., & Schuett-Hames, J. P. (2015). Focal species and landscape "naturalness" corridor models offer complementary approaches for connectivity conservation planning. *Landscape Ecology*, 30(10), 2121-2132.

Latta, G., Temesgen, H., & Barrett, T. M. (2009). Mapping and imputing potential productivity of Pacific Northwest forests using climate variables. *Canadian Journal of Forest Research*, 39(6), 1197-1207.

Littell, J. S., McKenzie, D., Kerns, B. K., Cushman, S., & Shaw, C. G. (2011). Managing uncertainty in climate-driven ecological models to inform adaptation to climate change. *Ecosphere*, 2(9), 1-19.

Littell, J. S., Oneil, E. E., McKenzie, D., Hicke, J. A., Lutz, J. A., Norheim, R. A., & Elsner, M. M. (2010). Forest ecosystems, disturbance, and climatic change in Washington State, USA. *Climatic Change*, 102(1-2), 129-158.

Luo, Y., Ahlström, A., Allison, S. D., Batjes, N. H., Brovkin, V., Carvalhais, N., Chappell, A., Ciais, P., Davidson, E. A., Finzi, A., & Georgiou, K. (2016). Toward more realistic projections of soil carbon dynamics by Earth system models. *Global Biogeochemical Cycles*, 30(1), 40-56.

Masson, D., & Knutti, R. (2011). Climate model genealogy. *Geophysical Research Letters*, 38(8).

May, C., Luce, C., Casola, J., Chang, M., Cuhaciyan, J., Dalton, M. , Lowe, S., Morishima, G., Mote, P., Petersen, A., Roesch-McNally, G., & York, E. (2018). Northwest. In *Impacts,*

Risks, and Adaptation in the United States: Fourth National Climate Assessment, Volume II (pp. 1036-1100). U.S. Global Change Research Program, Washington, DC, USA.

Meddens, A. J., Kolden, C. A., Lutz, J. A., Smith, A. M., Cansler, C. A., Abatzoglou, J. T., Meigs, G. W., Downing, W. M., & Krawchuk, M. A. (2018). Fire Refugia: What Are They, and Why Do They Matter for Global Change? *BioScience*, 68(12), 944-954.

Meigs, G., & Krawchuk, M. (2018). Composition and Structure of Forest Fire Refugia: What Are the Ecosystem Legacies across Burned Landscapes? *Forests*, 9(5), 243.

Millar, C. I., Stephenson, N. L., & Stephens, S. L. (2007). Climate change and forests of the future: managing in the face of uncertainty. *Ecological Applications*, 17(8), 2145-2151.

Morelli, T. L., Daly, C., Dobrowski, S. Z., Dulen, D. M., Ebersole, J. L., Jackson, S. T., Lundquist, J. D., Millar, C. I., Maher, S. P., Monahan, W. B., & Nydick, K. R. (2016). Managing climate change refugia for climate adaptation. *PLoS One*, 11(8), e0159909.

National Research Council. *Adaptive Management for Water Resources Planning* (2004). The National Academies Press, Washington, D. C., USA.

Neary, D. G., Ice, G. G., & Jackson, C. R. (2009). Linkages between forest soils and water quality and quantity. *Forest Ecology and Management*, 258(10), 2269-2281.

Omernik, J. M., & Griffith, G. E. (2014). Ecoregions of the conterminous United States: evolution of a hierarchical spatial framework. *Environmental Management*, 54(6), 1249-1266.

Pachauri, R. K., Allen, M. R., Barros, V. R., Broome, J., Cramer, W., Christ, R., Church, J. A., Clarke, L., Dahe, Q., Dasgupta, P., & Dubash, N. K. (2014). *Climate change 2014: synthesis report. Contribution of Working Groups I, II and III to the fifth assessment report of the Intergovernmental Panel on Climate Change* (p. 151). IPCC Geneva, Switzerland.

Petrou, Z. I., Kosmidou, V., Manakos, I., Stathaki, T., Adamo, M., Tarantino, C., Tomaselli, V., Blonda, P. and Petrou, M. (2014). A rule-based classification methodology to handle uncertainty in habitat mapping employing evidential reasoning and fuzzy logic. *Pattern Recognition Letters*, 48, 24-33.

Pianosi, F., Beven, K., Freer, J., Hall, J. W., Rougier, J., Stephenson, D. B., & Wagener, T. (2016). Sensitivity analysis of environmental models: A systematic review with practical workflow. *Environmental Modelling & Software*, 79, 214-232.

Rehfeldt, G. E., Crookston, N. L., Warwell, M. V., & Evans, J. S. (2006). Empirical analyses of plant-climate relationships for the western United States. *International Journal of Plant Sciences*, 167(6), 1123-1150.

Rehfeldt, G. E., Jaquish, B. C., López-Upton, J., Sáenz-Romero, C., St Clair, J. B., Leites, L. P., & Joyce, D. G. (2014a). Comparative genetic responses to climate for the varieties of *Pinus ponderosa* and *Pseudotsuga menziesii*: Realized climate niches. *Forest Ecology and Management*, 324, 126-137.

Rehfeldt, G. E., Leites, L. P., St Clair, J. B., Jaquish, B. C., Sáenz-Romero, C., López-Upton, J., & Joyce, D. G. (2014b). Comparative genetic responses to climate in the varieties of *Pinus ponderosa* and *Pseudotsuga menziesii*: Clines in growth potential. *Forest Ecology and Management*, 324, 138-146.

Rehfeldt, G. E., Jaquish, B. C., Sáenz-Romero, C., Joyce, D. G., Leites, L. P., St Clair, J. B., & López-Upton, J. (2014c). Comparative genetic responses to climate in the varieties of *Pinus ponderosa* and *Pseudotsuga menziesii*: reforestation. *Forest Ecology and Management*, 324, 147-157.

Rogers, B. M., Neilson, R. P., Drapek, R., Lenihan, J. M., Wells, J. R., Bachelet, D., & Law, B. E. (2011). Impacts of climate change on fire regimes and carbon stocks of the US Pacific Northwest. *Journal of Geophysical Research: Biogeosciences*, 116, G03037.

Rupp, D. E., Abatzoglou, J. T., Hegewisch, K. C., & Mote, P. W. (2013). Evaluation of CMIP5 20th century climate simulations for the Pacific Northwest USA. Journal *of Geophysical Research: Atmospheres*, 118(19), 10-884.

Sheehan, T., Bachelet, D., & Ferschweiler, K. (2019). Fire, CO_2, and climate effects on modeled vegetation and carbon dynamics in western Oregon and Washington. *PloS One*, 14(1), e0210989.

Sheehan, T., Bachelet, D., & Ferschweiler, K. (2015). Projected major fire and vegetation changes in the Pacific Northwest of the conterminous United States under selected CMIP5 climate futures. *Ecological Modelling*, 317, 16-29.

Sheehan, T., & Gough, M. (2016). A platform-independent fuzzy logic modeling framework for environmental decision support. *Ecological Informatics*, 34, 92-101.

Smith, M. J., Wagner, C., Wallace, K. J., Pourabdollah, A., & Lewis, L. (2016). The contribution of nature to people: Applying concepts of values and properties to rate the management importance of natural elements. *Journal of Environmental Management*, 175, 76-86.

Soto, M. E. C. (2012). The identification and assessment of areas at risk of forest fire using fuzzy methodology. *Applied Geography*, 35(1-2), 199-207.

Theobald, D. M., Harrison-Atlas, D., Monahan, W. B., & Albano, C. M. (2015). Ecologically-relevant maps of landforms and physiographic diversity for climate adaptation planning. *PloS One*, 10(12), e0143619.

Thom, D., Rammer, W., Dirnböck, T., Müller, J., Kobler, J., Katzensteiner, K., Helm, N. and Seidl, R. (2017). The impacts of climate change and disturbance on spatio-temporal trajectories of biodiversity in a temperate forest landscape. *Journal of Applied Ecology*, 54(1), 28-38.

Urban, D., Roberts, M. J., Schlenker, W., & Lobell, D. B. (2012). Projected temperature changes indicate significant increase in interannual variability of US maize yields. *Climatic Change*, 112(2), 525-533.

Whitlock, C., Shafer, S. L., & Marlon, J. (2003). The role of climate and vegetation change in shaping past and future fire regimes in the northwestern US and the implications for ecosystem management. *Forest ecology and Management*, 178(1-2), 5-21.

Williams, B. K. (2011). Adaptive management of natural resources – framework and issues. *Journal of Mnvironmental Management*, 92(5), 1346-1353.

Zabihi, K., Paige, G. B., Hild, A. L., Miller, S. N., Wuenschel, A., & Holloran, M. J. (2017). A fuzzy logic approach to analyse the suitability of nesting habitat for greater sage-grouse in western Wyoming. *Journal of Spatial Science*, 62(2), 215-234.

Zadeh, L. A. (1973). Outline of a new approach to the analysis of complex systems and decision processes. *IEEE Transactions on Systems, Man, and Cybernetics*, (1), 28-44.

4.7 Acknowledgements

Funding for this research was provided by the U.S. Department of the Interior via the Northwest Climate Science Center through agreement #G12AC20495 within the framework of the research project entitled “Integrated Scenarios of climate, hydrology and vegetation for the Northwest”, P. Mote (Oregon State University) principal investigator.

We thank Ken Ferschweiler for development work on MC2 and data processing support, Tara Hudiburg for model result data, Mike Gough for support of EEMS software, and Meg Krawchuk for guidance on this study.

4.8 Supporting Information

Table S4.1. Lookup table for vegetation type differences.

	0	**1**	**2**	**3**	**4**	**5**	**6**	**7**	**8**	**9**	**1**	**1**	**1**	**1**	**1**	**1**	**1**	**1**	**1**	**1**	**2**	**2**	**2**	**2**	**2**	**2**	**2**	**2**	**2**	**2**	**3**	**3**	**3**	**3**	**3**	**3**	**3**	**3**
0	0	5	5	5	5	5	5	5	5	5	5	5	5	5	5	5	5	5	5	5	5	5	5	5	5	5	5	5	5	5	5	5	5	5	5	5	5	5
1	5	0	1	2	5	4	5	5	5	5	5	5	4	4	4	4	3	2	1	5	5	5	5	5	4	4	4	3	2	1	5	5	3	3	2	1	5	5
2	5	1	0	1	3	2	4	5	5	5	5	5	5	5	5	5	5	5	5	5	5	5	5	5	5	5	5	5	5	5	5	5	5	5	5	5	5	5
3	5	2	1	0	2	1	3	5	5	5	5	5	5	5	5	5	5	5	5	5	5	5	5	5	5	5	5	5	5	5	5	5	5	5	5	5	5	5
4	5	5	3	2	0	2	1	2	2	4	3	4	2	4	3	5	5	5	5	5	5	5	5	5	5	5	5	5	5	5	5	5	5	5	5	5	2	5
5	5	4	2	1	2	0	2	4	3	3	2	3	2	2	1	2	3	4	5	5	5	5	5	5	5	5	5	5	5	5	5	5	5	5	5	5	3	5
6	5	5	4	3	1	2	0	1	1	3	2	3	2	4	2	3	2	3	4	2	4	4	5	3	5	5	4	5	5	5	5	5	5	5	5	5	4	5
7	5	5	5	5	2	4	1	0	1	3	2	2	2	4	2	3	4	5	5	2	4	4	3	2	4	4	3	4	5	5	5	5	5	5	5	5	1	5
8	5	5	5	5	2	3	1	1	0	2	1	1	1	2	2	2	3	4	5	1	3	3	2	2	4	4	3	4	5	5	5	5	5	5	5	5	1	5
9	5	5	5	5	4	3	3	3	2	0	1	1	2	1	2	2	3	4	5	3	2	3	2	3	1	2	3	4	5	5	5	5	5	5	5	5	3	5
10	5	5	5	5	3	2	2	2	1	1	0	1	2	2	1	2	3	4	5	2	2	3	1	3	3	4	2	4	5	5	5	5	5	5	5	5	1	5
11	5	5	5	5	4	3	3	2	1	1	1	0	2	2	2	1	3	4	5	2	2	3	1	3	3	4	2	4	5	5	5	5	5	5	5	5	2	5
12	5	4	5	5	2	2	2	2	1	2	2	2	0	2	1	1	1	2	3	2	3	4	3	1	3	4	2	2	3	4	5	5	5	5	5	5	2	5
13	5	4	5	5	4	2	4	4	2	1	2	2	2	0	1	1	1	2	3	4	2	4	3	3	1	3	2	2	3	4	5	5	5	5	5	5	4	5
14	5	4	5	5	3	1	2	2	2	2	1	2	1	1	0	1	1	2	3	3	3	3	2	2	2	3	1	2	3	4	5	5	5	5	5	5	3	5
15	5	4	5	5	5	2	3	3	2	2	2	1	1	1	1	0	1	2	3	3	3	3	2	2	2	3	1	2	3	4	5	5	5	5	5	5	4	5
16	5	3	5	5	5	3	2	4	3	3	3	3	1	1	1	1	0	1	2	3	3	3	3	2	2	2	2	1	2	3	5	5	5	5	5	5	5	5
17	5	2	5	5	5	4	3	5	4	4	4	4	2	2	2	2	1	0	1	4	4	4	4	3	3	3	3	2	1	2	5	5	5	5	5	5	5	5
18	5	1	5	5	5	5	4	5	5	5	5	5	3	3	3	3	2	1	0	5	5	5	5	4	4	4	4	3	2	1	5	5	5	5	5	5	5	5
19	5	5	5	5	5	5	2	2	1	3	2	2	2	4	3	3	3	4	5	0	2	2	1	1	3	3	2	3	4	5	2	3	4	4	5	5	1	5
20	5	5	5	5	5	5	4	4	3	2	2	2	3	2	3	3	3	4	5	2	0	1	1	3	2	3	2	3	4	5	2	2	3	4	5	5	3	5
21	5	5	5	5	5	5	4	4	3	3	3	3	4	4	3	3	3	4	5	2	1	0	1	2	2	1	2	3	4	5	1	3	3	4	5	5	3	5
22	5	5	5	5	5	5	5	3	2	2	1	1	3	3	2	2	3	4	5	1	1	1	0	2	2	2	1	3	4	5	2	3	4	4	5	5	5	5

Table S4.1, continued.

	0	1	2	3	4	5	6	7	8	9	10	11	12	13	14	15	16	17	18	19	20	21	22	23	24	25	26	27	28	29	30	31	32	33	34	35	36
23	5	5	5	5	5	5	3	2	2	3	3	3	1	3	2	2	2	3	4	1	3	2	2	0	2	2	1	1	2	3	3	4	5	5	5	5	4	5
24	5	4	5	5	5	5	5	4	4	1	3	3	3	1	2	2	2	3	4	3	2	2	2	2	0	1	2	1	2	3	2	3	4	4	5	5	2	5
25	5	4	5	5	5	5	5	4	4	2	4	4	4	3	3	3	2	3	4	3	3	1	2	2	1	0	1	2	3	4	2	1	2	2	3	4	4	5
26	5	4	5	5	5	5	4	3	3	3	2	2	2	2	1	1	2	3	4	2	2	2	1	1	2	1	0	1	2	3	3	2	2	2	3	4	4	5
27	5	3	5	5	5	5	5	4	4	4	4	4	2	2	2	2	1	2	3	3	3	3	3	1	1	2	1	0	1	2	4	3	2	1	2	3	5	5
28	5	2	5	5	5	5	5	5	5	5	5	5	3	3	3	3	2	1	2	4	4	4	4	2	2	3	2	1	0	1	4	3	2	2	1	2	5	5
29	5	1	5	5	5	5	5	5	5	5	5	5	4	4	4	4	3	2	1	5	5	5	5	3	3	4	3	2	1	0	5	4	3	3	2	1	5	5
30	5	5	5	5	5	5	5	5	5	5	5	5	5	5	5	5	5	5	5	2	2	1	2	3	2	2	3	4	4	5	0	1	2	2	3	4	5	5
31	5	5	5	5	5	5	5	5	5	5	5	5	5	5	5	5	5	5	5	3	2	3	3	4	3	1	2	3	3	4	1	0	1	1	2	3	5	5
32	5	3	5	5	5	5	5	5	5	5	5	5	5	5	5	5	5	5	5	4	3	3	4	5	4	2	2	2	2	3	2	1	0	1	1	2	5	5
33	5	3	5	5	5	5	5	5	5	5	5	5	5	5	5	5	5	5	5	4	4	4	4	5	4	2	2	1	2	3	2	1	1	0	1	2	5	5
34	5	2	5	5	5	5	5	5	5	5	5	5	5	5	5	5	5	5	5	5	5	5	5	5	5	3	3	2	1	2	3	2	1	1	0	1	5	5
35	5	1	5	5	5	5	5	5	5	5	5	5	5	5	5	5	5	5	5	5	5	5	5	5	5	4	4	3	2	1	4	3	2	2	1	0	5	5
36	5	5	5	5	2	3	4	1	1	3	1	2	2	4	3	4	5	5	5	1	3	3	5	4	2	4	4	5	5	5	5	5	5	5	5	5	0	5
37	5	5	5	5	5	5	5	5	5	5	5	5	5	5	5	5	5	5	5	5	5	5	5	5	5	5	5	5	5	5	5	5	5	5	5	5	5	0

(0: Undefined; 1: Barren; 2: Tundra; 3: Taiga Tundra; 4: Boreal Evergreen Needleleaf Forest; 5: Boreal Mixed Woodland; 6: Subalpine; 7: Maritime Evergreen Needleleaf Forest; 8: Temperate Evergreen Needleleaf Forest; 9: Temperate Deciduous Broadleaf Forest; 10: Temperate Cool Mixed Forest; 11: Temperate Warm Mixed Forest; 12: Temperate Evergreen Needleleaf Woodland; 13: Temperate Deciduous Broadleaf Woodland; 14: Temperate Cool Mixed Woodland; 15: Temperate Warm Mixed Woodland; 16: Temperate Shrubland; 17: Temperate Grassland; 18: Temperate Desert; 19: Subtropical Evergreen Needleleaf Forest; 20: Subtropical Deciduous Broadleaf Forest; 21: Subtropical Evergreen Broadleaf Forest; 22: Subtropical Mixed Forest; 23: Subtropical Evergreen Needleleaf Woodland; 24: Subtropical Deciduous Broadleaf Woodland; 25: Subtropical Evergreen Broadleaf Woodland; 26: Subtropical Mixed Woodland; 27: Subtropical Shrubland; 28: Subtropical Grassland; 29: Subtropical Desert; 30: Tropical Evergreen Broadleaf Forest; 31: Tropical Deciduous Woodland; 32: Tropical Savanna; 33: Tropical Shrubland; 34: Tropical Grassland; 35: Tropical Desert; 36: Cool Needleleaf Forest; 37: Agriculture and Grazing)

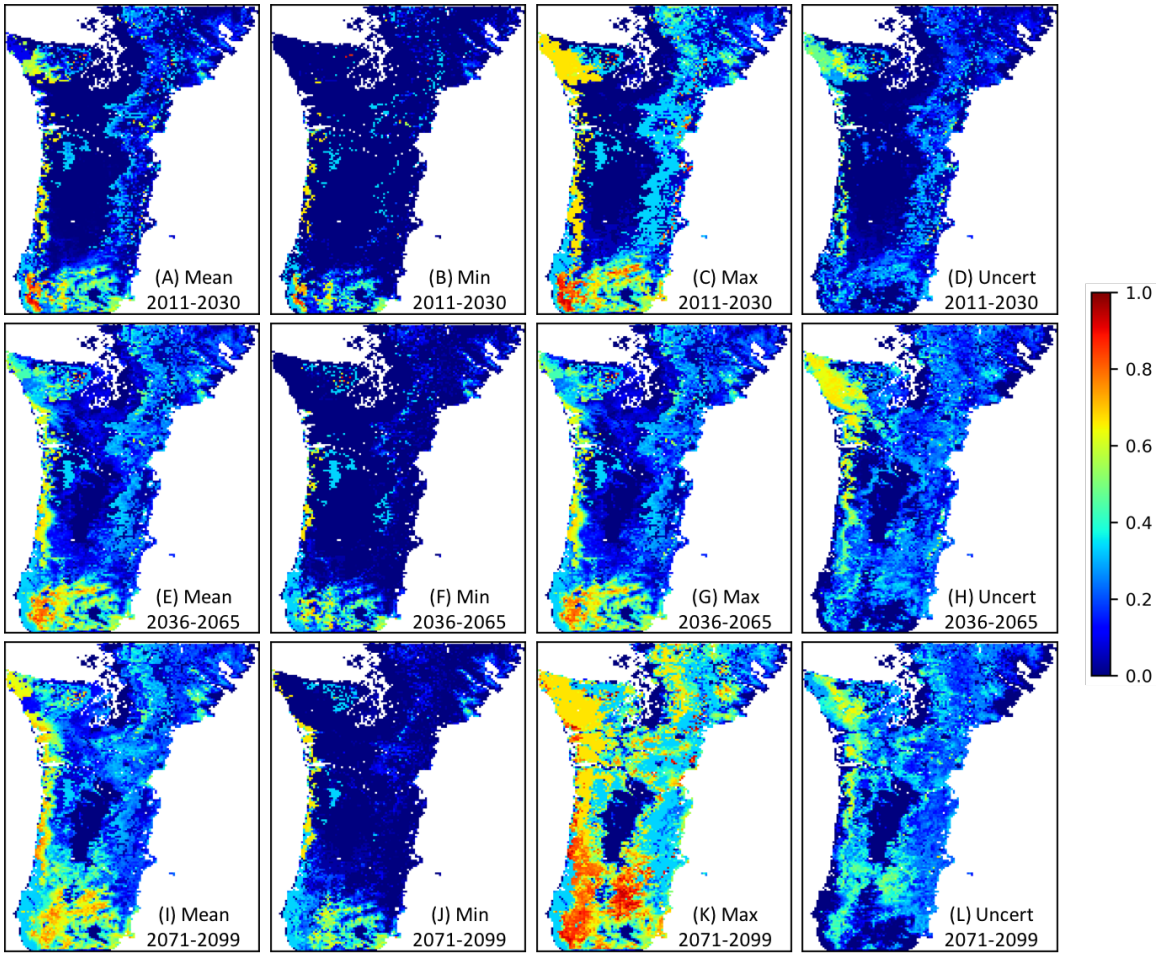

Fig. S4.1. Maps of *Biomass Loss Risk* from EEMS model for the RCP 4.5 FS scenario. Figure rows include the mean, minimum, maximum, and uncertainty representation for one time period. (min: minimum; max: maximum; uncert: uncertainty)

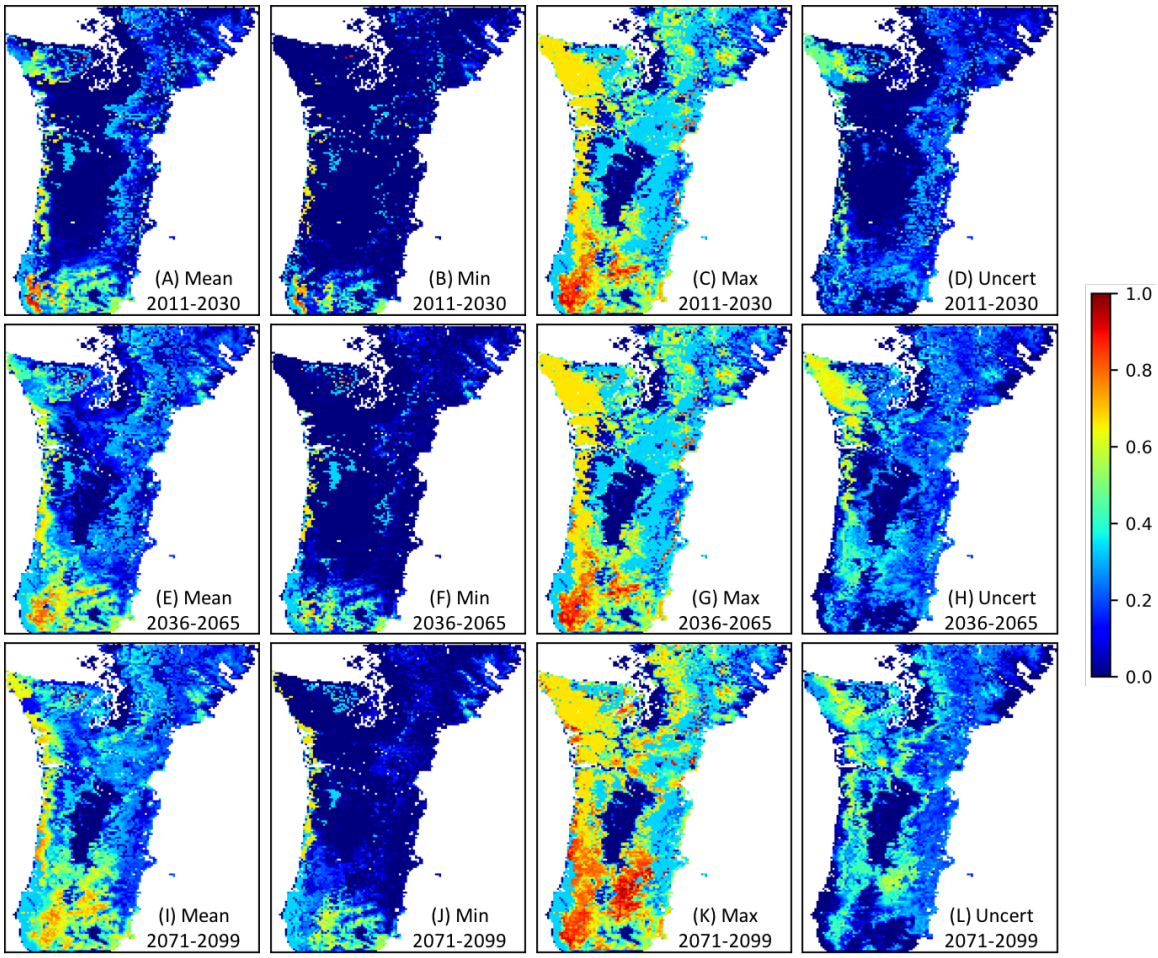

Fig. S4.2. Maps of *Biomass Loss Risk* from EEMS model for the RCP 4.5 NFS scenario. Figure rows include the mean, minimum, maximum, and uncertainty representation for one time period. (min: minimum; max: maximum; uncert: uncertainty)

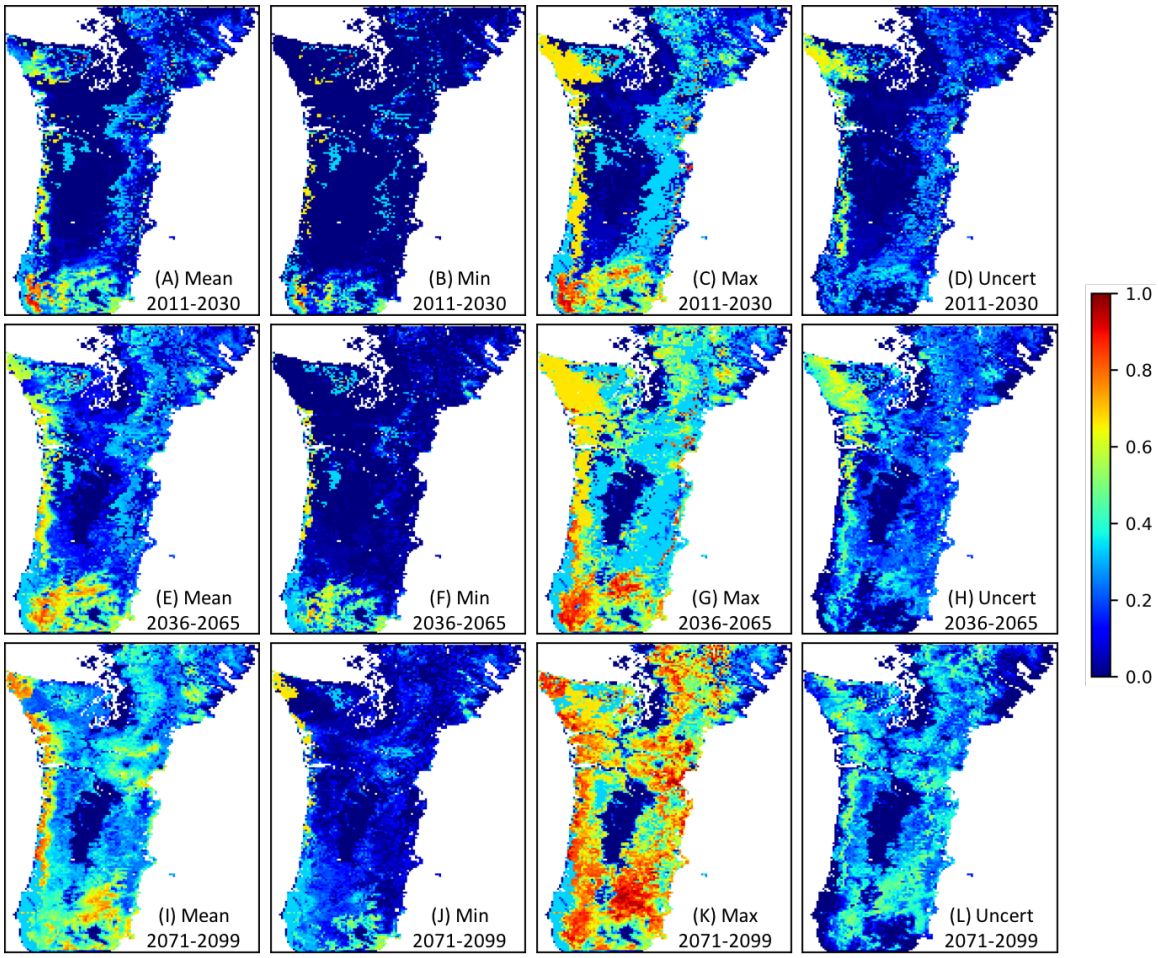

Fig. S4.3. Maps of *Biomass Loss Risk* from EEMS model for the RCP 8.5 FS scenario. Figure rows include the mean, minimum, maximum, and uncertainty representation for one time period. (min: minimum; max: maximum; uncert: uncertainty)

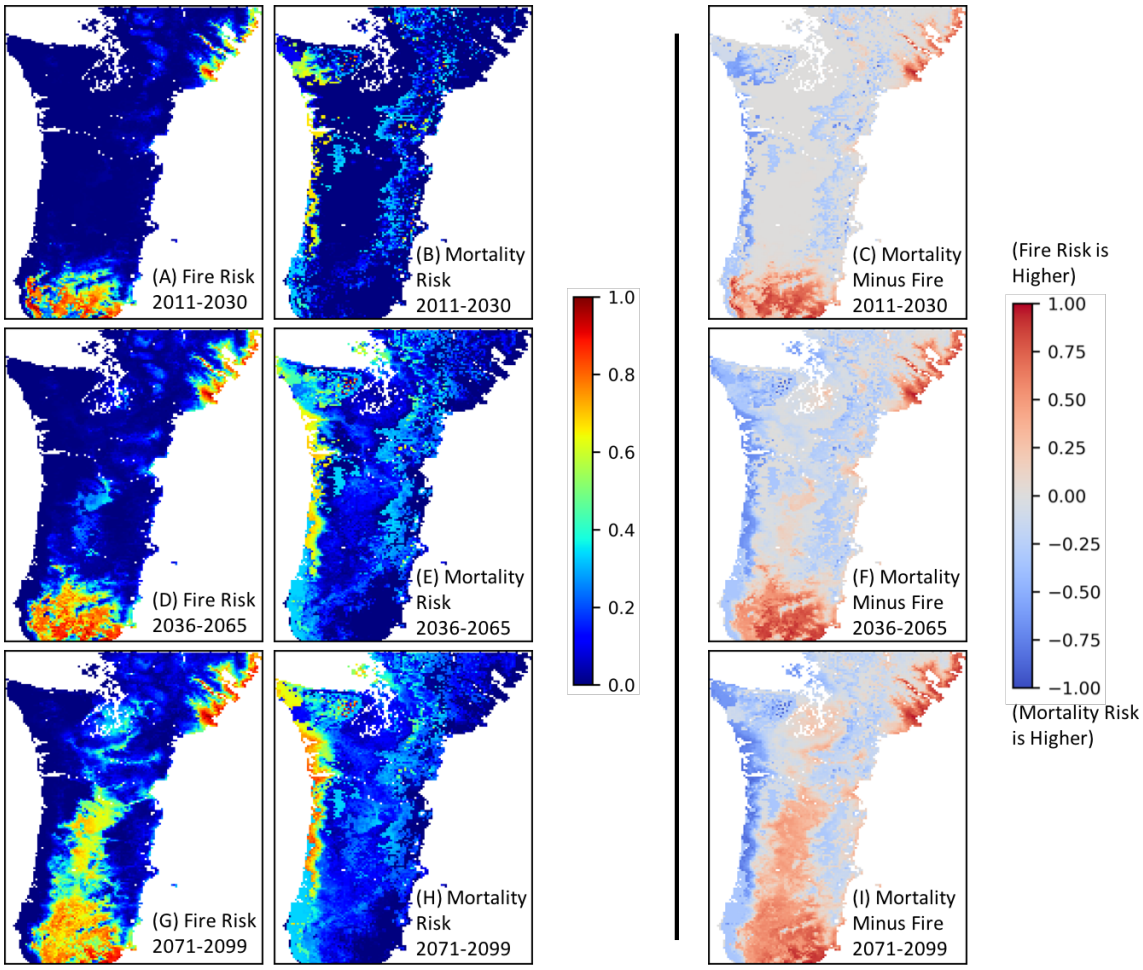

Fig. S4.4. Drivers of *MC2 Mortality Risk.* Maps of *MC2 Fire Loss Risk* (A, D, G), *MC2 Mortality Risk* (B, E, H), and *MC2 Fire Loss Risk* minus *MC2 Mortality Risk* (C, F, I) from EEMS model for the RCP 4.5 FS scenario. Figure rows represent time periods.

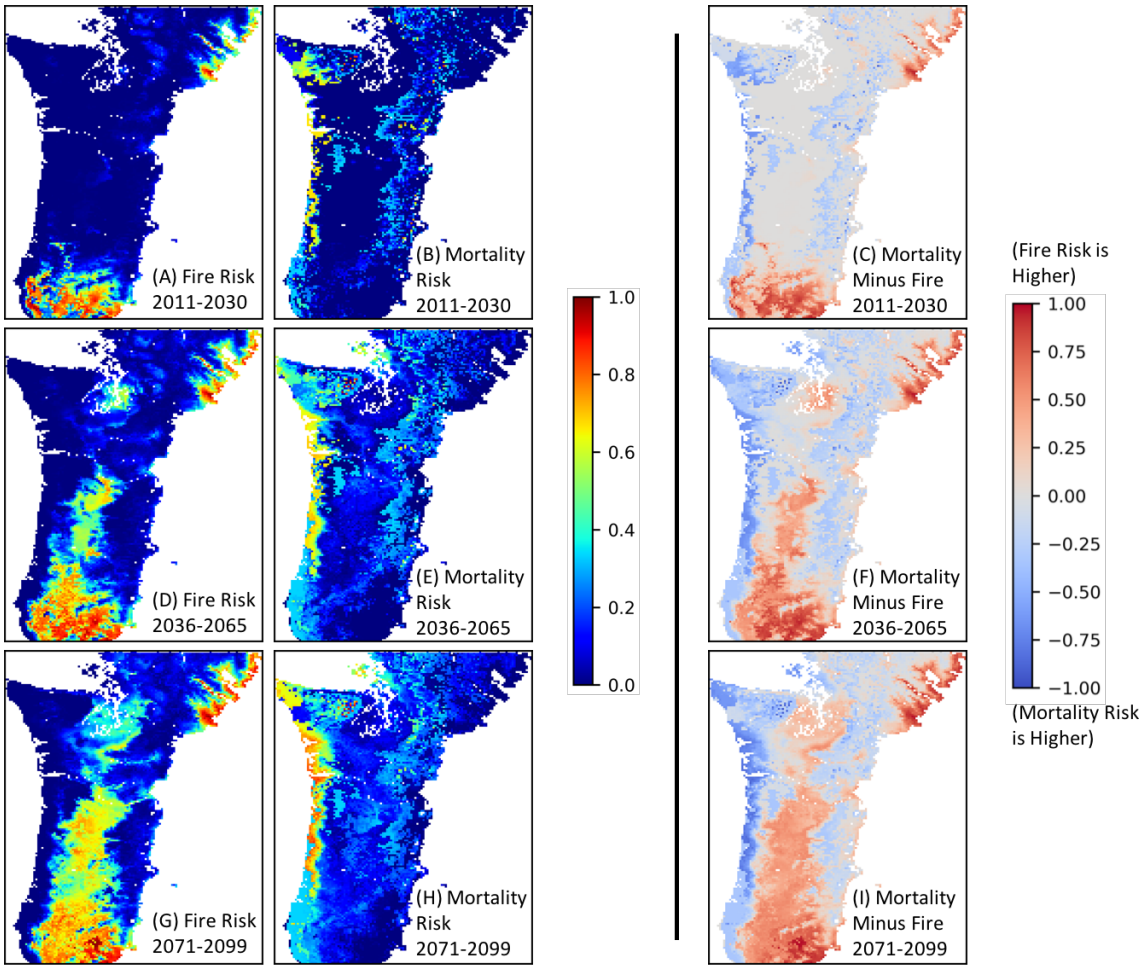

Fig. S4.5. Drivers of *MC2 Mortality Risk.* Maps of *MC2 Fire Loss Risk* (A, D, G), *MC2 Mortality Risk* (B, E, H), and *MC2 Fire Loss Risk* minus *MC2 Mortality Risk* (C, F, I) from EEMS model for the RCP 4.5 NFS scenario. Figure rows represent time periods.

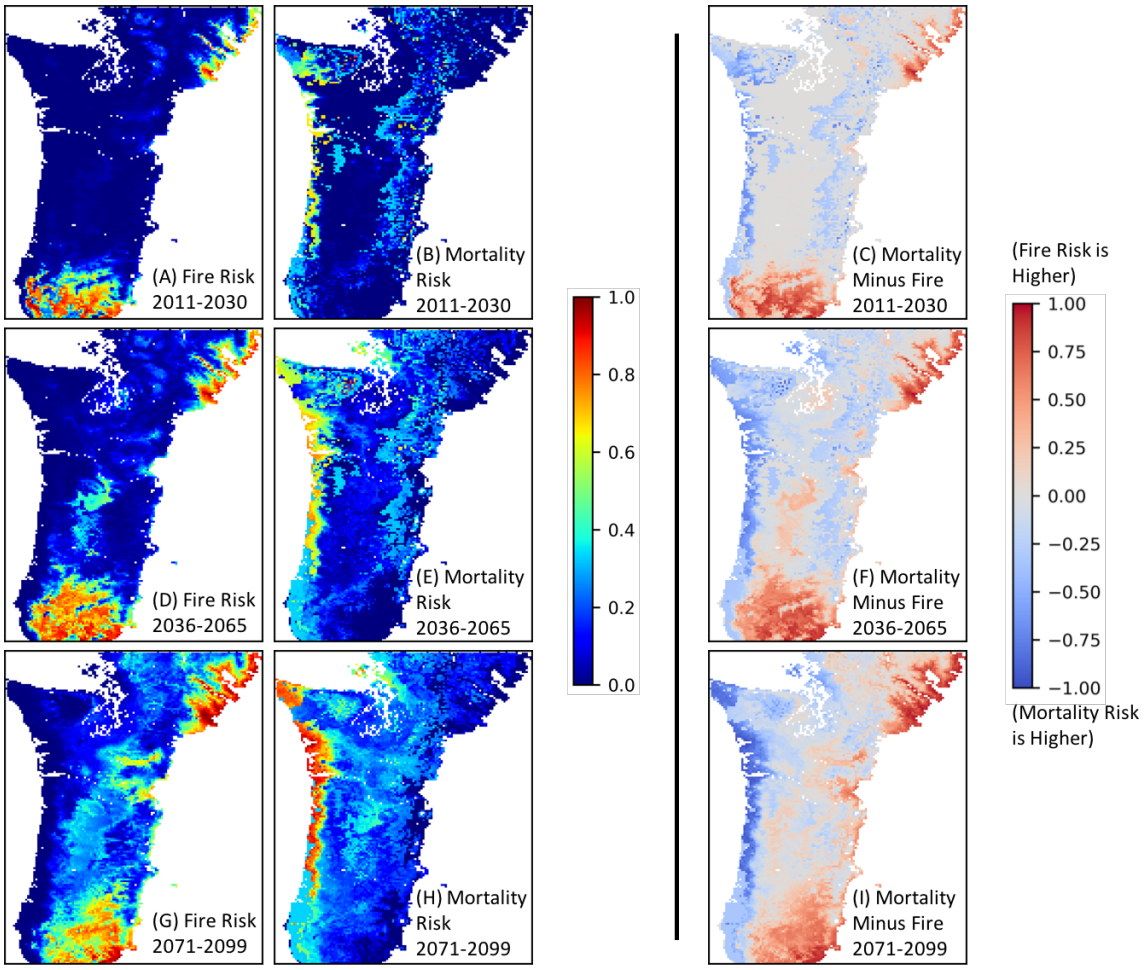

Fig. S4.6. Drivers of *MC2 Mortality Risk.* Maps of *MC2 Fire Loss Risk* (A, D, G), *MC2 Mortality Risk* (B, E, H), and *MC2 Fire Loss Risk* minus *MC2 Mortality Risk* (C, F, I) from EEMS model for the RCP 8.5 FS scenario. Figure rows represent time periods.

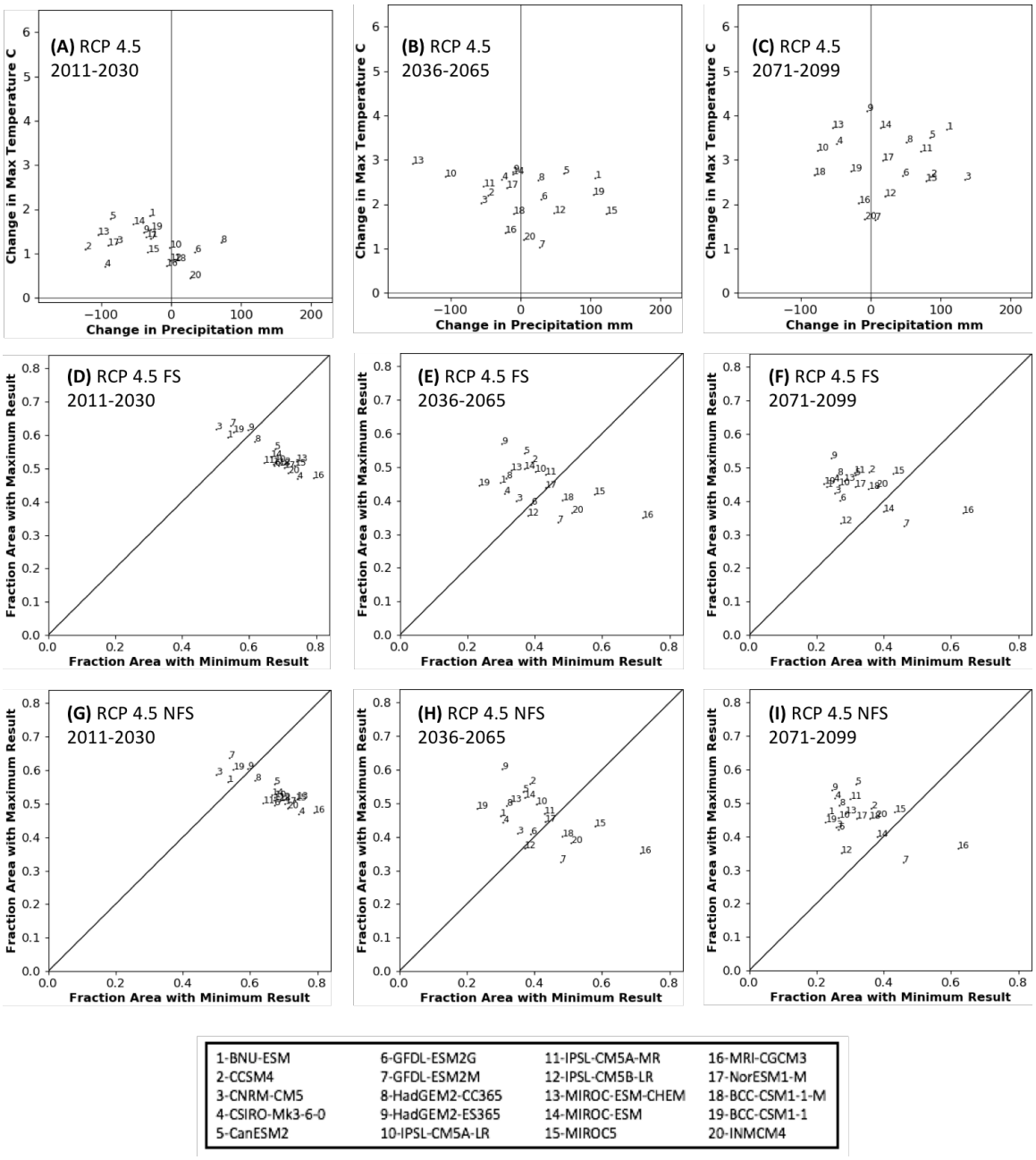

1-BNU-ESM	6-GFDL-ESM2G	11-IPSL-CM5A-MR	16-MRI-CGCM3
2-CCSM4	7-GFDL-ESM2M	12-IPSL-CM5B-LR	17-NorESM1-M
3-CNRM-CM5	8-HadGEM2-CC365	13-MIROC-ESM-CHEM	18-BCC-CSM1-1-M
4-CSIRO-Mk3-6-0	9-HadGEM2-ES365	14-MIROC-ESM	19-BCC-CSM1-1
5-CanESM2	10-IPSL-CM5A-LR	15-MIROC5	20-INMCM4

Fig. S4.7. Relationship between climate change summary and MC2 Biomass Loss Risk. Change (1971-2000 vs future period) in average maximum temperature vs change in average annual precipitation for each of the 20 RCP 4.5 climate futures (A-C), and fraction of the simulated area with maximum and minimum values *MC2 Biomass Loss Risk* for the RCP 4.5 FS scenario (D-F) and the NFS scenario (G-I). In graphs D-I, a point above the 45° line indicates that the results of the MC2 run driven by that climate future showed a greater number of high vs low values of biomass loss over more of the study area. Points below the 45° line indicate that MC2 results showed a greater number of low vs high values over more of the area. (mm: millimeters)

5 Conclusions

5.1 Study and findings

I have used the most recent downscaled climate futures to simulate vegetation dynamics, carbon dynamics, and fire in the Pacific Northwest of the conterminous United States. The bulk of my work focused on Oregon and Washington west of the Cascade Mountain Range crest. In order to characterize overall uncertainty in MC2 results and explore avenues for model improvements, I performed uncertainty and sensitivity analyses with the model. Chapter 2 examined the effects of fire suppression and emission scenarios with climate futures from 20 different global climate models (GCMs) and earth system models (ESMs). Chapter 3 examined the effects of embedded assumptions about fire and CO_2 fertilization in the MC2 dynamic global vegetation model (DGVM). Chapter 4 quantified the risk of biomass loss, identified the drivers of that risk, and evaluated the sources of uncertainty associated with that risk.

In Chapter 2, I described major findings for each of the three regions I studied. In the eastern Northwest mountains (ENWM), conifer forests persist under all scenarios. However subalpine forests are replaced by warmer forest types. Sudden vegetation shifts could be triggered by large fires as modeled, or other disturbances the model does not simulate. In the Northwest plains and plateau (NWPP), simulated fire suppression leads to the expansion of woody vegetation indicating the importance of fire in shaping local vegetation. Invasive species (such as medusahead and cheatgrass; Davies et al., 2011), which were not simulated, have a strong influence in this region and may change fire regime and vegetation succession trajectory. Finally, in the western Northwest (WNW), the model projects that most conifer forests are replaced by mixed forests, and large fires occur in the 21st c. over much of the region. A combination of maladapted vegetation with large fires indicates the potential for sudden, large-scale vegetation change.

In Chapter 3, assumptions about both CO_2 fertilization and fire occurrence had strong effects on simulated C dynamics. The CO_2 fertilization effect is not sufficient to overcome C losses due to fire in the 21st c., and the only scenario where C losses were minimal was the case with CO_2 fertilization effect and no fire. One implication is that the WNW region will become a C source during the 21st c. When ignitions were assumed to be unlimited, fire suppression had little effect on fire occurrence or carbon dynamics. However simulating stochastic ignitions and

ignition propagation resulted in less variable carbon fluxes and carbon pools. This points to the importance of considering ignition source probabilities in modeling fire occurrence in this region. Modifying the effects of raising atmospheric CO_2 on plant production and the frequency of fire occurrence had virtually no effect on vegetation change in the region, indicating that vegetation change in the model is entirely climate driven.

Chapter 4 introduces a novel method and results. I built an Environmental Evaluation Modeling System (EEMS) logic model to quantify the risk of biomass loss and its drivers. My EEMS model provides a transparent, useable model for evaluating risk as well as enabling data exploration to discover what the drivers are. Mortality generally drives *Biomass Loss Risk* along the coast while fire is a stronger driver inland. The differences between the projections of various climate models for the same emission and fire suppression scenario contributed more to uncertainty than the choice of emission (RCP) or +/- fire suppression.

5.2 Dissertation context

Research is carried out for many purposes and in different ways. At one end of the spectrum is the pursuit of science disconnected from the influence of society or decision making; on the other end is coproduction in which scientists work interactively with those who will use the science in decision making (Kirchhoff et al., 2013). As mentioned in the introduction, examples of coproduction in climate science are common.

While the research performed in this dissertation was not part of a coproduction project, it was at least partially motivated by a desire to provide the best available science to other scientists and decision makers. The only outside funding contribution to this dissertation came from the Northwest Climate Science Center's *Integrated Scenarios of climate, hydrology and vegetation for the Northwest* project, whose goals included "a series of freely available datasets that can be used to address specific management questions" and supporting "a range of management activities to increase the resilience of Northwest ecosystems, agricultural systems, and built environments" (https://www.sciencebase.gov/catalog/item/55db7caae4b0518e35470be5). Data from runs used in Chapter 1 are available as part of that project. A measure of the early success of this dissertation's research is the 34 references Chapter 2 has amassed since its 2015 publication

(scholar.google.com). As an example, MC2 model results from that chapter have been used to model Canada lynx habitat suitability (Robbins, 2017).

EEMS was created to produce decision support models (Sheehan and Gough, 2016). In addition to the implementations of EEMS for creating models within ArcGIS or using the EEMS scripting language, its online version (www.eemsonline.org) allows users to upload, share, explore, modify, and save models and data layers. Data Basin's (www.databasin.org) EEMS explorer allows users to explore models and data layers within Data Basin. EEMS has been used in a variety of coproduced projects resulting in online tools such as the California Climate Console (http://climateconsole.org/). A motivation to use EEMS in Chapter 4 was to produce results suitable for environmental decision support. One section in that chapter outlines how the model and results could be used in the future for a variety of management questions and implicitly makes the case for EEMS as a platform for use in coproduction.

5.3 Opportunities for future study and contributions

Using MC2 or other climate-driven models with a broad range of climate futures is one way to explore future vegetation, climate, and fire trajectories. Differences in results, however, are tied to specific climate futures. An alternative would be to run the vegetation model under a set of synthetic climates in order to discover what climatic changes would contribute to crossing tipping points in the model and lead to alternative future states.

The difference in MC2 results using stochastic ignition occurrences and ignition propagation point to a rich area of research in DGVM fire dynamics under realistic conditions. The use of ignition source probability surfaces along with a rigorous fuel condition/ignition propagation model would likely enhance the realism of fire occurrence and effects. Cell-to-cell fire propagation would likely allow for larger fires to develop in a more realistic way. Such improvements would allow for fire and its effects to become an emergent property of the model, obviating the need for the currently embedded FRI-limited burning. Some preliminary work has been done with MC2's fire algorithm (Sheehan et al., 2015) that could be an important first step towards improvement in modeling mega-fires (Stephens et al., 2014).

MC2 is implemented in a combination of C++ and Fortran. Program flow is intricately linked with functionality. Algorithms are commonly spread among modules and source files in ways that are not readily apparent. The mapping of data and variable names between the C++

code and the Fortran code is neither straightforward nor well-documented. Initialization of computational and control variables is complicated, involving a combination of initialization files and code modifications in multiple C++ methods. In short, MC2 is neither easy to use, easy to understand, nor easy to modify. For MC2 to be a productive research tool into the future, it should be rewritten in a modular format, using a modern programming language. Separating the higher-level logic of module execution from the implementation of modules would allow users to easily update or replace modules in order to experiment with alternative modules and combinations of modules. It would also allow for different timesteps for different modules. Some early work was started on a new version of MC2, appropriately called MC3. However funding was unavailable to do more than preliminary design work.

EEMS is a platform with great potential as both a research tool and an instrument to inform management decisions. Its ability to easily integrate different types of data from disparate sources makes it suitable for integrating results from multiple models, as was done in Chapter 4. Whether using EEMS' drag-and-drop interface in ArcGIS or its scripting language, EEMS' ease of use gives modelers a system with a small learning curve. EEMS has been integrated with an evolutionary algorithm to find the best fit operators and parameters for an EEMS model to simulate fire resistance in the Sierra Nevada (Sheehan et al., 2017). This technique opens up the possibility for EEMS to be used as a statistical tool in a decision support setting.

With the combination of remotely sensed time series data, cloud data storage, and cloud computing, we have entered an era of more democratic environmental modeling. Google Earth Engine (GEE; https://earthengine.google.com/) has become very popular for GIS processing. For interactive use, GEE requires scripting in JavaScript, which is a constraint for many users. An EEMS-like graphical and/or scripting interface to GEE would make using it and sharing models easier, opening the power of the platform to a wider audience.

5.4 Future personal research stream

As I complete this dissertation, I find myself in an atypical position for a finishing Ph. D. student. My body of work consists not only of what I have done for this dissertation, but also what I have done over a multi-decade research and professional career and a multi-graduate degree academic career. While working on this degree I have worked full time for an environmental nonprofit best characterized as a bridging organization. I have contributed to a

large number of projects in roles including software architect, software developer, system analyst, vegetation modeler, carbon cycle modeler, decision support modeler, data analyst, and supervisor. I am fortunate that my background has allowed me to switch roles depending on funded project requirements.

However, the ability to perform many roles can lead to a lack of direction. One of the reasons I chose to get a Ph. D. was to pursue a research path with depth rather than just breadth. In some ways I succeeded by focusing on modeling climate effects for a specific region. In some ways, perhaps, I did not succeed. During the course of the dissertation I broadened my focus by delving deeply into modeling uncertainty and then tying the results together with decision support modeling. Fortunately, though, my dissertation leaves me with multiple possible research avenues.

All that said, as I look to the future, my hope is to pursue research weighted towards decision support modeling. It is in this area I have made my most singular contribution to research methods. With EEMS, I have created a platform that I and others have used for myriad environmental modeling projects. While published results from EEMS models are still few, environmental projects using EEMS are manifold and include terrestrial and aquatic intactness models for the Utah and the Colorado Plateau (https://databasin.org/maps/2e6d671d25414d47b2e21072665eefb1, https://databasin.org/maps/2c11057b154c4158b0ee875447e6a48b); site sensitivity (to climate), climate exposure, and potential climate impacts models for California; climate exposure for the western conterminous United States; conservation targets in the Mojave and Modoc regions of California; and models related to the PNW Coastal Landscape Conservation Design project (all available at www.eemsonline.org).

As a follow-on to EEMS, I have created a software architecture, called MPilot, to construct hierarchical modeling frameworks. The current version of EEMS is built using this architecture, and I have also used it to build a set of tools for processing netCDF datasets (the standard format for climate data). With MPilot, programmers can build tool sets that allow users to easily construct workflows for GIS and statistical processing of large datasets. I have outlined an architecture and development plans for an interactive, MPilot-based modeling system for

Google Earth Engine. Called GEODE (Global Environmental Online Decision Engine), this system will blend EEMS' ease of use with the power of GEE.

My goal, however, is not simply to develop software. If possible, I would like to supervise or collaborate with colleagues on software development projects. The software is simply the means to the end of doing my own environmental research from local to global scales. I would like to develop a global intactness model and global risk models based on current landscape conditions, current landscape values, such as biodiversity, and future climate protections. These models would be available to other projects as starting points for regional models for any number of purposes.

Additionally, I would like to continue regional modeling work, collaborating with researchers in fields of environmental sciences including ecology, fire, and climate. I am well positioned to work with ecologists, sociologists, resource managers, and other stakeholders to develop models for valuing landscapes using different criteria and finding areas of conflict and least potential impact. Doing this work will require the right funded position. Procuring that is my next challenge.

5.5 References

Davies, K. W., Boyd, C. S., Beck, J. L., Bates, J. D., Svejcar, T. J., & Gregg, M. A. (2011). Saving the sagebrush sea: an ecosystem conservation plan for big sagebrush plant communities. *Biological Conservation*, 144(11), 2573-2584.

Kirchhoff, C. J., Lemos, M. C., & Dessai, S. (2013). Actionable knowledge for environmental decision making: broadening the usability of climate science. *Annual Review of Environment and Resources*, 38, 393-414.

Robbins, T. O. (2017). *The Future of Southern Periphery Canada Lynx (Lynx canadensis): Habitat Suitability Projections for Lynx in the Washington-British Columbia Transboundary Region.* Master of Science thesis, University of Washington, Seattle, WA, USA.

Sheehan, T., Bachelet, D., & Ferschweiler, K. (2015). Fire in a changing climate: stochastic versus threshold-constrained ignitions in a dynamic global vegetation model (Poster). American Geophysical Union Fall Meeting, San Francisco, CA, Dec 14-18, 2015.

Sheehan, T. H. L. Romsos, W. D. Spencer (2017). Optimizing a fuzzy logic model of forest resilience in the Sierra Nevada, California (Poster). Ecological Society of America Annual Meeting, Portland, OR, August 6-11, 2017.

Stephens, S. L., Burrows, N., Buyantuyev, A., Gray, R. W., Keane, R.E., Kubian, R., Liu, S., Seijo, F., Shu, L., Tolhurst, K. G., & Van Wagtendonk, J. W. (2014). Temperate and

boreal forest mega-fires: characteristics and challenges. *Frontiers in Ecology and the Environment*, 12(2), 115-122.